

Insights into Heterogeneous Catalysts for the HMF Synthesis from Biomass

vorgelegt von
M. Sc.
Sylvia Reiche
aus Dahlen

Von der Fakultät II-Mathematik und Naturwissenschaften
der Technischen Universität Berlin
zur Erlangung des akademischen Grades
Doktor der Naturwissenschaften
Dr. rer. nat.

genehmigte Dissertation

Promotionsausschuss:

Vorsitzender: Prof. Dr. rer. nat. Reinhard Schomäcker

Gutachter: Prof. Dr. rer. nat. Robert Schlögl

Gutachter: Prof. Dr. rer. nat. Arne Thomas

Gutachter: Prof. Dr. rer. nat. Dangsheng Su

Tag der wissenschaftlichen Aussprache: 27.03.2012

Berlin 2012

D83

La gravitation de l'esprit nous fait tomber vers le haut.
Die Schwerkraft des Geistes lässt uns nach oben fallen.

Simone Weil

Kurzzusammenfassung

Die säurekatalysierte Dehydratation von Fructose unter Bildung von 5-(Hydroxymethyl)furfural (HMF) stellt eine wichtige Modelreaktion für den notwendigen Rohstoffwandel in der chemischen Industrie dar. In der vorgelegten Arbeit wurde eine Vielzahl heterogener Katalysatoren für die HMF-Synthese getestet und mit Ergebnissen der Literatur verglichen. Es wurde deutlich, dass alle Materialien bereits nach der ersten Anwendung deutlich deaktivierten und Untersuchungen zur Stabilität der Katalysatoren nur unzureichend dokumentiert sind. Im Rahmen der Dissertation wurde ein einphasiges Verfahren entwickelt, durch das die Nebenreaktion der Levulinsäurebildung verhindert werden konnte. Die Nutzung von 2-Butanol als einziges Lösungsmittel hat den weiteren Vorteil, dass Produktverunreinigungen, z. B. durch die notwendige Zugabe von Salzen im zweiphasigen Verfahren, vermieden werden können. Zudem kann eine Produktakkumulation an der Katalysatoroberfläche graphitischer Kohlenstoffkatalysatoren verhindert werden, welche andernfalls Folgereaktionen in Form von Polymerization begünstigen können.

Unter Verwendung des einphasigen Verfahrens in 2-Butanol wurde die Desaktivierung saurer Kohlenstoffkatalysatoren systematisch untersucht. Dabei konnten drei verschiedene Deaktivierungsprozesse unterschieden werden: (1) Das Auslaugen der funktionellen Gruppen unter Reaktionsbedingungen, (2) die Ablagerung unlöslicher Nebenprodukte, sogenannter Humine, auf der Katalysatoroberfläche und (3) die Desaktivierung der Katalysatoroberfläche durch die Reaktion mit dem alkoholischen Lösungsmittel. Das Auslaugen funktioneller Gruppen (Leaching) wurde für alle post-funktionalisierten Katalysatoren detektiert. Daher sind Leaching-Tests ein essentielles Element vollständiger Katalysatorcharakterisierung und entsprechende Vorbehandlungsschritte eine notwendige Voraussetzung für stabile Katalysatoren. Auch wenn für ein Material das Auslaugen der Säuregruppen aufgrund entsprechender Vorbehandlung ausgeschlossen werden konnte, so ist die Stabilität in der Fructose Dehydratation nicht automatisch gegeben. Die Vielzahl möglicher Nebenreaktion führt zu unlöslichen Nebenprodukten, welche wiederum die aktiven Säurezentren blockieren und den Katalysator sukzessive deaktivieren. Aufgrund dessen wurde eine Referenzreaktion mit monofunktionalem Reaktant, die säurekatalysierte Veresterung von Essigsäure mit Ethanol, zur vergleichenden Betrachtung herangezogen. Eine stabile Katalysatoraktivität bei erneutem Einsatz (Recycling) in der Veresterung konnte dabei, ähnlich wie die Leaching-Tests, als notwendige aber nicht hinreichende Bedingung für die Stabilität des Katalysators in der Fructosedehydratation angesehen werden. Dieses Ergebnis unterstreicht die Notwendigkeit zusätzlicher mechanistischer Kenntnisse des komplexen Reaktionsnetzwerks der Fructosedehydratation an heterogenen Katalysatoren. Schließlich konnte mittels in-situ XPS gezeigt werden, dass eine Vorbehandlung sehr wohl Einfluss auf die Oberflächenchemie der untersuchten Kohlenstoffmaterialien haben kann. Speziell die Reaktivitäten gegenüber Wasser änderten sich für die oxidierten mesoporösen Materialien nach der Vorbehandlung.

Abstract

The acid catalyzed dehydration of fructose in 5-hydroxymethyl furfural (HMF) is an important model reaction for the necessary feedstock change in chemical industry. In the present work, multiple heterogeneous catalysts have been tested for the HMF synthesis from fructose and the results have been compared to literature data. It could be shown that the materials deactivated strongly already after the first reaction run. The comparative studies of the literature showed the lack of stability tests for heterogeneous catalysts in fructose dehydration.

For comparable studies of the catalysts, a one-phase dehydration procedure in 2-butanol has been elaborated. The use of 2-butanol as the only reaction solvent inhibits the product accumulation on hydrophobic catalysts (e.g. functionalized carbon nanotubes), as confirmed by adsorption studies. In addition, the rehydration to the side products levulinic acid and formic acid are suppressed. The process avoids impurities in the HMF-product that can be problematic in subsequent processing steps, such as S- and N-containing solvents or salt residues applied in the biphasic process. Hence the one-phase system in 2-butanol would require lower purification costs than other established processes.

Comparative studies on carbon based heterogeneous catalysts revealed three different deactivating processes: (1) the leaching of instable acid functional groups, (2) the surface coverage or side blocking by insoluble polymeric byproducts (humins) and (3) the surface passivation by the alcoholic solvent. The stability of acid functional groups was investigated by activity tests of the solvent after preconditioning of the catalyst (leaching tests). It was found that leaching is a common problem for all post-functionalized, e. g. sulfonated, catalysts and appropriate pretreatments are required, in order to start with a stable fraction of acid functional groups. Leaching tests are essential for thorough proof of catalyst stability and hence are suggested to be adapted as common test for heterogeneous catalysts in fructose dehydration. Furthermore we established the comparison to the reference reaction, the esterification of acetic acid in ethanol, as successful tool for the estimation of catalyst stability. The deactivation by leaching or solvent reactions can be traced by the reference reaction. However, the successful recycling in the esterification reaction does not guarantee a stable catalyst for HMF synthesis, which underlines the necessity of further mechanistic understanding of the fructose dehydration on heterogeneous catalysts.

Finally, it could be shown by in-situ XPS that the catalyst pretreatment can significantly influence the surface chemistry of the carbon materials. In particular, the reactivity towards water differed for the oxidized mesoporous carbon after the pretreatment in alcoholic solvent.

TABLE OF CONTENTS

Table of Contents	I
List of Figures	III
List of Tables	VII

I	Introduction	1
I.1	The Feedstock Cellulosic Biomass	2
I.2	HMF Synthesis from Biomass	4
I.3	Mechanism of Fructose Dehydration to HMF	9
I.3.1	Overview scheme of reaction network	10
I.3.2	Historic development of mechanistic ideas on fructose dehydration	13
I.3.3	Mechanistic solvent effects	19
I.4	References	20
II	Outline of the Work	23
III	Heterogeneous Catalysts in the Dehydration of Fructose to HMF	25
III.1	Introduction	26
III.2	Results	27
III.3	Discussion	32
III.4	Experimental Section	35
III.4.1	Materials	35
III.4.2	Catalyst Performance Tests	36
III.5	References	37
IV	Deactivation Pathways of Carbon Catalysts for Fructose Dehydration	39
IV.1	Introduction	40
IV.2	Experimental	44
IV.2.1	Catalyst Preparation	44
IV.2.2	Catalyst Characterization	46
IV.2.3	Catalyst Performance Tests	47
IV.3	Results and Discussion	49
IV.3.1	Catalyst Testing in the Dehydration of Glucose to HMF	49

IV.3.2	Dehydration of Fructose in 2-butanol.....	55
IV.4	Summary and Conclusion.....	66
IV.5	References.....	68
V	Reactivity of Mesoporous Carbon Against Water – an In-Situ XPS Study	70
V.1	Introduction	71
V.2	Experimental	75
V.2.1	Material synthesis and preliminary characterization	75
V.2.2	Instrumental	76
V.3	Results and Discussion	77
V.3.1	Differences in original carbon samples	77
V.3.2	Differences during heating in vacuum	84
V.3.3	Behavior during heating in water atmosphere	87
V.3.4	Cl impurities and their evolution during heat and vapor treatment.....	91
V.4	Conclusions	93
V.5	References.....	95
VI	Final Discussion and Outlook.....	98
VII	Supplementary Information	i
VII.1	Appreciations	ii
VII.2	Database Sample Numbers.....	iii
VII.3	BET Isotherms.....	iv
VII.4	XPS	v

LIST OF FIGURES

I	Introduction.....	1
	Figure 1: Schematic of secondary cell-wall structure of grass ^[3]	3
	Figure 2: Important products from HMF	5
	Figure 3: Overview of reaction network for the dehydration of fructose.....	12
	Figure 4: Dehydration steps as suggested by Nef in 1910 ^[22]	13
	Figure 6: Comparison of possible conformations for glucose and fructose	15
	Figure 5: Lobry-de-Bruyn-Alberda-van-Ekenstein-rearrangement.....	16
	Figure 7: Structural model of hydrothermal carbon particles ^[47]	18
	Figure 8: Proposed mechanism for the catalytic effect of DMSO ^[50]	19
II	Outline of the Work.....	23
III	Heterogeneous Catalysts in the Dehydration of Fructose to HMF.....	25
	Figure 1: Catalytic performance of differently functionalized Baytube catalysts.....	28
	Figure 2: Comparison of BET isotherms of BTs and MC_H ₂ O ₂	30
	Figure 3: Comparison of different oxidic materials in the dehydration of fructose to HMF.....	31
	Figure 4: Characteristic color changes of the catalysts after the fructose dehydration reaction	32
IV	Deactivation Pathways of Carbon Catalysts for Fructose Dehydration.....	39
	Figure 1: Overview of carbon material basis.....	41
	Figure 2: Comparison of the dehydration of fructose and the reference reaction the esterification of acetic acid in ethanol.....	43
	Figure 3: Catalytic testing facilities	48
	Figure 4: Optimal reaction temperature for the glucose dehydration in aqueous phase	50
	Figure 5: G&F conversion, HMF selectivity, and HMF yield for different reaction times at 40 bar N ₂ for 10 wt% glucose solutions in water.....	50
	Figure 6: Comparison of differently functionalized Baytube® catalysts in the dehydration of glucose in aqueous media	52

Figure 7: Adsorption isotherms of glucose and HMF on BTs in different solvents after 20 h at 30°C.....	53
Figure 8: HMF yield over reaction time for the dehydration of glucose and fructose in aqueous phase in comparison to the one-phase system in 2-butanol.....	54
Figure 9: Schematic reaction assembly of one phase system in 2-butanol.....	56
Figure 10: Catalytic testing modes	57
Figure 11: BTs catalyst in the dehydration of fructose in 2-butanol.....	58
Figure 12: BTs catalyst in the esterification of acetic acid	59
Figure 13: Catalytic performance of BS-CNF in the dehydration of fructose.....	60
Figure 14: Left: Amberlyst® 15 (Amb) in the fructose dehydration. Right: Nafion® (Naf) in the fructose dehydration. Comparison of first run (RUN1), leaching test (LEACH) and reuse of the catalyst after RUN1 in a recycling run (RECYCL)	61
Figure 15: Left: Comparison of first run activities of AGPs and BTs. Right: Number of acid functional groups determined by titration	62
Figure 16: Upper: Catalytic performance of AGPs after four preconditioning step (AGPs_PC4) in dehydration of fructose in 2-butanol. Lower: Recyclability of AGPs_PC4 in the esterification reaction.....	63
Figure 17: Left: OMCs in the dehydration of fructose in 2-butanol after preconditioning (PC), and recycling of the preconditioned OMCs (RECYCL). Right: Leaching activity of OMCs in the esterification of acetic acid (LEACH).....	64
Figure 18: Mesoporous carbon catalyst TDP0.2 in the dehydration of fructose in 2-butanol.....	65
Figure 19: Mesoporous TDP0.2-catalyst in the esterification of acetic acid.	65
V Reactivity of Mesoporous Carbon Against Water – an In-Situ XPS Study	70
Figure 1: Possible reaction mechanism for the formation of the resorcinol-formaldehyde polymer as the precursor for OMC synthesis ^[5, 9]	72
Figure 2: Fructose dehydration into 5-hydroxymethyl furfural under liberation of 3 molecules of water	73
Figure 3: Catalytic performance of mesoporous carbon materials in the dehydration of fructose to HMF.....	74
Figure 4: Schematic drawing of the high pressure XPS system at BESSY II ^[11]	77
Figure 5: Scheme of possible carbon structure	79
Figure 6: O1s fits of MC_0, MC_1 and MC_2 of ex-situ XPS measurements	80
Figure 7: C1s fits of MC_0, MC_1 and MC_2 of ex-situ XPS measurements.....	83

Figure 8: TG-MS experiment of MC_1	85
Figure 9: Evolution of C1s components during heating in vacuum and subsequent addition of water (0.1 mbar) at 130°C	87
Figure 10: Reactivity of different oxygen functional groups towards water ^[28] and consequential changes in the solvation chemistry.....	89
Figure 11: Evolution of C1s components during heating in vacuum and subsequent addition of water (0.1 mbar) at 130°C	90
Figure 12: Insitu XPS spectra of sample MC1 (left) and MC2 (right)	94
 VI Final Discussion and Outlook	98
Figure 1: Mechanism of fructose dehydration catalyzed by homogeneous acids.....	100
 VII Supplementary Information	i
Figure 1: O1s fits (left panel) and C1s fits (right panel) of MC_0, MC_1 and MC_2 obtained by ex-situ XPS	v
Figure 2: Fits for O1s spectra of MC_1 and MC_2 during heating in vacuum	vi
Figure 3: Fits for C1s spectra of MC_1 and MC_2 during heating in vacuum.....	vi
Figure 4: Fits for O1s spectra of MC_1 and MC_2 during heating in 0.1 mbar vapor	vii
Figure 5: Fits for C1s spectra of MC_1 and MC_2 during heating in 0.1 mbar vapor	vii
Figure 6: Cl 2p spectra for MC_1 and MC_2 during heating in vacuum	viii
Figure 7: Cl 2p spectra for MC_1 and MC_2 during heating in vapor.....	viii

LIST OF TABLES

I	Introduction.....	1
	Table 1: Monosaccharide building blocks of biomass	7
II	Outline of the Work.....	23
III	Heterogeneous Catalysts in the Dehydration of Fructose to HMF.....	25
	Table 1: Overview of catalytic performance of tested materials and comparison to literature references	29
IV	Deactivation Pathways of Carbon Catalysts for Fructose Dehydration.....	39
	Table 1: Overview of catalysts.....	46
	Table 2: BET surface area before and after reaction.....	52
V	Reactivity of Mesoporous Carbon Against Water – an In-Situ XPS Study	70
	Table 1: Summary of material basis including BET areas and titration results.....	76
	Table 2: O1s peak assignment according to the literature	78
	Table 3: Quantification of oxygen species of MC_0, MC_1 and MC_2 by ex-situ XPS.....	81
	Table 4: C1s peak assignment according to literature	82
	Table 5: Quantification of carbon species in the C1s spectra of MC_0, MC_1 and MC_2 obtained by ex-situ XPS	84
	Table 6: Quantification of oxygen species of MC_1 and MC_2 during heating in vacuum and subsequent addition of water (0.1 mbar) at 130°C	85
	Table 7: Quantification of oxygen species for MC_1 and MC_2 during heating in 0.1 mbar vapor	88
	Table 8: Quantification of Cl species of MC_1 and MC_2 during in-situ XPS.....	92
VI	Final Discussion and Outlook	98
VII	Supplementary Information	i
	Table 1: BET isotherms of mesoporous carbon samples investigated by XPS	v

Table 2: Quantification of carbon species in the O1s peak during heating in vacuum and subsequent addition of water at 130°C	x
Table 3: Quantification of carbon species in the C1s peak during heating in vacuum and subsequent addition of water at 130°C.....	x
Table 4: Quantification of carbon species in the O1s peak during heating in 0.1 mbar vapor pressure	xi
Table 5: Quantification of carbon species in the C1s peak during heating in 0.1 mbar vapor pressure	xi

I INTRODUCTION

The diminishing reserves of fossil fuels coupled with the steady growth in their consumption necessitate the exploration of alternative resources. In order to secure the future supply of fuels and chemicals, a renewable feedstock is required to provide the sustainable foundation of prospective processes. Biomass, as steadily produced by photosynthesis, is not only a renewable feedstock, it also offers a CO₂-neutral bases for the production of essential chemicals and transportation fuels. However, the change in feedstock requires the complete reconstruction of today's infrastructure and technology. All established processes for the refining of alkane based crude oil are founded on the introduction of functional groups, mainly by selective oxidation. The existing functionalization technology needs to be transferred into strategies of selective oxygen removal for the highly functionalized biomass feedstocks.

Starting from the choice of proper raw materials, over economic and ecological cultivation, down to the development of new refining strategies, there are several complex challenges that require multidisciplinary solutions. It is in the responsibility of scientific research to contribute to the implementation of necessary feedstock changes, starting from in-depth analysis and the successive compilation of fundamental understanding.

I.1 The Feedstock Cellulosic Biomass

The choice of a suitable biomass feedstock for future chemical and fuel production has to be taken with care. Political criteria, as well as ethical issues and technical feasibility need to be taken into account. Political criteria can be global dependencies and requirements in development and industrialization. The ethical arguments concern price competition to food sources or the question of sustainability of biomass production and use. Last but not least, the question of technical feasibility is important for large scale, industrial processes. Herein, the number and costs of necessary reaction and purification steps, as well as the financial investments for the development of new production lines, compared to the price of the final product play a role. Since esculent plants are generally easier to digest and existing technology of food processing can be used; they are preferred feedstocks according to the argument of technical applicability. For this reason, the first generation biofuels are made of sugar, starch and vegetable oil^[1].

In contrast, second generation biofuels are produced from sustainable sources, i. e. available feedstocks preventing impact on greenhouse gas emission, biodiversity and land use. In fact, the most abundant class of biomass raw materials is carbohydrates, contributing 95% of the 200 billion tones of annual biomass production by photosynthesis^[2]. Considering the other sustainability criteria of biodiversity and land use change, possible second generation feedstocks are harvest waste (sugar cane begasse, corn stover), forest industry side streams or fast growing energy crops. The main component of those materials is lignocellulose which consists of a complex network of benzylic lignin, hemicellulose and cellulose (compare grass structure **Figure 1**)^[3].

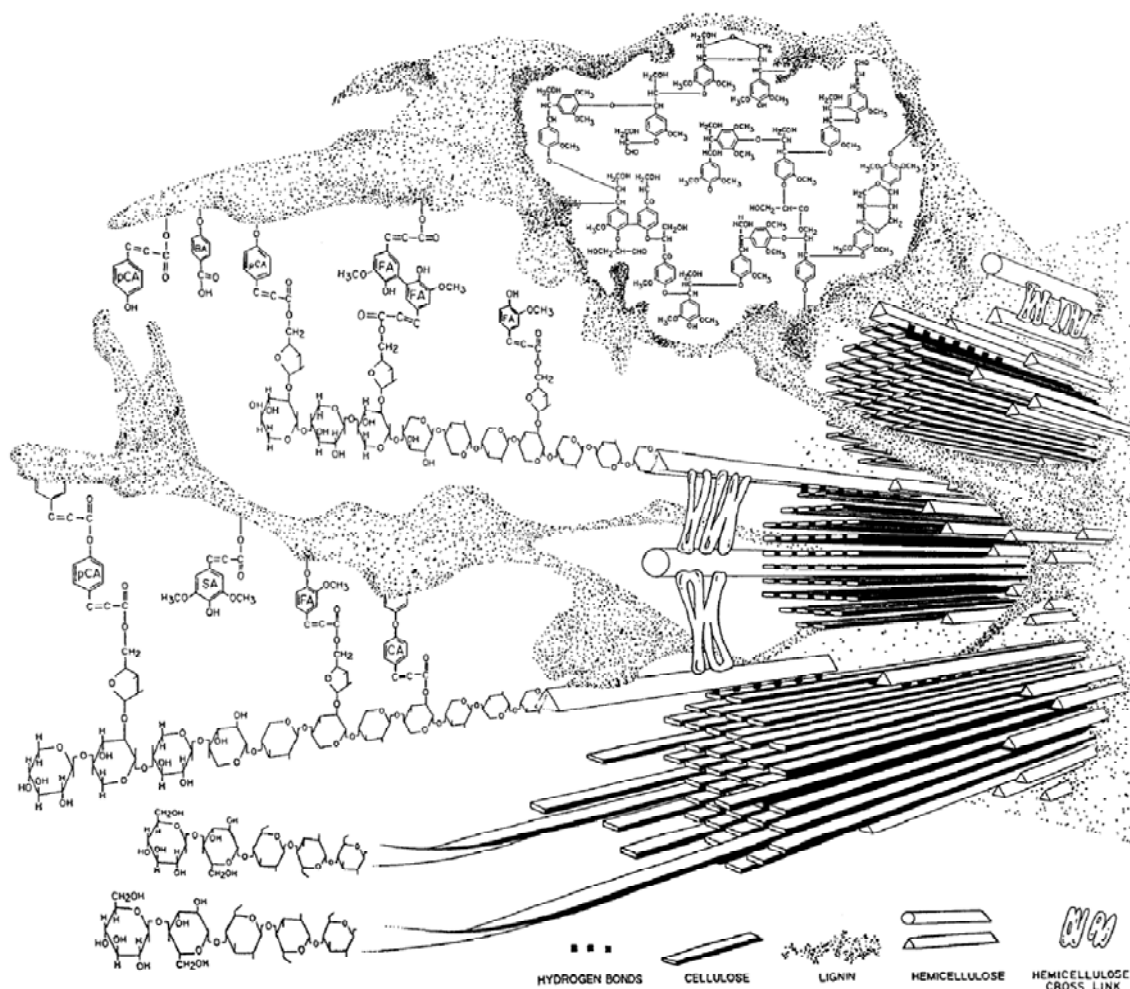


Figure 1: Schematic of secondary cell-wall structure of grass. The main components are cellulose hemicelluloses and lignin, interconnected by p-coumaric acid (pCA), ferulic acid (FA), p-hydroxybenzoic acid (BA), sinapic acid (SA) and cinnamic acid (CA)^[3].

The carbohydrate fraction based on hemicellulose and cellulose comprises hexose- and pentose-units that are polymerized by the formation of very stable glycosidic bonds. In cellulose, β -(1,4)-linked D-glucose units form long-chained polymers. Through interconnection by hydrogen bonds, those cellulose chains result in fibers with partly crystalline areas. Hemicellulose, by contrast, is of a less ordered structure, due to the variety of sugar units in the polymer which are cross-linked to form a network rather than linear structures. Typical sugar

units of hemicellulose are the pentoses xylose and arabinose, as well as the hexoses glucose, mannose and galactose. Lignin is incorporated into the carbohydrate network of hemicellulose and cellulose, and leads to the typical wooden appearance of plants. All fragments are interconnected by non-core lignin components, such as p-coumaric acid, ferulic acid, p-hydroxybenzoic acid, sinapic acid or cinnamic acid.

In nature, those robust structures give the plant structural stability. Only few organisms, such as ruminant animals, are able to break the structure, hydrolyze glycosidic bonds and metabolize the monosaccharides from cellulosic biomass. This indicates the difficulty of controlled cleavage of lignocellulose into well defined building blocks. Since lignocellulose is the only biomass feedstock that can be exploited in sustainable manner in large scale, the main challenge of its industrial use is the development of an adequate refining technology. This implies the improvement of enzymatic and chemical hydrolysis strategies on the one hand, and processes for the selective conversion of lignocelluloses derived building blocks on the other hand.

I.2 HMF Synthesis from Biomass

The main carbohydrate units of lignocellulose, as well as of first generation feedstocks, are summarized in **Table 1**. They provide a pool of potential building blocks for the synthesis of chemicals and fuels. One important property of the materials is the high oxygen content. The consequence of the high oxygen content is the lower heating value, which is disadvantageous for the application as fuels. Additionally the high density of functional groups results in a high and

unspecific reactivity of monosaccharides. Thus the major challenge is the selective, chemical removal of oxygen which is efficiently done in acid catalyzed dehydration reactions.

One important dehydration product is 5-hydroxymethyl furfural (HMF). HMF can be further converted to dimethyl furan (DMF) and used as a fuel or fuel additive^[4]. In addition, HMF is an important intermediate for the production of polymers^[5], e.g. in form of the further oxidized derivate furandicarboxylic acid (FDCA) which is seen as potential alternative to terephthalic acid derived from crude oil processing. Another process already applied in industrial scale is the use of the HMF-derivate 3,5-dihydroxy methylfuran by Oaker Oats for the production of polyurethane foams^[6]. Furthermore, essential future platform chemicals can be produced of HMF, such as levulinic acid^[7] or pyrrols^[8] (**Figure 2**).

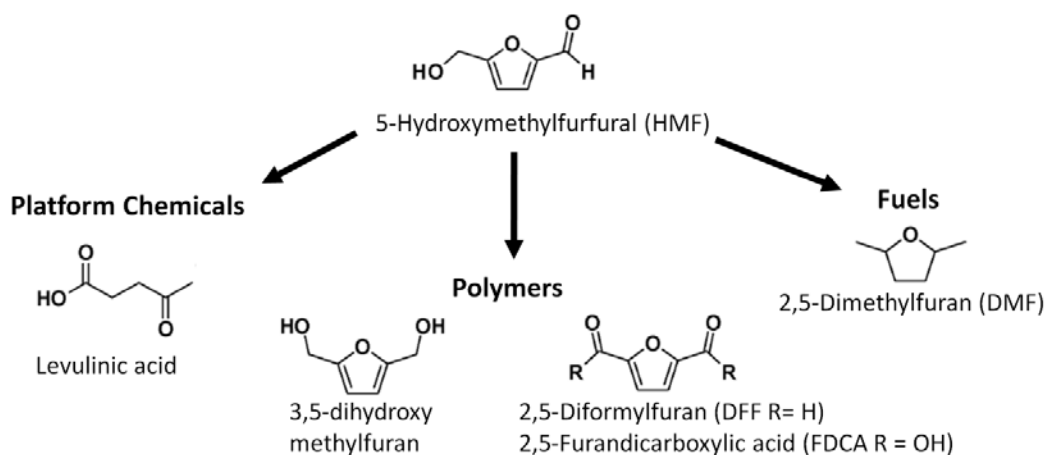


Figure 2: Important products from HMF

In addition to the direct industrial relevance of the reaction studied, the dehydration of fructose is one general pathway of effective oxygen removal in biomass conversion chemistry^[9]. HMF has consequently been listed as one of the “key substance between carbohydrate chemistry and mineral oil based chemistry”^[10]. Therefore this reaction was also studied as an important model

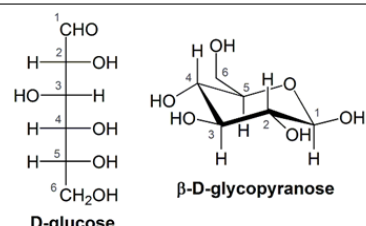
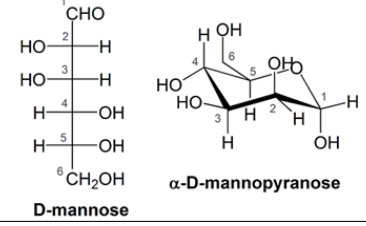
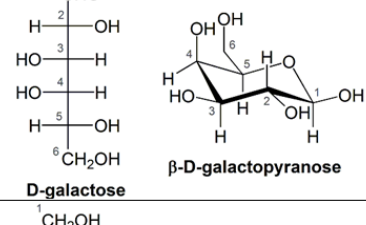
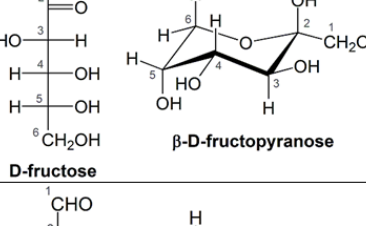
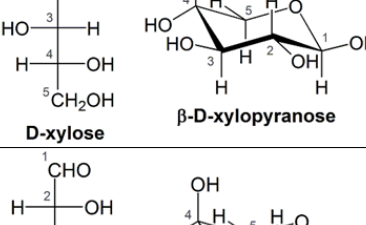
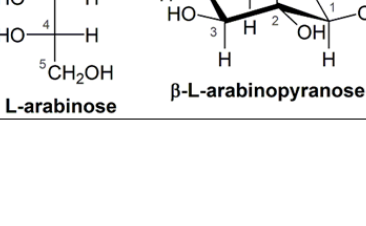
reaction in the extension and the improvement of already existing concepts of biorefinery^[11].

Due to the reasons mentioned, the number of publications on HMF synthesis increased exponentially within the last decade. Great efforts have been made to study a variety of possible feedstocks. The spectrum ranges from monosaccharide and polysaccharide, over cellulose and hemicellulose up to biomass raw materials, such as woodchips or straw. The latter require special digestion or extraction mechanisms. One approach is to apply ball milling to mechanocatalytically break natural cellulose sources^[12] prior to further dehydration steps. However, even by addition of a homogeneous acid (p-toluenesulfonic acid, p-TSA) the mechanically assisted depolymerization process yields only into less than 0.3 % furfural products^[13]. So far ball milling studies have aimed the production of soluble, short-chained polysaccharides, and there might be more potential for this method to assist direct production of HMF from natural lignocellulose sources.

The most promising possibility to efficiently dissolve lignocellulosic biomass and convert it directly to HMF or HMF-derivatives is the use of ionic liquids (ILs). Binder and Raines reported the use of N,N-dimethylacetamide (DMA) in combination with 1-ethyl-3-methylimidazolium chloride ([EMIM]Cl), lithium chloride (LiCl) and CrCl₃ for the direct production of HMF from corn stover in a single reaction step^[14]. In applying microwave heating (400 W for 3 min), Zhang et al. were able to obtain 45-52% HMF yields from corn stalk, rice straw and pine wood^[15]. The solvent used in that work was 1-butyl-3-methylimidazolium chloride ([BMIM]Cl), again together with CrCl₃. Thus the reaction mixture might contain toxic chromium species. In addition, there are the general problems of product separation and purification, as well as the high solvent costs. On this account, the direct conversion of raw biomass into HMF can be still seen as in a “proof-of-principle”-state.

Introduction

Table 1: Monosaccharide building blocks of biomass

Monosaccharide unit	Biomass derived polymers	Raw biomass feedstock
 <p>D-glucose β-D-glycopyranose</p>	lignocelluloses, hemicelluloses cellulose starch cellubiose sucrose lactose raffinose	corn stover, wood, grass cotton, jute, linen potatoes, corn, wheat, rice cotton, jute, linen sugar cane, sugar beet milk legumes, sugar cane
 <p>D-mannose α-D-mannopyranose</p>	lignocelluloses, hemicelluloses	corn stover, wood, grass
 <p>D-galactose β-D-galactopyranose</p>	lignocelluloses, hemicelluloses lactose raffinose	corn stover, wood, grass milk legumes, sugar cane
 <p>D-fructose β-D-fructopyranose</p>	sucrose inulin	sugar cane, sugar beet composite plants
 <p>D-xylose β-D-xylopyranose</p>	lignocelluloses, hemicelluloses	corn stover, wood, grass
 <p>L-arabinose β-L-arabinopyranose</p>	lignocelluloses, hemicelluloses	corn stover, wood, grass

In principal, there are similar procedures applied while using purified cellulose as feedstock for HMF synthesis. In combination with column chromatography on silica gel isolated HMF yields of 61% were obtained from cellulose^[16]. Here 10 wt% CrCl₃ in [BMIM]Cl were irradiated by microwave heating at 400 W for 2 min. Other groups, such as Valente et al.^[17], reported lower yields for HMF production from cellulose in similar complex systems. They did not detect HMF formation after 4 h at 100°C (oil bath heating), while using a 2-phase mixture of [BMIM]Cl and methyl isobutyl ketone (MIBK) together with CrCl₃ as catalyst. The addition of 1-ethyl-3-methylimidazolium hydrogen sulfate ([EMIM][HSO₄]) leads to 9% HMF yield after 4 h at 100°C. Binder and Raines could increase the HMF yield to 53% by the addition of HCl using oil bath heating at 140°C for 1 h^[14]. Although the reaction systems are similar, a direct comparison of those results is difficult due to the differences in reaction conditions applied. In general, it can be concluded that microwave heating and high ion contents favor high HMF yields from cellulose^[16].

One example for an ionic-liquid-free method for the direct conversion of cellulose to HMF was reported by Chareonlimkun et al.^[18]. They used hot compressed water (HCW) and a heterogeneous ZrO₂-TiO₂ catalyst. A stainless steel reactor was filled by 0.1 g cellulose and 1 ml water, and heated to 250°C for 5 min. Due to constant N₂-pressure of 34.5 MPa water is in the state of liquid phase during the experiment. Although this method avoids the used of toxic additives and expensive ionic liquids, the obtained HMF selectivity of 13% at 70% conversion is rather low.

The selected examples on the use of raw biomass or cellulose should show that, despite the partially promising HMF yields, the currently required reaction conditions do not allow a sustainable synthesis. Highly complex production routes, including toxic additives, expensive solvents and impractical product separation, are required. Additionally, the systematic variation of reaction

conditions, in order to validate the influence of the individual parameters and provide a comparable basis of reactivity results remains to be carried out.

Due to the reasons mentioned, all following considerations will focus on the use of the monosaccharides glucose and fructose as initial product for the synthesis of HMF. In parallel comprehensive research efforts are observable in the selective breakage of raw biomass into monosaccharide by enzymatic and chemical hydrolysis, as well as mechanocatalytical ball milling process.

I.3 Mechanism of Fructose Dehydration to HMF

As described above, sugars are complex structures containing reactive carbonyl and hydroxyl functional groups in high density. In biological systems sugars can be selectively converted by perfectly designed enzymes under mild conditions. The formation of byproducts is suppressed by the constrained local environment of the active site. Chemical sugar conversion however, such as an acidic treatment of aqueous fructose solutions, leads to a complex reaction network of many possible reaction routes and byproducts. Driven by different motives, various scientists tried to map this reaction network over the last century. In this section, a summary of their findings is comprised in an overall reaction scheme. Secondly, the literature basis for the current mechanistic understanding is summarized, in order to distinguish between the scientific level of knowledge, ongoing debates, and remaining queries down to the present day.

I.3.1 Overview scheme of reaction network

An overview of the reaction network of the acid catalyzed dehydration of fructose into HMF is depicted in **Figure 2**. In the center of the scheme stands the overall reaction, indicated by the bold arrows. Fructose reacts over intermediates to the dehydration product HMF. In aqueous media HMF can further react via re-hydration levulinic acid and formic acid, again passing certain intermediate steps. The explanatory boxes (dotted) for the intermediates contain the mechanisms discussed in the literature. For the dehydration of fructose to HMF two general pathways are reported (upper dotted box). The upper one, comprising the intermediates **1-5**, maintains the five-membered ring structure of fructofuranose (**F α f** or **F β f**). In the first step, fructose is protonated in the C-2-OH position. The formed C-2-OH₂⁺ splits off water as a good leaving group. Thus the first dehydration step results in the fructofuranosyl cation (**2**). At the same time, all initial stereoisomeric information in C-2 position is lost, as indicated by wavy lines. By the following deprotonation, the enol intermediate **3** evolves which is in equilibrium with the corresponding keto form **4**. Subsequently, either the C-4-OH or the C-3-OH position can be dehydrated by water abstraction, resulting in **5a** or **5b**, respectively. Finally the last dehydration step, which is the only irreversible step in the mechanism, results in the formation of aromatic HMF.

Alternatively, the dehydration can follow an open-chain mechanism over the acyclic keto-form of fructose (**6**). Thereby **6** is in equilibrium to the enol- tautomer **7** and can be dehydrated at the C-3-OH position. A 3-deoxyhexosulose intermediate is formed, labeled as **8**. The subsequent dehydration at C-4-OH position results in the unsaturated osone **9**. Finally, the abstraction of the third water molecule leads to the formation of the five-ring structure of HMF.

Introduction

In aqueous media the dehydration product HMF can further react with water over the intermediates **11-15** (lower explanatory box). The “rehydration” reaction is as well catalyzed by the acid abundant in the reaction mixture. The formal addition of one water molecule results in the cleavage of formic acid, and further water addition to intermediate **15** results in the formation of levulinic acid. Both levulinic acid and formic acid lead to a lowering of the total pH of the solution and autocatalyze the decomposition of fructose.

A major contribution to the overall reaction network comes from unwanted byproducts. They can be classified into soluble and insoluble polymerization products. Soluble polymers can be formed by intermolecular condensation of fructose. The reaction of two fructose molecules under water abstraction results in the dimer di-fructose-di-anhydride. The formation of insoluble byproducts, so-called humins, can proceed over oligomerization of fructose with itself and with HMF. Furthermore side products of levulinic acid formation (**17**) can undergo unwanted polymerization reactions. Generally, all intermediates carry multiple functional groups predestinated for the formation of side products and humins, in particular in acidic environment. Thus the process of humin formation is highly complex and a throughout mechanistic understanding of this process is still missing.

Introduction

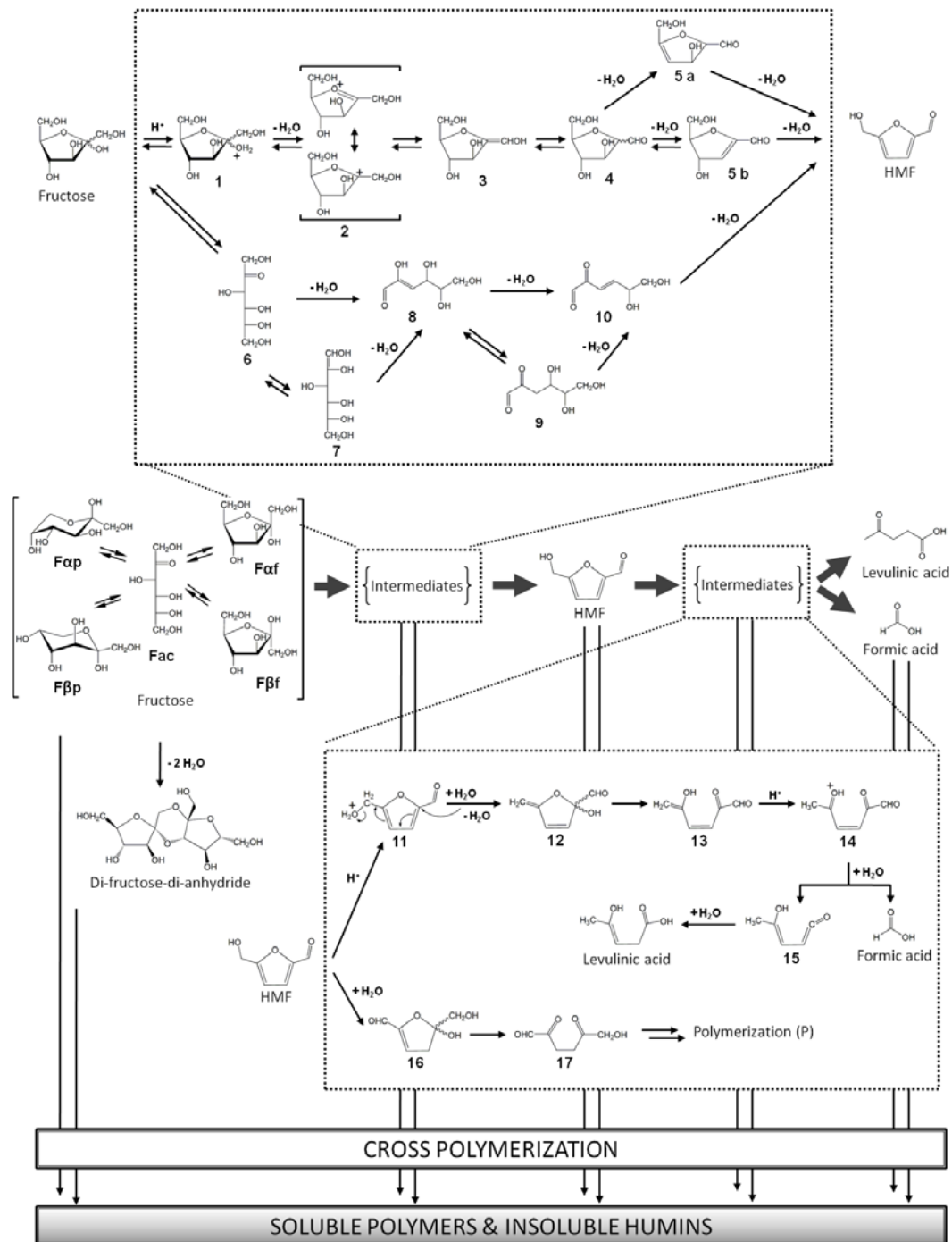
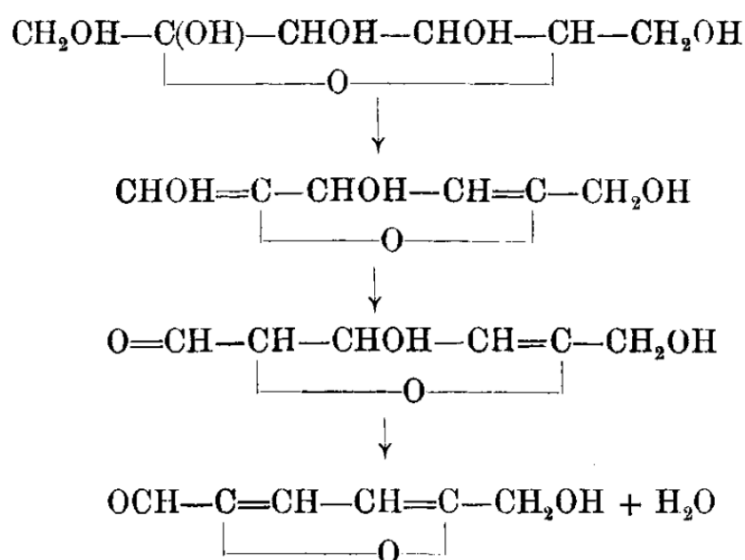


Figure 3: Overview of reaction network for the dehydration of fructose under acidic conditions in aqueous media. The overall reaction (\Rightarrow) appears in the middle of the scheme. The explanatory boxes show the mechanism of HMF formation (upper dotted box) and the re-hydration of HMF to levulinic acid and formic acid (lower dotted box).



dehydration products of chitose (5-(hydroxymethyl)-tetrahydrofuran-2,3,4-triol) in combination with further specific color reactions. Based on the identification of HMF as the dehydration product, Nef suggested a mechanism in 1910 (**Figure 4**)^[22]. Nef already proposed cyclic intermediates similar to **5 a**, compare **Figure 2** upper reaction mechanism. One general argument for a dehydration mechanism over cyclic intermediates (compare **1-5**, **Figure 2**) is the higher activity of fructose in comparison to glucose. Blanksma and van Ekenstein found only 1% yield of HMF from glucose whereas fructose gave 20-25% yield under the same reaction conditions^[24]. Kiermayer^[19], as well as later Haworth and Jones^[25] found that in acidic treatments of sucrose only the fructose half reacts to form HMF, the glucose half remains unreacted in the reaction mixture. As already summarized in the previous chapter the highest HMF yields have been achieved by either using fructose as a direct feedstock or facilitating isomerization to fructose prior to the actual dehydration step^[26, 27]. Since the five-membered ring structure of fructofuranose is close to the suggested fructofuranosyl cation (**2**), the measurable advantage of fructose in comparison to glucose supports the cyclic mechanisms. Although fructose occurs in the 5-ring state only to an extent of 24% at 20°C, the furanose content increases with temperature (at 80°C 42% furanose^[28]).

In the case of glucose none of the possible cyclic conformers provides a suitable structural element for a direct HMF formation (**Figure 6**). Consequently an epimerization is necessary described as the Lobry-de-Bruyn-Alberda-van Ekenstein-rearrangement (**Figure 5**)^[29]. The epimerization between the aldose glucose and the ketose fructose is typically base catalyzed, and passes the open chain conformation of glucose (0.002% at 31°C). The enediol intermediate is also discussed as first possible intermediate **7** (**Figure 2**) in the acyclic reaction mechanism.

Introduction

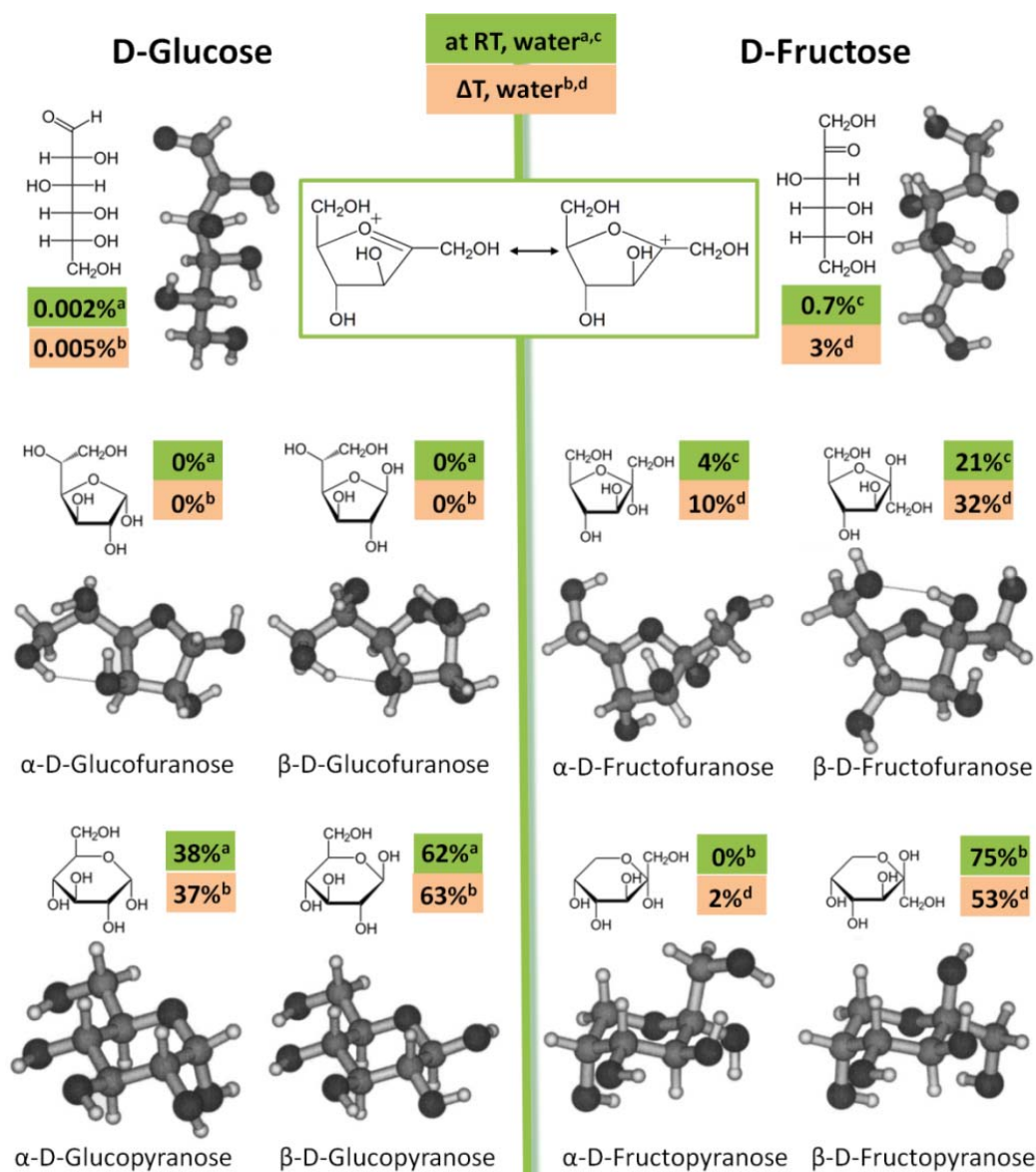


Figure 6: Comparison of possible conformations for glucose and fructose with their abundance in aqueous solution^[30]: a) 31°C, glucose^[31, 32]; b) 44°C, glucose^[31, 32]; c) 27°C, fructose^[32, 33]; d) 80°C, fructose^[28]

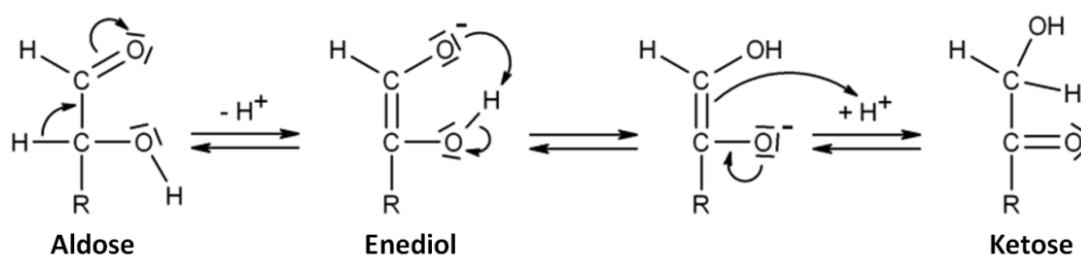


Figure 5: Lobry-de-Bruyn-Alberda-van-Ekenstein-rearrangement

The acyclic reaction mechanism, i. e. another possible mechanism via open chain intermediates (compound **6-8**, **Figure 2**), has first been discussed by Hurd and Isenhour in 1932^[34]. It is based on the well known, base-catalyzed β -elimination of the hydroxyl group via enediol intermediates (**7**), as discussed for the epimerization. Since fructose forms a more stable open chain conformer than glucose (**Figure 5**), the higher abundance of the same can be an explanation for the higher dehydration activity of fructose. The phenylosazone derivate of **9** has been isolated by Wolfrom et al.^[35]. The same group further proceeded UV absorption studies to add further evidence to the abundance of acyclic intermediates^[36]. However, those studies did compare absorption bands which are not part of the UV spectrum of 3-deoxyhexosulose (**8**) as critically discussed later^[37, 38]. Anet et al. also supported the idea of a dehydration mechanism over acyclic intermediates^[39, 40]. They were able to isolate osazone derivatives of 3-deoxyhexulose (**8**) and 3,4-dideoxyhexulose intermediates (**9**) by paper column chromatography and identified the same by NMR^[40]. Later isotope exchange studies were performed in D_2O ^[41, 42] showing that the HMF product does not contain any deuterium incorporation. Since the acyclic mechanism includes several equilibria with enolic tautomers (**7**, **9**), carbon-linked deuterium is expected in the final product. Thus the isotope exchange experiments in D_2O support the idea of the cyclic mechanism^[38]. The question remained how measurable amounts of deuterium free HMF can be obtained

from glucose, since here an epimerization is the first requirement for HMF formation and in basic media deuterium incorporation was detected.^[42] The answer was given by Harris and Feather^[43] who observed an intramolecular C-2 \rightarrow C-1 hydrogen transfer in the dehydration of C-2 tritium labeled glucose (glucose-2-³H). However, an intramolecular hydrogen transfer C-3 \rightarrow C-2, which could prove an acyclic mechanism in the absence of deuterium incorporation, has not been presented down to the present day. In 2008, Yaylayan et al. reported a relative efficiency in HMF formation for glucose, 3-desoxyglucosone (**9**) and fructose of 0.16 : 1 : 2.4^[44]. Hence **9** cannot be the main precursor of HMF from fructose; otherwise it would have lead to more HMF than in the case relative to glucose.

The present compilation of literature on sugar dehydration strongly supports the cyclic mechanism over the furanosyl cation. If at all, the open-chain mechanism only plays a minor role in the formation of HMF from fructose.

Despite the significant influence of insoluble polymerization products on the HMF selectivity, very little is known on the formation mechanism of humins. One possible reaction, which can lead to the formation of humins, is the intermolecular condensation of fructose^[45, 46]. Furthermore, side reactions of fructose with the product HMF are reported^[46], such as the acetalization between the aldehyde functional group of HMF and hydroxyl functional groups of the sugar. More general, Kuster et al. mentioned that side reactions between all intermediates contribute to the humin formation^[26]. More recently, the structural analysis of hydrothermally synthesized carbon materials from glucose gave further insight in the constitution of humins (**Figure 7**)^[47]. The results of the ¹³C solid-state MAS NMR experiments can be directly applied on the structure determination of humins, since the hydrothermal carbon synthesis from glucose is performed under very similar conditions as common dehydration reactions, i. e. 10 wt% glucose solution in water at 180°C for 24 h.

Only the choice of longer reaction times provokes the preferential formation of solid carbon materials, instead of maximizing HMF yields. The main structural motif detected for the hydrothermal carbon was with approximately 65% the furan ring, originated from HMF. About 23% was assigned to sp^3 carbon and the remaining fraction attributed to C=O and residual glucose. Consequently, the NMR results support the idea of a complex polymerization procedure with major contribution of HMF. However, the question of the origin of the interconnecting carbon chains containing 23% sp^3 carbon and about 13% C=O remains unsolved. Hence the elucidation of the humin formation mechanism is still open to prospective research activities.

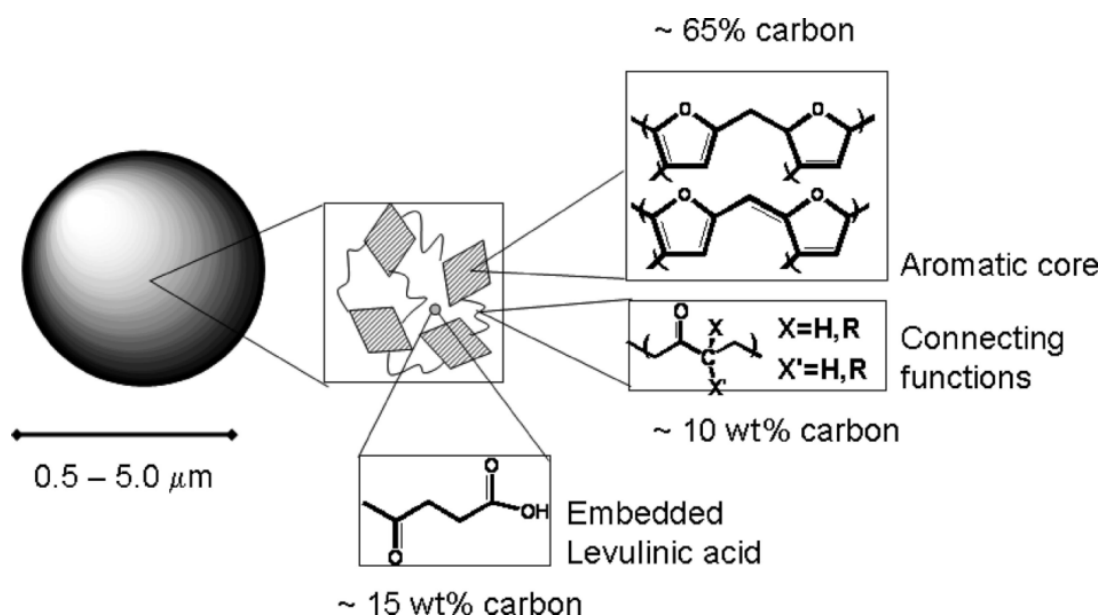


Figure 7: Structural model of hydrothermal carbon particles according to [47]

I.3.3 Mechanistic solvent effects

The (ring) structure and conformation of the initial sugar apparently play a major role in the facileness of the dehydration reaction. Since solvents have the property to influence the structural appearance of sugars, there have been several mechanistic considerations on solvent effects. The most prominent example is DMSO. Dais and Perlin^[48] observed a higher content of furanose conformers of fructose in DMSO compared to water already at 20°C, with 20% α -furanose (**F α f**), 55% β -furanose (**F β f**) and only 26% β -pyranose (**F β p**). It is known that intramolecular hydrogen bonds are stronger in DMSO than in water^[49]. However a direct connection between stronger intramolecular hydrogen bonds and conformeric preferences cannot be concluded because the influence of hydrogen bonds is similar in pyranose and furanose conformers. An explanation for the distribution of fructose conformers in DMSO is still outstanding. Amarasekara et al.^[50] found a further decrease of **F β p** down to 16% at 150°C and proposed a mechanism for the catalytic effect of DMSO beyond the furanose stabilization (**Figure 8**). Additionally they could identify the cyclic intermediate **5 b** (compare **Figure 3**) by combination of ¹H and ¹³C NMR data and therewith provide further evidence for the cyclic mechanism.

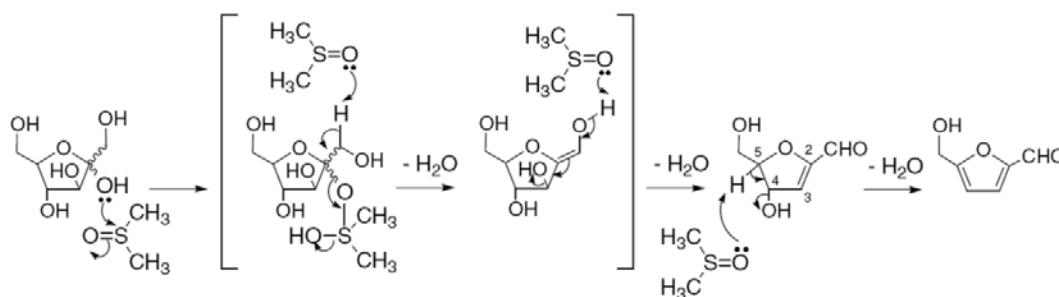


Figure 8: Proposed mechanism for the catalytic effect of DMSO on the dehydration of fructose^[50]

I.4 References

- [1] European Biofuels Technology Platform (EBTP), *Biofuel Production*, <http://www.biofuelstp.eu/fuelproduction.html>, **17th November 2011**.
- [2] N. E. Bassam, International Research Center for Renewable Energy (IFEED), **2009**.
- [3] J. Bidlack, M. Malone, R. Benson, *Proceedings of the Oklahoma Academy of Science* **1992**, 72, 51-56.
- [4] Y. Roman-Leshkov, C. J. Barrett, Z. Y. Liu, J. A. Dumesic, *Nature* **2007**, 447, 982-U985.
- [5] A. Gandini, M. N. Belgacem, *Progress in Polymer Science* **1997**, 22, 1203-1379; C. Moreau, M. N. Belgacem, A. Gandini, *Topics in Catalysis* **2004**, 27, 11-30.
- [6] W. J. Pentz, in *Patent*, C08G 1814 ed. (Ed.: Q. O. Company), Quaker Oats Company, US, **1984**.
- [7] A. Corma, S. Iborra, A. Velty, *Chemical Reviews* **2007**, 107, 2411-2502; G. Dautzenberg, M. Gerhardt, B. Kamm, *Holzforschung* **2011**, 65, 439-451.
- [8] F. W. Lichtenthaler, A. Brust, E. Cuny, *Green Chemistry* **2001**, 3, 201-209.
- [9] R. Rinaldi, F. Schuth, *Energy & Environmental Science* **2009**, 2, 610-626.
- [10] H. Schiweck, M. Munir, K. M. Rapp, B. Schneider, M. Vogel, *Zuckerindustrie* **1990**, 115, 555-565.
- [11] B. Kamm, P. Gruber, M. Kamm, *Biorefineries - Industrial Processes and Products*, Vol. 2, Wiley-VCH, Weinheim, **2005**.
- [12] S. M. Hick, C. Griebel, D. T. Restrepo, J. H. Truitt, E. J. Buker, C. Bylda, R. G. Blair, *Green Chemistry* **2010**, 12, 468-474; S. Van de Vyver, J. Geboers, P. A. Jacobs, B. F. Sels, *Chemcatchem* **2011**, 3, 82-94.
- [13] N. Meine, J. Hilgert, R. Rinaldi, F. Schüth, in *XV. International Symposium on Relations between Homogeneous and Heterogeneous Catalysis*, Berlin, **2011**.
- [14] J. B. Binder, R. T. Raines, *Journal of the American Chemical Society* **2009**, 131, 1979-1985.
- [15] Z. Zhang, Z. K. Zhao, *Bioresource Technology* **2010**, 101, 1111-1114.
- [16] C. Z. Li, Z. H. Zhang, Z. B. K. Zhao, *Tetrahedron Letters* **2009**, 50, 5403-5405.

- [17] S. Lima, P. Neves, M. M. Antunes, M. Pillinger, N. Ignatyev, A. A. Valente, *Applied Catalysis a-General* **2009**, 363, 93-99.
- [18] A. Chareonlimkun, V. Champreda, A. Shotipruk, N. Laosiripojana, *Bioresource Technology* **2010**, 101, 4179-4186.
- [19] J. Kiermayer, *Chem. Zeit.* **1895**, 19, 1003-1005.
- [20] G. Düll, C. J. Lintner, *Chemiker-Zeitung* **1895**, 19, 216-217.
- [21] G. Düll, C. J. Lintner, *Chem. Zeit.* **1895**, 19, 216-217.
- [22] J. U. Nef, *Justus Liebigs Annalen Der Chemie* **1910**, 376, 1-119.
- [23] W. A. van Ekenstein, J. J. Blanksma, *Recueil Des Travaux Chimiques Des Pays-Bas Et De La Belgique* **1906**, 25, 153-161.
- [24] W. A. van Ekenstein, J. J. Blanksma, *Berichte der deutschen chemischen Gesellschaft* **1910**, 43, 2355-2361.
- [25] W. N. Haworth, E. L. Hirst, V. S. Nicholson, *Journal of the Chemical Society* **1927**, 1513-1526; W. N. Haworth, W. G. M. Jones, *Journal of the Chemical Society* **1944**, 667-670.
- [26] B. F. M. Kuster, *Starch-Starke* **1990**, 42, 314-321.
- [27] S. H. Khajavi, Y. Kimura, R. Oomori, R. Matsuno, S. Adachi, *Journal of Food Engineering* **2005**, 68, 309-313.
- [28] W. Funcke, C. von Sonntag, C. Triantaphylides, *Carbohydrate Research* **1979**, 75, 305-309.
- [29] S. Angyal, A. Stütz, *Vol. 215*, Springer Berlin / Heidelberg, **2001**, pp. 1-14.
- [30] M. Jetzki, R. Signorell, *Journal of Chemical Physics* **2002**, 117, 8063-8073; H. E. Vandam, A. P. G. Kieboom, H. Vanbekkum, *Starch-Starke* **1986**, 38, 95-101.
- [31] S. J. Angyal, V. A. Pickles, *Australian Journal of Chemistry* **1972**, 25, 1695-&.
- [32] L. D. Hayward, S. J. Angyal, *Carbohydrate Research* **1977**, 53, 13-20.
- [33] S. J. Angyal, G. S. Bethell, D. E. Cowley, V. A. Pickles, *Australian Journal of Chemistry* **1976**, 29, 1239-1247.
- [34] C. D. Hurd, L. L. Isenhour, *Journal of the American Chemical Society* **1932**, 54, 317-330.
- [35] M. L. Wolfrom, E. G. Wallace, E. A. Metcalf, *Journal of the American Chemical Society* **1942**, 64, 265-269.

Introduction

- [36] M. L. Wolfrom, R. D. Schuetz, L. F. Cavalieri, *Journal of the American Chemical Society* **1948**, *70*, 514-517; M. L. Wolfrom, R. D. Schuetz, L. F. Cavalieri, *Journal of the American Chemical Society* **1949**, *71*, 3518-3523.
- [37] J. Lewkowski, *Arkivoc* **2001**, *2*; G. Machell, G. N. Richards, *Journal of the Chemical Society* **1960**, 1938-1943.
- [38] M. J. Antal, W. S. L. Mok, G. N. Richards, *Carbohydrate Research* **1990**, *199*, 91-109.
- [39] E. F. L. J. Anet, *J. Am. Chem. Soc.* **1960**, *82*, 1502; E. Anet, *Australian Journal of Chemistry* **1960**, *13*, 396-403; E. F. L. Anet, *Australian Journal of Chemistry* **1962**, *15*, 503-&; E. Anet, *Advances in Carbohydrate Chemistry* **1964**, *19*, 181-218.
- [40] E. F. L. Anet, *Australian Journal of Chemistry* **1965**, *18*, 240-&.
- [41] G. Fodor, J. P. Sachetto, *Tetrahedron Letters* **1968**, 401-&.
- [42] M. S. Feather, J. F. Harris, *Carbohydrate Research* **1970**, *15*, 304-&.
- [43] D. W. Harris, M. S. Feather, *Journal of Organic Chemistry* **1974**, *39*, 724-725.
- [44] C. P. Locas, V. A. Yaylayan, *Journal of Agricultural and Food Chemistry* **2008**, *56*, 6717-6723.
- [45] Y. D. Chu, K. A. Berglund, *Starch-Starke* **1990**, *42*, 112-117.
- [46] Y. Roman-Leshkov, J. N. Chheda, J. A. Dumesic, *Science* **2006**, *312*, 1933-1937; B. F. M. Kuster, H. S. Vanderbaan, *Carbohydrate Research* **1977**, *54*, 165-176; P. Vinke, H. van Bekkum, *Starch-Starke* **1992**, *44*, 90-96.
- [47] N. Baccile, G. Laurent, F. Babonneau, F. Fayon, M. M. Titirici, M. Antonietti, *Journal of Physical Chemistry C* **2009**, *113*, 9644-9654.
- [48] P. Dais, A. S. Perlin, *Carbohydrate Research* **1987**, *169*, 159-169.
- [49] S. J. Angyal, J. C. Christofides, *Journal of the Chemical Society-Perkin Transactions 2* **1996**, 1485-1491.
- [50] A. S. Amarasekara, L. D. Williams, C. C. Ebede, *Carbohydrate Research* **2008**, *343*, 3021-3024.

II OUTLINE OF THE WORK

The literature on HMF synthesis is bulky and showed various different approaches for the common target reaction of sugar dehydration. The majority of research efforts went into catalyst screening of commercially available materials under different reaction conditions. However, since there is no common agreement on the conditions of catalyst testing, a detailed comparison of the results is hardly possible. Furthermore the literature is lacking on detailed characterization of the catalytically active materials. Consequently questions on catalyst stability or the structure of the actual active component remain unsolved. Ideas on both aspects would be needed for a more directed synthesis of the catalysts as the basis of improvements in the final HMF yields.

The highly diverse literature basis can be seen as the natural response on the complexity of the reaction. Since the dehydration of sugars implies a broad reaction network, the elucidation of the reaction mechanism, in particular the function of the heterogeneous catalyst is by no means trivial. The intention of this work is to provide a tiny but solid stepping stone on the long way of mechanistic understanding of HMF synthesis on heterogeneous catalysts. Under this aspect one class of heterogeneous catalysts, i. e. carbon based catalysts, has been studied in depth in the dehydration of glucose and fructose into HMF. In a first process, suitable reaction conditions and catalytic testing modes have been elaborated, in order to compare performance and stability of the different carbon material. Subsequently, the effect of the carbon

structure and the influence of the functionalization method on stability and performance have been investigated. The stability of the catalyst was tested in terms of resistance of the functional groups against applied reaction conditions, site blocking of the active component by humin accumulation and structural changes of the catalyst by solvent or heat treatment. The latter was further investigated by in-situ XPS experiments.

III HETEROGENEOUS CATALYSTS IN THE DEHYDRATION OF FRUCTOSE TO HMF

Authors: Sylvia Reiche, Edward Kunkes, Nuruzatulifah Bt. Asari Mansor, Xiao Chen Zhao, Koteswara Rao Vuyyuru, Alberto Villa, Jean-Philippe Tessonnier, Dangsheng Su, Malte Behrens, Peter Strasser, Robert Schlögl

Abstract

Several heterogeneous catalysts have been reported in the dehydration of fructose to 5-hydroxymethyl furfural (HMF). Despite the obvious arguments for the preferential use of heterogeneous catalyst, their performance is lower than for the further optimized homogeneous system. In addition, the direct comparison of literature results is hindered by the huge variety of reaction conditions applied. We tested multiple promising heterogeneous catalyst in a work-up-friendly one-phase system in 2-butanol and compared performance as well as recyclability.

III.1 Introduction

The discovery of 5-hydroxymethyl furfural (HMF) and first mechanistic ideas were reported more than 100 years ago^[1]. Still, an inexpensive and sustainable production route from biomass derived feedstocks remains a challenge to current research. Even though, the awareness of future feedstock changes in the chemical industry and HMF being a key molecule^[2] in the pool of biomass derived building blocks lead to an exponential increase in research interest. Recently published reviews^[3, 4] summarized the most critical points in HMF synthesis by deficient mechanistic understanding of the complex reaction network, the low reactivity of glucose in comparison to the less abundant isomer fructose and the lack of efficient separation methods, due to the unfavorably high hydrophilicity of HMF^[3]. Groundbreaking progress was achieved in the optimization of homogeneously catalyzed fructose dehydration in the development of efficient biphasic systems^[5, 6]. The addition of phase modifiers, such as inorganic salts, typically NaCl^[6], or polar aprotic solvents, such as dimethyl sulfoxid (DMSO) or 1-methyl-2-pyrrolidinone (NMP), and/or the hydrophilic polymer poly(1-vinyl-2-pyrrolidinone) (PVP) into the aqueous phase and 2-butanol to the organic phase further enhanced the HMF yield^[5]. However, with every additive used the purification of HMF is hampered. Hence, practicable solutions for the complete elimination of impurities in the product stream are still outstanding.

More efficient would be the direct use of heterogeneous catalysts. Also here, intensive research efforts have been reported in the literature^[7-9]. The type of heterogeneous catalysts applied ranged from oxides^[10, 11], over polymer resin down^[9, 12-14] to sulfonated carbon materials^[15, 16]. However a direct comparison of the data is difficult due to the variety of different reaction conditions applied.

For this reason, we retested acidic heterogeneous catalysts that gave promising results in the literature, among them, the zeolites H-mordenite and H-ZSM5, as well as other oxidic materials, such as niobium oxide and sulfated zirconia. Furthermore, niobium phosphate and vanadyl pyrophosphate were tested, as well as the ion exchange resins Amberlyst® 15 and Nafion®. Finally the study involves carbon catalysts based on functionalized multi-walled carbon nanotubes (MWCNTs)^[17], amorphous carbon from glucose pyrolysis (AGP)^[18] and ordered mesoporous carbon (OMC) based on polymeric precursors^[19]. The catalyst screening was performed, in order to achieve comparable data as the basis for further studies in the direction of a better understanding of the active surface, structural requirements of the materials and ideally the final implementation of the findings into improvements of the catalyst synthesis. By systematic re-run (= recycling), it was checked for often neglected irreversible catalyst modifications.

III.2 Results

For the present study, we moved from an aqueous system into a one-phase system in 2-butanol. This has the advantage that part of possible side reactions, e. g. the re-addition of water to HMF under the formation of levulinic acid and formic acid, are suppressed. Furthermore, the final extraction of the product is not necessary and impurities due to phase modifiers can be avoided. The advantages mentioned prevail the lower solubility of fructose in 2-butanol and the use of lower concentrated feed solutions.

The fructose dehydration experiments were performed in a batch reactor at 130°C. For a typical experiment, 2.5 g fructose were added to 100 ml 2-butanol

and 250 mg catalyst. The results are summarized in **Table 1**. Comparing the MWCNT-based catalysts (**Figure 1**), we could observe the highest activity for the Baytubes ® functionalized in sulfuric acid (BTs) with 28% yield of HMF after 3 h reaction time. The catalysts obtained by the functionalization with boronic acid (BTb), as well as the gas phase functionalized carbon nanotubes (BTsG200, BTsG600) did not exhibit high dehydration activities. In the recycling run, i. e. the reuse of the material in a second experiment, the HMF yield using BTs decreased to 4%. Hence the material deactivated strongly already after one reaction run.

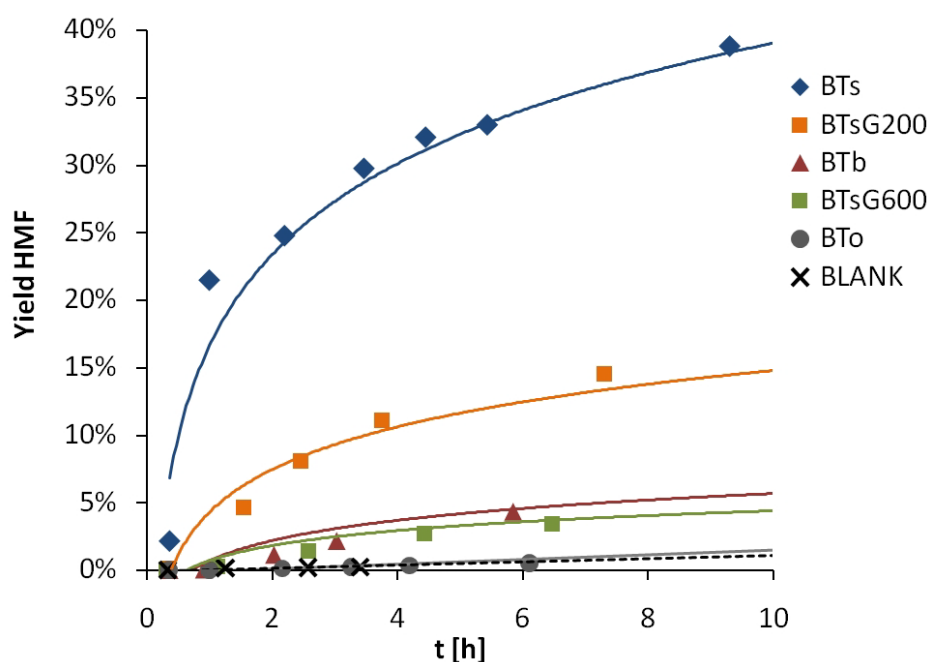


Figure 1: Catalytic performance of differently functionalized Baytube catalysts in the dehydration of fructose into HMF (130°C, one phase system 2-butanol). At t = 0.33 h the reaction temperature of 130°C is reached

Heterogeneous Catalysts in the Dehydration of Fructose to HMF

Table 1: Overview of catalytic performance of tested materials and comparison to literature references

Catalyst	BET surface area [m ² /g]	Yield HMF [%] (Recycling Run)	r_0^* $\left[\frac{\mu\text{mol HMF}}{2\text{h}\cdot\text{m}^2} \right]$	Reference HMF Yield [%] / conditions
BT ₀	227	0	0	-
BTs	245	28 (4)	56.1	
BTsG200	258	8	17.4	
BTsG600	265	2	2.9	
BTb	253	2	2.5	
AGPs	nonporous	50; 37 ^a (5 ^a)	-	-
OMCs	683	17	7.8	-
MC_TDP	654	61 (17)	51.5	
MC_H ₂ O ₂	596	59 (34)	55.7	
Nafion®	flexible structure, swellable in liquid phase	36 (28)	-	^[9] 94 / 0.3 g F, 10 g DMSO, 0.02 g cat., 120°C, 2 h
Amberlyst® 15		50	-	^[9] 92 / 0.3 g F, 10 g DMSO, 0.02 g cat., 120°C, 2 h ^[13] 87 /
Sulfated zirconia	424	11	12.6	^[9] 92 / 0.3 g F, 10 g DMSO, 0.02 g catalyst, 120°C, 2 h ^[20] 68 / 0.045 g F, 1 ml DMSO, 0.018 g cat, 130°C, 4 h
H-mordenite	387	4	5.7	^[10, 11] 69 / 1-7 g F, 0.5-2 g cat., 35 ml H ₂ O, 175 ml MIBK, 10 bar N ₂ , 165°C, 60 min
H-ZSM5	418	27 ^b ; 14 ^c	8.6	^[10] 53 / 1-7 g F, 0.5-2 g cat., 35 ml H ₂ O, 175 ml MIBK, 10 bar N ₂ , 165°C, 60 min
Nb ₂ O ₅	n. d.	1	-	^[21] 29 / 10 wt% F in H ₂ O, 0.7-1.7 g, 100°C, 30 min
NbOPO ₄	141	24 (6)	89.0	^[22] 23 / 6 wt% F in H ₂ O, 0.7 g, 100 °C
(VO) ₂ P ₂ O ₇	10.8	6	239.6	^[23] 42 / H ₂ O, 50°C, 1 h

All catalytic tests were performed in a one-phase system of 2-butanol at 130°C. The yields (calculated per mol initial fructose) refer to the amount of HMF formed after t = 3 h.

r_0^* specific apparent initial rate

^a HMF yield for the preconditioned catalyst (catalyst was pretreated 4 times in 2-butanol at 130°C for 15 h each)

^b 500 mg catalyst

^c 1 g catalyst

F fructose

The further tested mesoporous materials AGPs, MC_TDP and MC_H₂O₂ exhibit even higher HMF yields, up to 61% for MC_TDP, in the first reaction run. However, also here the catalysts could not preserve their activity in the recycling run. Comparing the specific apparent initial rate of the graphitic Baytube-catalyst BTs with the amorphous, mesoporous material MC_H₂O₂, we can conclude similar activities of both materials when normalizing to the surface area. However, the BET isotherms show the significant differences in the pore structures of the two materials. The direct comparison according the surface area, neglects the influence of the pore structure on the catalytic performance, as well possible changes in the surface area due to different swelling behavior of material during the reaction.

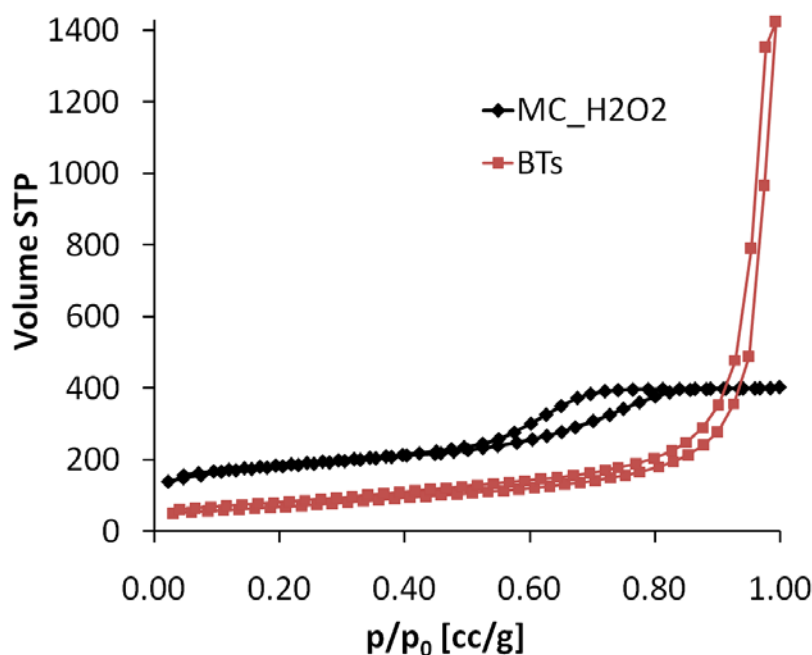


Figure 2: Comparison of BET isotherms of BTs and MC_H₂O₂. From the graph it can be concluded that the MC_H₂O₂ catalyst has the higher amount of mesopores, as well as micropores.

The activity losses in case of the ion exchange resins are less pronounced comparing the first run and the recycling run. In case of Nafion® the HMF yield decreases from 36% to 28% ($t = 3$ h). In comparison to the carbon catalysts that are naturally black, the ion exchange resins change their color and appearance upon catalytic testing (**Figure 4**). Considering the dramatic impact of the reaction conditions on the nafion beads, the long-term stability of the material is questionable.

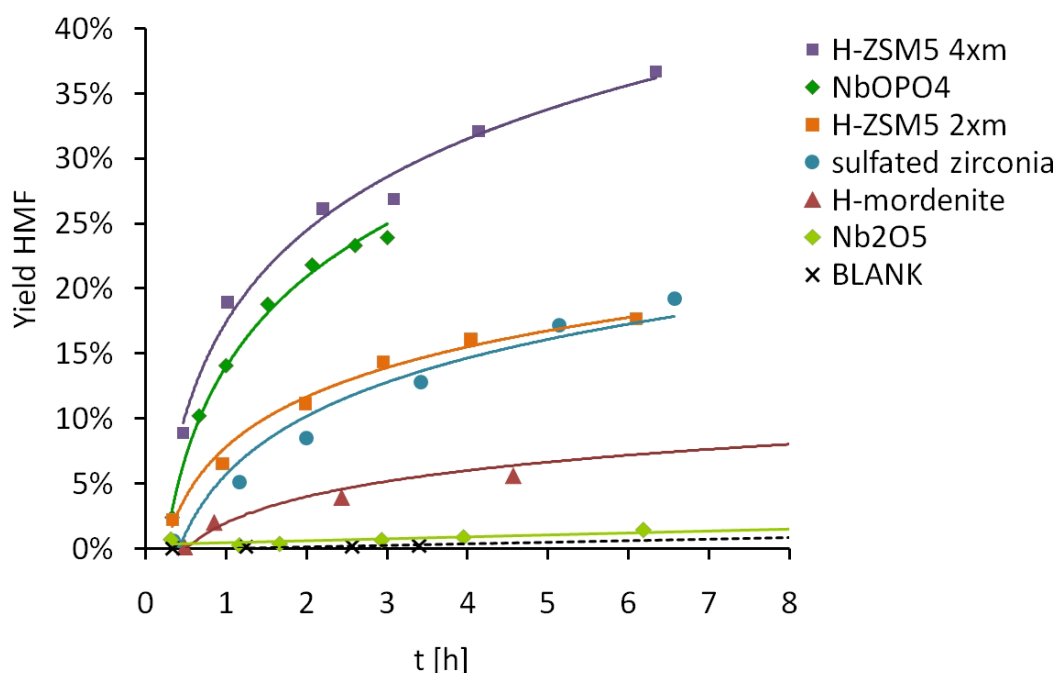


Figure 3: Comparison of different oxidic materials in the dehydration of fructose to HMF. For the H-ZSM5 catalyst 500 mg (=2xm) and 1 g (=4xm) were used. For all other materials 250 mg were tested. At $t = 0.33$ h the reaction temperature of 130°C is reached.

For the white oxidic catalysts similar darkening of the material can be observed (**Figure 4**). The color change is associated with the often reported formation of insoluble humins^[8, 24], side products of the fructose dehydration that can be accumulated onto the catalysts surface during the reaction. Comparing the catalytic activity of the different oxide based catalysts

(**Figure 3**), the niobium phosphate catalyst provided the highest HMF yields per mass catalyst. By increasing the mass of H-ZSM5 to 1 g, the HMF yield could also be pushed to 27% ($t = 3$ h). However, the elevated HMF formation is combined with more pronounced humin accumulation, as observable in the brownish color of the material (**Figure 4**).

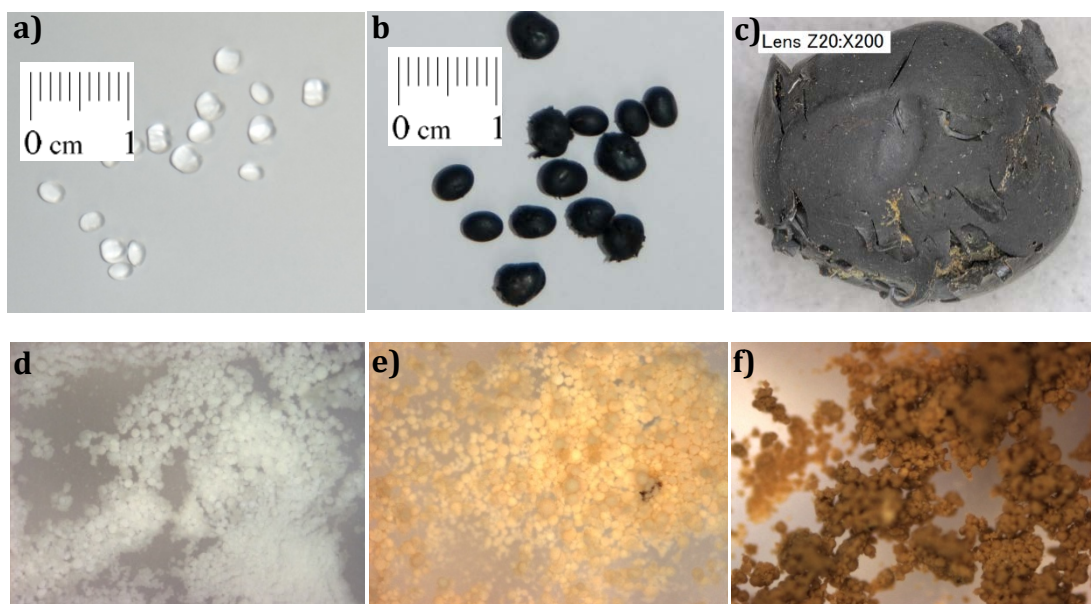


Figure 4: Characteristic color changes of the catalysts after the fructose dehydration reaction. a) Nafion before reaction (photography), b) Nafion beads after reaction (photography), c) one Nafion bead at magnification of 200x (optical microscope), d) H-ZSM5 before reaction, e) H-ZSM5 2xm after reaction, f) H-ZSM5 4xm after reaction (d-f: optical microscope, magnification 50x)

III.3 Discussion

In summary, the tested heterogeneous catalysts showed either low performance from the very beginning or did not maintain their catalytic activity in the recycling run. Comparing our findings to the results in the literature

(**Table 1**), we can conclude that in principal higher HMF yields are possible using the same heterogeneous catalysts. However, in most cases reported in the literature, the use of heterogeneous catalysts is combined with solvents of intrinsic catalytic activity such as DMSO^[9] or ionic liquid additives^[25]. Another possibility to enhance the HMF yields is the parallel extraction using a 2-phase system of water with methyl isobutyl ketone (MIBK)^[10, 11]. The latter can be seen as an elegant option for the longterm use of heterogeneous catalysts. However, the method would not be compatible with catalysts of a highly hydrophobic surface, such as carbon based catalysts, because of their preferential abundance in the organic phase. Hence, the use of an organic extraction solvent would not only hinder the contact between the catalyst and the initial product, the extended impact of the catalyst on the HMF product, could even provoke side reactions. Furthermore, the use of an additional extracting solvent, in general, is accompanied by the same technical difficulties as described for the homogeneously catalyzed reactions.

The other critical point is the recycling of the material. Often only the first-run-performance is reported leaving questions on the catalyst stability open to the reader. Recently, the first review which includes the comparison of recyclability of the materials was published by Rosatella et al.^[3]. Only for 18 out of 100 entries on the use of heterogeneous catalysts in the production of HMF, data on the recyclability could be found. Most commonly the recycling capability is reported for ion exchange resins, where our results also point to relatively good recyclability. However, special attention is required when comparing the reaction times and the fructose to resin ratio. If the material was reused 5 times after a reaction time of 5-20 min per run and a fructose to resin ratio of one or smaller, it is hard to predict the longterm stability of the material^[14].

Another option of possible recycling of oxidic catalysts was reported by Yan et al.^[20] for sulfated zirconia catalysts. They demonstrated the successive

deactivation of the material over four dehydration runs in DMSO. However, by calcination of the catalyst at 550°C for 2 h after each dehydration run, the catalytic activity could be partially recovered. The most significant loss in activity was observed in the first recycling (about one quarter lower HMF yield). In subsequent reaction runs the activity was preserved by calcination.

Based on the catalytic data presented and the critical comparison of the same to the literature, it can be concluded that deeper studies of the catalyst stability are essential, in order to excel established homogeneous solutions and to guarantee a long-term application. So far, little is known on possible structural changes of the catalyst in the course of the fructose dehydration reaction. Hence, only post-treatments can be applied for the reactivation of the catalyst, such as calcination^[20], extractive washings by different solvents^[21, 26] or recovery of surface functional group by re-treatments in diluted mineral acids^[27]. Consequently, it is the future aim of our research to further elucidate possible deactivation mechanisms, in order to comprise structural requirements on the heterogeneous catalyst.

The promising results on carbon based catalysts in first dehydration experiments, strongly suggest the further exploration of the same. The hydrothermal stability and structural diversity of carbon catalysts provide a prospective basis, widely applied in other biomass relevant reactions, such as esterification^[18] or cellulose hydrolysis^[16, 28].

III.4 Experimental Section

I.4.1 Materials

Baytubes®(BT) were purchased from Bayer® and functionalized in concentrated sulfuric acid (97% Merck, 500 ml for 10 g BT) or nitric acid (65% Merck, 500 ml for 10 g BT) at 100°C for 20 h. Subsequently, the material was filtered, intensively washed by water until the pH of the washing solution was neutral. The material was redispersed in water and stirred over night, in order to completely desorb remaining acid. Finally the resulting sulfuric acid treated Baytubes® (BTs) or nitric acid treated Baytubes® (BTn) were dried at 100°C for 10 h. For the preparation of boronic acid functionalized Baytubes (BTb), 10 g of BTn were impregnated with 0.75 M H_3BO_3 by incipient wetness impregnation. Subsequently, the material was heat treated in Ar at 1500°C for 4h.

For the preparation of the gas phase functionalized sulfonated Baytubes, 3 g BTn were treated in oleum saturated argon atmosphere at 200°C (BTsG200) or 600°C (BTsG600) for 20 h. In order to guarantee an optimal mixing during the functionalization process, a horizontal rocking furnace was used, providing an agitated sample bed^[29]. The oleum saturation was achieved by leading the Ar carrier gas through 50 ml oleum solution (20% fuming oleum in concentrated sulfuric acid).

Sulfonated amorphous carbon material was prepared as reported by Hara et al.^[18]. The functionalization of the amorphous carbon obtained by glucose pyrolysis (AGP), was performed as described for BTs. The resulting material is sulfonated amorphous carbon from glucose pyrolysis (AGPs).

For the catalysts based on ordered mesoporous carbon (OMC), 5.5 g of resorcinol and 5.0 g of formaldehyde solution (37 wt%) undergo an acid catalyzed polymerization in 50 ml of a water-ethanol-mixture (1:1 by weight). The obtained polymer is carbonized in N₂ atmosphere at 350°C and 600°C for 2h, respectively. The detailed procedure of OMC synthesis is described elsewhere^[19]. Subsequently, 2 g OMC are stirred in 100 ml H₂SO₄ (97%) at 100°C for 20 h, resulting in sulfuric acid treated OMC, denoted as OMCs. To prepare TDP-donated S-containing mesoporous carbon, 20 mol% of resorcinol is replaced by 4,4'-thiodiphenol (TDP). After the carbonization at 350 and 600°C, the TDP containing mesoporous carbon is oxidized by H₂O₂ in a mixture of methanol and 2 M HCl (1:1, V:V) to obtain MC-TDP^[19].

The ion exchange resins Amberlyst® 15 and Nafion® NR50 were purchased from Sigma Aldrich. Additional commercial catalysts were sulfated zirconia (MEL Chemicals), H-mordenite (Südchemie), H-ZSM5 (Degussa), niobium oxide (Roth) and niobium phosphate (CBMM). The vanadyl pyrophosphate material was produced by Ecole Polytechnique Montréal.

I.4.2 Catalyst Performance Tests

The catalytic tests were performed in a one-phase system in 2-butanol. For a typical experiment 2.5 g fructose were loaded together with 100 ml 2-butanol. If not stated differently 250 mg catalyst were added and the system was heated under stirring (450 rpm) to 130°C. All reactions were performed in a 200 ml Parr® autoclave using a teflon liner and a teflon-coated stirrer.

III.5 References

- [1] J. Kiermayer, *Chem. Zeit.* **1895**, 19, 1003-1005; J. U. Nef, *Justus Liebigs Annalen Der Chemie* **1910**, 376, 1-119.
- [2] H. Schiweck, M. Munir, K. M. Rapp, B. Schneider, M. Vogel, *Zuckerindustrie* **1990**, 115, 555-565.
- [3] A. A. Rosatella, S. P. Simeonov, R. F. M. Frade, C. A. M. Afonso, *Green Chemistry* **2011**, 13, 754-793.
- [4] M. J. Climent, A. Corma, S. Iborra, *Green Chemistry* **2011**, 13, 520-540; X. L. Tong, Y. Ma, Y. D. Li, *Applied Catalysis a-General* **2010**, 385, 1-13; K. D. Vigier, F. Jerome, in *Carbohydrates in Sustainable Development II: a Mine for Functional Molecules and Materials, Vol. 295*, **2010**, pp. 63-92.
- [5] Y. Roman-Leshkov, J. N. Chheda, J. A. Dumesic, *Science* **2006**, 312, 1933-1937; J. N. Chheda, Y. Roman-Leshkov, J. A. Dumesic, *Green Chemistry* **2007**, 9, 342-350.
- [6] Y. Roman-Leshkov, C. J. Barrett, Z. Y. Liu, J. A. Dumesic, *Nature* **2007**, 447, 982-U985.
- [7] L. Cottier, G. Descotes, *Trends Heterocycl. Chem.* **1991**, 2, 233-248.
- [8] B. F. M. Kuster, *Starch-Starke* **1990**, 42, 314-321.
- [9] K. Shimizu, R. Uozumi, A. Satsuma, *Catalysis Communications* **2009**, 10, 1849-1853.
- [10] P. Rivalier, J. Duhamet, C. Moreau, R. Durand, *Catalysis Today* **1995**, 24, 165-171.
- [11] C. Moreau, R. Durand, S. Razigade, J. Duhamet, P. Faugeras, P. Rivalier, P. Ros, G. Avignon, *Applied Catalysis a-General* **1996**, 145, 211-224.
- [12] Y. Nakamura, S. Morikawa, *Bulletin of the Chemical Society of Japan* **1980**, 53, 3705-3706; J. N. Chheda, J. A. Dumesic, *Catalysis Today* **2007**, 123, 59-70.
- [13] C. Lansalot-Matras, C. Moreau, *Catalysis Communications* **2003**, 4, 517-520.
- [14] X. Qi, M. Watanabe, T. M. Aida, R. L. Smith, Jr., *Green Chemistry* **2008**, 10, 799-805; X. H. Qi, M. Watanabe, T. M. Aida, R. L. Smith, *Industrial & Engineering Chemistry Research* **2008**, 47, 9234-9239.
- [15] S. Suganuma, K. Nakajima, M. Kitano, D. Yamaguchi, H. Kato, S. Hayashi, M. Hara, *Solid State Sciences* **2010**, 12, 1029-1034.

- [16] S. Suganuma, K. Nakajima, M. Kitano, D. Yamaguchi, H. Kato, S. Hayashi, M. Hara, *Journal of the American Chemical Society* **2008**, *130*, 12787-12793.
- [17] J. P. Tessonnier, D. Rosenthal, T. W. Hansen, C. Hess, M. E. Schuster, R. Blume, F. Girgsdies, N. Pfander, O. Timpe, D. S. Su, R. Schlögl, *Carbon* **2009**, *47*, 1779-1798.
- [18] A. Takagaki, M. Toda, M. Okamura, J. N. Kondo, S. Hayashi, K. Domen, M. Hara, *Catalysis Today* **2006**, *116*, 157-161.
- [19] X. C. Zhao, A. Q. Wang, J. W. Yan, G. Q. Sun, L. X. Sun, T. Zhang, *Chemistry of Materials* **2010**, *22*, 5463-5473.
- [20] H. P. Yan, Y. Yang, D. M. Tong, X. Xiang, C. W. Hu, *Catalysis Communications* **2009**, *10*, 1558-1563.
- [21] C. Carlini, M. Giuttari, A. M. R. Galletti, G. Sbrana, T. Armaroli, G. Busca, *Applied Catalysis a-General* **1999**, *183*, 295-302.
- [22] T. Armaroli, G. Busca, C. Carlini, M. Giuttari, A. M. R. Galletti, G. Sbrana, *Journal of Molecular Catalysis a-Chemical* **2000**, *151*, 233-243.
- [23] C. Carlini, P. Patrono, A. M. R. Galletti, G. Sbrana, *Applied Catalysis a-General* **2004**, *275*, 111-118.
- [24] J. Horvat, B. Klaic, B. Metelko, V. Sunjic, *Croatica Chemica Acta* **1986**, *59*, 429-438; J. Horvat, B. Klaic, B. Metelko, V. Sunjic, *Tetrahedron Letters* **1985**, *26*, 2111-2114; S. K. R. Patil, C. R. F. Lund, *Energy Fuels* **2011**, *25*, 4745-4755.
- [25] X. H. Qi, M. Watanabe, T. M. Aida, R. L. Smith, *Green Chemistry* **2009**, *11*, 1327-1331.
- [26] A. Takagaki, M. Ohara, S. Nishimura, K. Ebitani, *Chemical Communications* **2009**, 6276-6278.
- [27] F. S. Asghari, H. Yoshida, *Carbohydrate Research* **2006**, *341*, 2379-2387.
- [28] A. Onda, T. Ochi, K. Yanagisawa, *Topics in Catalysis* **2009**, *52*, 801-807.
- [29] N. Giliard, Technische Universität Berlin (Berlin), **2011**.

IV DEACTIVATION PATHWAYS OF CARBON CATALYSTS FOR FRUCTOSE DEHYDRATION

Authors: Sylvia Reiche, Xiao Chen Zhao, Matthew Aronson, Klaus Friedel, Edward Kunkes, Jean-Philippe Tessonnier, Dangsheng Su, Malte Behrens, Sharifah Bee Abdul Hamid, Robert Schlögl

Abstract

A variety of acid functionalized carbon based catalysts has been synthesized and tested for the dehydration of fructose to 5-hydroxymethyl furfural (HMF). The stability of the materials has been studied under three different aspects: Firstly, the stability of the acid functional groups was evaluated in leaching tests. Secondly, the influence of surface poisoning was determined by comparing the catalytic performance in the dehydration of fructose to the esterification of acetic acid in ethanol. The latter was used as reference reaction, due to the milder reaction conditions and the obviation of humin formation. Thirdly, we tested for the influence of the reaction solvent by preconditioning the catalyst prior to the actual reaction.

IV.1 Introduction

As extensively reported in previous chapters, several crucial steps in the upgrading of biomass-derived raw materials involve acid catalyzed reactions. The use of homogeneous acids involves the contamination of the product with the corrosive catalyst, as well as the introduction of other impurities, such as chlorine or sulfur containing compounds from counter ions of mineral acids. Hence, thorough product separation is required to avoid on the one hand consecutive side reactions, and to eliminate potential catalyst poisons for further processing steps. The required product separation is challenging and cost intensive. In the case of sugar dehydration to HMF, more advanced biphasic processes yielded promising results^[1, 2]. However, also here product separation is limited by partition coefficients between the reaction solvent water and the extraction solvent, e. g. 2-butanol or methyl isobutylketon (MIBK). Therefore, such a process would involve a solvent recovery and purification system, if implemented on a large scale. Thus heterogeneous catalysts are desired in large scale industrial processes. The application of heterogeneous catalysts is limited by several challenges concerning the conversion of highly functionalized feedstocks. All the more, a deeper understanding of heterogeneous catalysts, their relevant properties for this highly complex reaction systems, catalyst stability and causes of deactivation are essential for the development of sustainable processes.

Deactivation Pathways of Carbon Catalysts for Fructose Dehydration

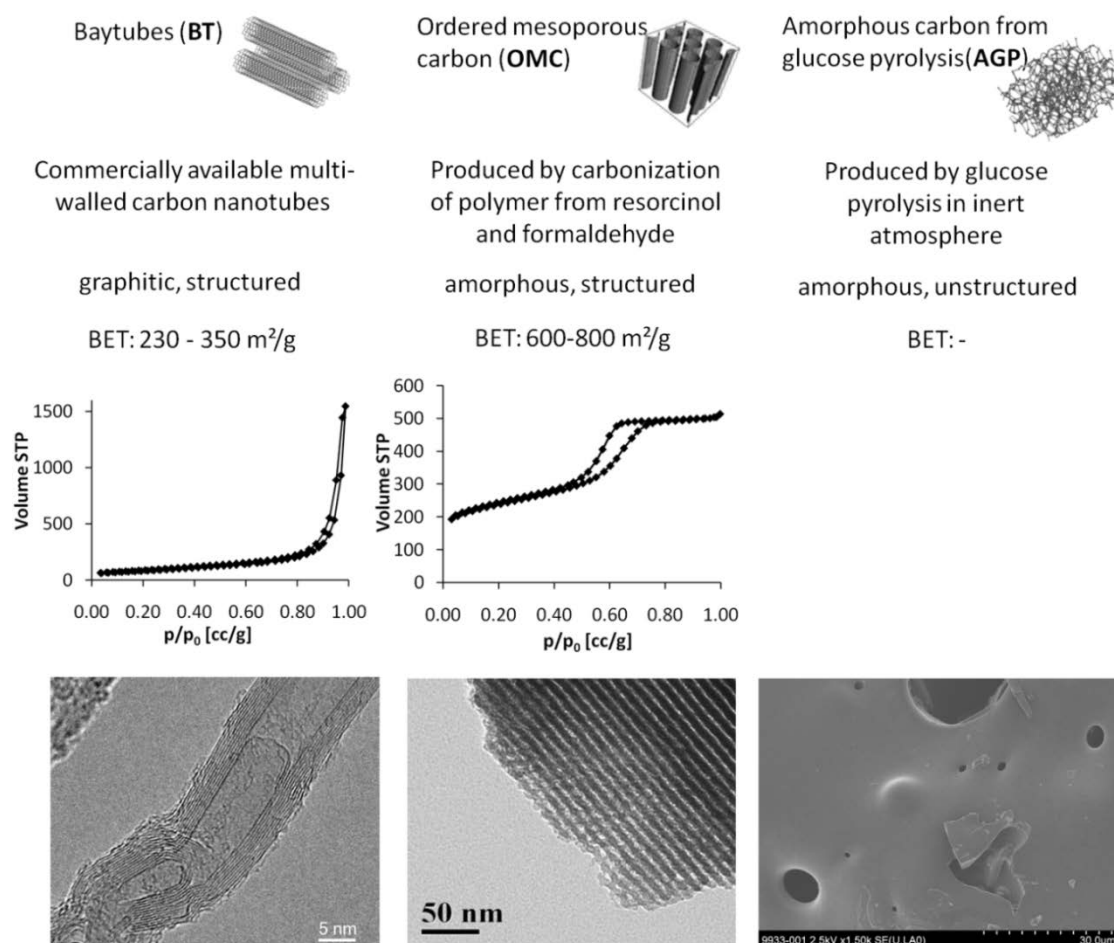


Figure 1: Overview of carbon material basis

The focus of this study is on carbon based heterogeneous catalysts. Carbon catalysts themselves can be produced from biomass feedstocks on a sustainable basis^[3, 4]. Furthermore, carbonized structures are hydrothermally stable, which is critical for water based processes and a major advantage in comparison to the more commonly used metal oxide based catalysts. In addition, carbon provides a broad structural diversity. Bulky solvated biomolecules need wide pores for preferential mass transport^[5]. One suitable concept of carbon structures was suggested by Lefferts and Schouten^[6, 7] who described carbon nanofibers (CNF)

as an inverse of the conventional porous catalyst. Large surfaces provided by the outside surface of tubular CNFs, which is more easily accessible than long narrow pores. Another concept for suitable carbon structures can be found in mesoporous carbon. By altering the choice of the template the pore size can be adjusted according to the requirements from the reaction network. Within this work, both, carbon nanotubes (CNTs) as well as ordered mesoporous carbon (OMC) catalysts were applied. Finally, an unstructured amorphous carbon from glucose pyrolysis (AGP) completes the carbon basis of the catalysts tested in this chapter. A summary of major properties of the pristine carbon materials is given in **Figure 1**.

Carbon catalysts offer a huge variety of functionalization possibilities^[8, 9]. They can be acidified by treatments in concentrated acid, as applied in this work. They can also be used as a catalyst support; for instance for metal nanoparticles allowing for the synthesis of multifunctional catalysts. By chemical grafting it is possible to immobilize functional groups more selectively on the carbon structures. In the case of graphitic structures, such as CNTs, a selective backbone functionalization is only possible if relatively harsh conditions are applied. Examples are fluorination treatments followed by substitution reactions or diazotizations. The latter technique was also applied here.

The acidified carbon catalysts were tested for glucose and fructose dehydration reactions in water as well as in 2-butanol. The esterification of acetic acid in ethanol was used as a reference reaction. Both reactions, the fructose dehydration in 2-butanol and the esterification of acetic acid, are acid catalyzed and form water as byproduct. Additionally both reactions use an alcoholic solvent; in case of the esterification the ethanol is solvent and reactant at the same time. Based on these commonalities (**Figure 2**) the esterification is considered to be a suitable reference reaction. The main difference between the

Deactivation Pathways of Carbon Catalysts for Fructose Dehydration

esterification and the fructose dehydration is given by the reactivity of the initial product. Since carbohydrates carry multiple functional groups, they can react in acidic aqueous media under the formation of various side products in a complex reaction network^[10, 11]. As side product formation can be excluded for the esterification reaction, the stability of the acid functional groups and the catalyst against heat (80°C), the alcoholic solvent and the water formed in the course of the reaction, can be determined.

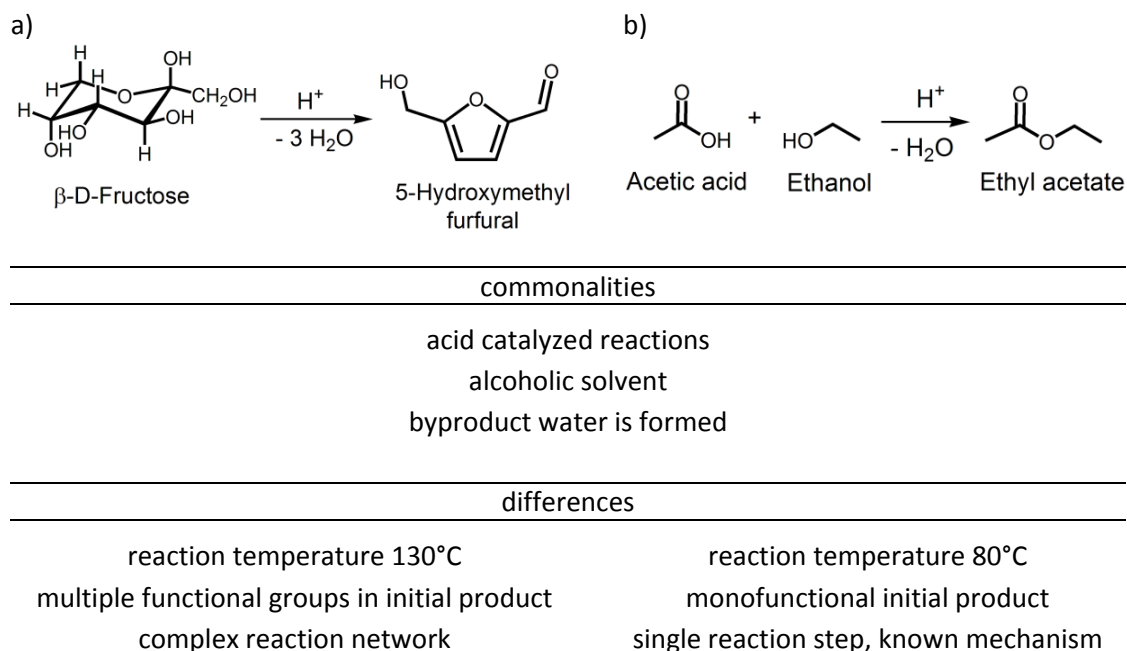


Figure 2: Comparison of the dehydration of fructose (a) and the reference reaction, the esterification of acetic acid in ethanol (b)

IV.2 Experimental

IV.2.1 Catalyst Preparation

Baytubes®(BT) were purchased from Bayer® and functionalized in concentrated sulfuric acid (97% Merck, 500 ml for 10 g BT) or nitric acid (65% Merck, 500 ml for 10 g BT) at 100°C for 20 h. Subsequently, the material was filtered, intensively washed by water until the pH of the washing solution was neutral. The material was redispersed in water and stirred over night, in order to completely desorb remaining acid. Finally the resulting sulfuric acid treated Baytubes® (BTs) or nitric acid treated Baytubes® (BTn) were dried at 100°C for 10 h. For the preparation of boronic acid functionalized Baytubes (BTb), 10 g of BTn were impregnated with 0.75 M B(OH)₃ by incipient wetness impregnation. Subsequently, the material was heat treated in Ar at 1500°C for 4h.

Highly graphitized carbon nanofibers (CNF) were purchased from Applied Sciences, Inc. (ASI, material PR24XT-HHT). For the grafting of benzene sulfonic acid onto the CNF-surface a diazotization was applied, similar to the one reported by Dyke et al.^[12]. Therein, 2.50 g PR24XT-HHT (0.21 mol) were stirred together with 1.80 g sulfanilic acid (10.4 mmol) in a 1 l three necked round bottom flask. Subsequently, 300 mL of 1,2-dichlorobenzene were added and the mixture was sonicated for 20 min in order to disperse the solids in the organic solution. The suspension was heated to 60 °C while vigorously stirred at 400 rpm. Subsequently, 2.80 mL of isoamyl nitrite (20.8 mmol) were added slowly via a dropping funnel into the flask and the mixture was further stirred at 60 °C for 16 h. After cooling to 45°C, 300 ml dimethylformamide were added and the suspension was sonicated for 10 min. The solid was filtered off and washed

thorough by DMF and dichloromethane. In order to remove unreacted, low soluble sulfanilic acid, the sample was stirred 2-time in 300 mL NaOH (1 M) for 30 minutes while being heated to 60 °C at 400 rpm. For neutralization, the sample was stirred in 500 mL 1 M HCl solution over night. Finally the material was filtered, washed with deionized water until the filtrate showed neutral pH and dried at 110 °C to obtain benzene sulfonic acid grafted CNF (BS-CNF).

Sulfonated amorphous carbon material was prepared as reported by Hara et al.^[3]. The functionalization of the amorphous carbon obtained by glucose pyrolysis (AGP), was performed as described for BTs. The resulting material is sulfonated amorphous carbon from glucose pyrolysis (AGPs).

For the catalysts based on ordered mesoporous carbon (OMC), 5.5 g of resorcinol and 5.0 g of formaldehyde solution (37 wt%) undergo an acid catalyzed polymerization in 50 ml of a water-ethanol-mixture (1:1 by weight). The obtained polymer is carbonized in N₂ atmosphere at 350°C and 600°C for 2h, respectively. The detailed procedure of OMC synthesis is described elsewhere^[13]. Subsequently, 2 g OMC are stirred in 100 ml H₂SO₄ (97%) at 100°C for 20 h, resulting in sulfuric acid treated OMC, denoted as OMCs.

To prepare TDP-donated S-containing mesoporous carbon, 20 mol% of resorcinol is replaced by 4,4'-thiodiphenol (TDP). After the carbonization at 350 and 600°C, the TDP containing mesoporous carbon is oxidized by H₂O₂ in a mixture of methanol and 2 M HCl (1:1, V:V) to obtain MC-TDP^[13].

The ion exchange resins Amberlyst® 15 and Nafion® NR50 were purchased from Sigma Aldrich.

An overview of the catalysts tested is given in **Table 1**.

Deactivation Pathways of Carbon Catalysts for Fructose Dehydration

Table 1: Overview of catalysts

Sample	Material description	BET [m ² /g]	Acid sites [mmol/g]
BT ₀	pristine Baytubes® from Bayer	293 ^a , 227 ^b	-
BT _s	Baytubes® functionalized by H ₂ SO ₄	304 ^a , 245 ^b	0.24 ^{a,c} , 0.09 ^{b,c}
BT _n	Baytubes® functionalized by HNO ₃	326 ^a	0.19 ^{a,c}
BT _b	Baytubes® functionalized by B(OH) ₃	253 ^a	
BS-CNF	PR24XT-HHT from Applied Sciences, Inc. (ASI) grafted by benzene sulfonic acid	36.1	
AGP	amorphous carbon from glucose pyrolysis	-	
AGPs	amorphous carbon from glucose pyrolysis functionalized by H ₂ SO ₄	-	1.7 ^{c,d} , 0.42 ^{c,e}
OMC	ordered mesoporous carbon	789	-
OMCs	ordered mesoporous carbon functionalized by H ₂ SO ₄	683	0.45 ^c
MC_TDP	mesoporous carbon, 20mol% of building block recorcinol replaced by thiodiphenyl	654	0.25 ^c
Naf	Nafion® NR50 from Aldrich		
Amb	Amberlyst® 15 from Aldrich		3.7 ^c

^a first batch of Baytubes®, ^b second batch of Baytubes®, ^c density of acid sites determined by titration of the material (100 mg in 50 ml KCl 0.001 M) with 0.01 M NaOH, ^d titration of material as synthesized, ^e titration result of pretreated material (4x 15 h at 130°C in 2-butanol)

IV.2.2 Catalyst Characterization

The BET surface areas were determined by measuring the N₂ adsorption-desorption-isotherms with a Quantachrome Autosorb automatic BET-sorptometer at -196°C with nitrogen as analysis gas.

SEM micrographs were acquired using a Hitachi S-4800 microscope. For the acquisition of TEM micrographs a Philips CM200 LaB6 microscope and a FEI Quanta 200 FEG was used.

The number of acid functional groups was determined by titration using an automatic titrator (Mettler Toledo). For each measurement, 100 mg catalyst

were dispersed in 10^{-3} mol KCl-solution and stirred over night. Following the dispersion was titrated under Ar atmosphere, using a 0.1 M NaOH solution.

IV.2.3 Catalyst Performance Tests

Catalytic test reactions in water were performed in a fully automated reactor system from Cambridge Reactor Design (CRD) with 5 independent 100-ml batch reactors made of hastelloy (**Figure 3a**). In a typical experiment 50 ml of an aqueous solution of 10 wt.% glucose (Sigma Aldrich) were stirred at 450 rpm together with 250 mg catalyst at 40 bar N_2 pressure.

For the catalyst performance tests in 2-butanol a 200-ml Parr autoclave (Series 4560) made of stainless steel using a Teflon liner and a Teflon-coated stirrer was used (**Figure 3b**). Fructose dehydration reactions consisted of 2.5 g fructose (Sigma Aldrich) in 100 ml 2-butanol. The reactions were conducted at 130°C and 7 bar N_2 pressure. Sampling was performed through an integrated sampling tube. All samples were filtered with a $0.2\text{-}\mu\text{m}$ syringe filter and diluted by water (1:50) prior to analysis.

For the analysis of sugars and HMF by liquid chromatography an Agilent 1200 HPLC instrument was used. Fructose and glucose were detected with a refractive index detector (RID), and HMF was detected with a UV-Vis detector (variable wavelength detector, VWD) at 284 nm (absorption maxima HMF^[14]). The column used was a Rezex™ RHM-Monosaccharide from Phenomenex®. The method includes a mobile phase of 0.005 M H_2SO_4 with a flow rate of 0.6 mL/min at 80°C column temperature.

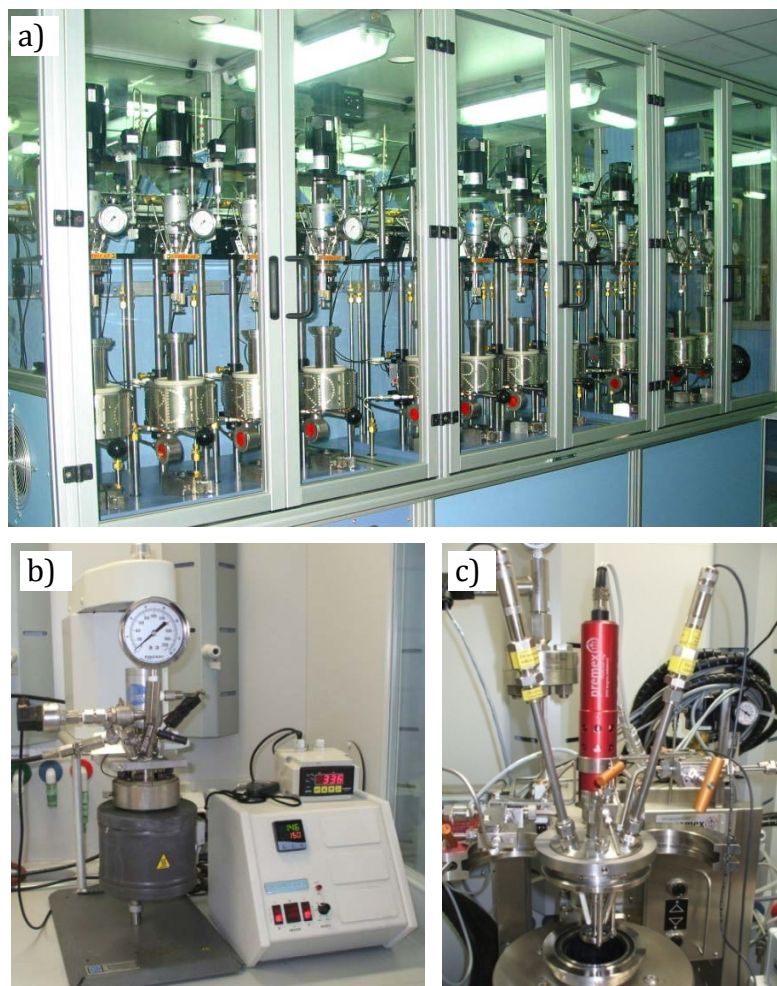


Figure 3: Catalytic testing facilities: a) 12 x 100 ml autoclaves in automated reactor system from CRD, b) 200 ml Parr reactor, c) 300 ml Premex reactor

The esterification reactions were carried out in a 300-ml batch reactor by premex reactor ag® (Figure 3c). Therein, 146 ml ethanol (2.5 mol) and 1.4 ml acetic acid (0.025 mol) were stirred at 800 rpm at 80°C. An integrated sampling tube allowed direct sampling. All samples were analyzed by GC-MS using an Agilent GC (6890 N) coupled to an Agilent 5975B MS detector. For the quantification of ethanol, acetic acid and ethyl acetate a flame ionization detector (FID) was used.

IV.3 Results and Discussion

IV.3.1 Catalyst Testing in the Dehydration of Glucose to HMF

The dehydration of glucose in water was studied in a fully automated reactor system developed for high-throughput screening. Since the single batch reactors did not provide a possibility of sampling during the reaction, we needed first to choose proper reaction conditions for a qualitative comparison of the catalysts. For the determination of an optimal reaction temperature, 5 experiments at 130°C, 150°C, 170°C, 180°C and 190°C were performed in 40 bar N₂ for 2 h. For each experiment, the autoclaves were loaded by 50 ml 10 wt% glucose solution together with 250 mg BTs catalyst. The optimal temperature was determined to be 180°C for the maximum HMF yield after 2 h reaction time (**Figure 4**). For better comparison we combined the quantities of glucose and fructose, as determined by HPLC analysis, in order to plot a total sugar conversion (G & F conversion, G... glucose, F... fructose). At 130 °C no HMF formation could be observed, merely a glucose isomerization into fructose was detected after 2 h reaction time. With further increase in temperature, the activity towards glucose dehydration generally increased. However, for temperatures higher than 180°C the selectivity to HMF drops, most likely due to the prevailing of the formation of secondary products. This is in agreement with studies from the literature that state that the formation of these insoluble humins is favored at high reaction temperatures.

For the choice of a proper reaction time in the batch reactor system, three separate experiments with of 20 min-, 60 min- and 120 min-duration were performed. As shown in **Figure 5** the HMF selectivity is decreasing over time with increasing G&F conversion. As reaction time, we have chosen 2 h for the

following comparison of the differently functionalized carbon nanotube catalysts, since the HMF yield is still in an increasing regime and the conversion of < 70% allows a reasonable comparison of the different catalysts.

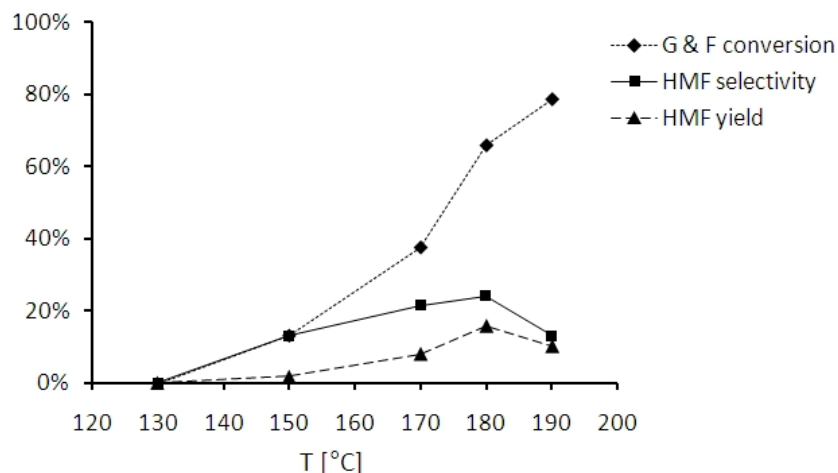


Figure 4: Determination of the optimal reaction temperature for the glucose dehydration in aqueous phase ($t = 120$ min, 40 bar N_2 , 10 wt% glucose solution, 250 mg BTs catalyst). The sugar conversion was summarized in G&F conversion (—◆—), which is calculated based on the sum of glucose and fructose concentrations measured, and plotted together with the HMF selectivity (—■—) and yield (—▲—).

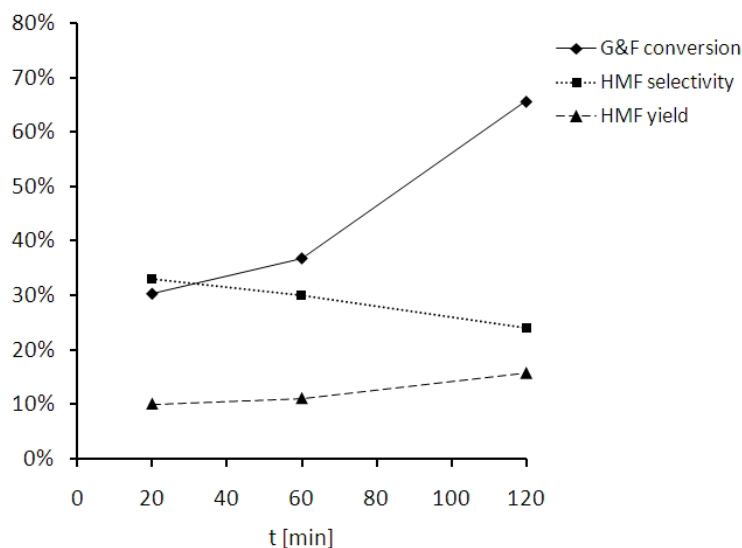


Figure 5: G&F conversion (—◆—), HMF selectivity (····■····), and HMF yield (—▲—) for different reaction times at 40 bar N_2 for 10 wt% glucose solutions in water and 250 mg BTs catalyst

Subsequently, we compared differently functionalized CNT catalysts in the dehydration of a 10 wt% glucose solution in water (**Figure 6**). Bronsted acid functional groups had been incorporated into the carbon surface by nitric acid- (BTn), sulfuric acid- (BTs) and boronic acid- (BTb) treatments. Furthermore iron nanoparticles were deposited by incipient wetness. Iron which is surface oxidized into iron oxide under ambient conditions can react as a Lewis acid. Fig x. depicts the sum of glucose and fructose conversion, as well as the HMF selectivities after 2 h reaction time at 180°C. All materials tested show a higher activity of G&F conversion compared to the BLANK experiment, i. e. a reaction performed under the same conditions without the addition of a heterogeneous catalyst. The greatest difference in sugar conversion and HMF selectivity compared to the blank experiment (45 % conversion, 26 % selectivity) was observed for the CNT catalyst treated in nitrid acid (53 % conversion, 24 % selectivity). The activity generally was measured to be increasing in the order blank < BTn < BTs \approx BTb. Comparing the equally active materials BTs and BTb in terms of selectivity towards HMF, we see a higher HMF selectivity for the sulfuric acid functionalized BTs. One reason for this tendency could be the occurrence of Lewis acid sites for the BTb sample. Lewis acid sites have been reported before to be active in the dehydration of sugars. However, they can catalyze more side reactions, e. g. the formation of humins from the reaction of furfural products with the initial sugars^[15]. Therefore the total furfural yield decreases with the amount of Lewis acid functional groups of heterogeneous catalysts. A similar behavior of higher activity but lower HMF selectivity could be observed for the materials after the deposition of iron. Another observation which agrees with the findings by Weingarten et al. ^[15].

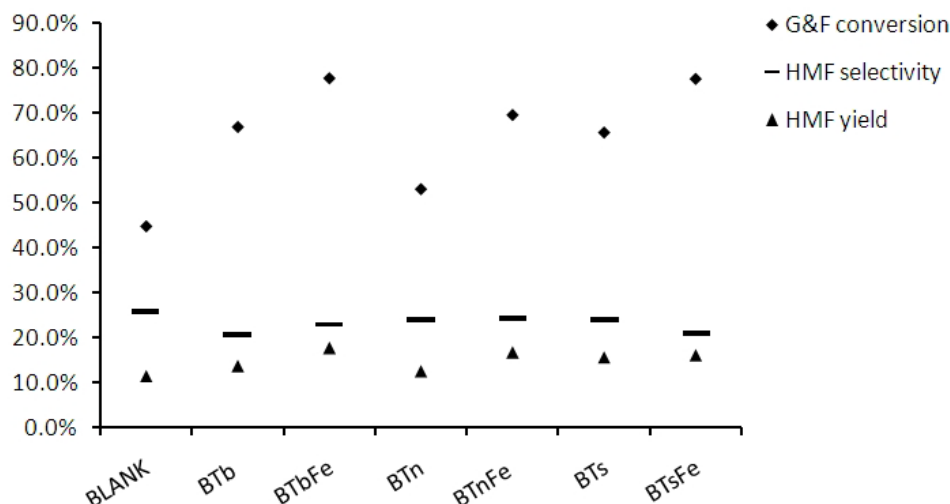


Figure 6: Comparison of differently functionalized Baytube® catalysts in the dehydration of glucose in aqueous media after 120 min reaction time at 40 bar N₂ and 250 mg catalyst

Although the activity of glucose dehydration could be enhanced by the heterogeneous catalysts we tested in aqueous phase, the selectivities of our targeted Product HMF were poor. In order to elucidate the reasons for the low selectivity of the carbon catalysts, all materials were characterized by BET and SEM, and compared to the unused catalysts. The analytical techniques applied clearly showed the coverage of the high surface area catalysts by insoluble byproducts. This leads to coverage of surface functional groups, i. e. the active sites in the reaction, as well to a tremendous decrease of catalyst surface area. In the case of the BTs-catalyst the surface area decreased by 98% from 351 to 7 m²/g (**Table 2**).

Table 2: BET surface area before and after reaction

Sample	before A _{BET} [m ² /g]	after A _{BET} [m ² /g]
BTs	351	7.25
BTn	326	26.6
BTb	253	32.0

One reason for enhanced humin accumulation onto the catalyst surface can be related to the surface properties of the catalysts. Since carbon nanotubes consist of a graphitic carbon structure with highly hydrophobic properties, this could favor high product reactivity on the catalyst surface. In order to study this phenomenon, adsorption experiments of glucose and HMF in aqueous medium as well as in 2-butanol were performed (**Figure 7**). 2-butanol is a more hydrophobic solvent that is widely used as extraction solvent in biphasic reaction systems in sugar dehydration processes [1, 2, 16]. For this reason, we have chosen 2-butanol for comparison to aqueous system. In Fig. x. the HMF and the glucose coverages are plotted as a function of their concentrations. HMF in aqueous solution adsorbs with a capacity that is one order of magnitude greater than that of HMF in 2-butanol solution. In contrast, the glucose adsorption onto the hydrophobic carbon surface is small.

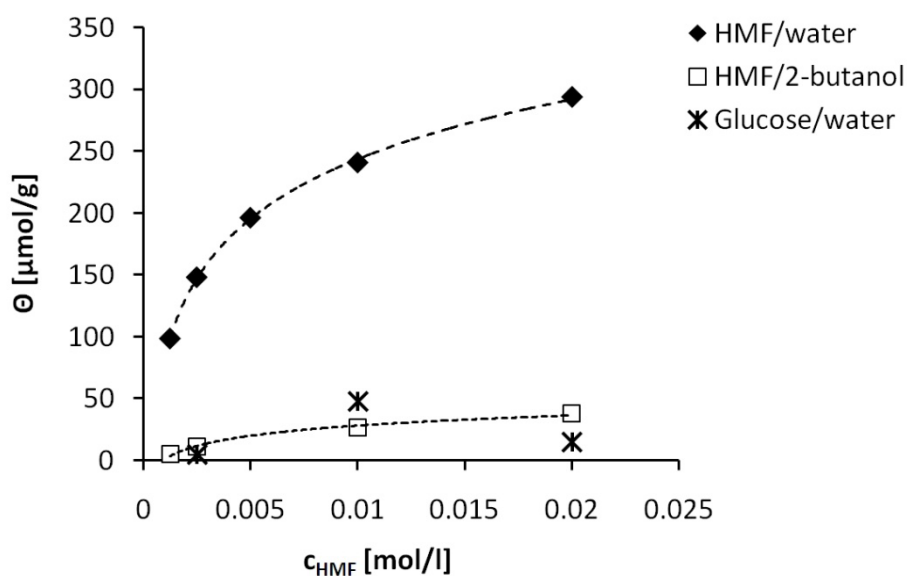


Figure 7: Adsorption isotherms of glucose and HMF on BTs in different solvents after 20 h at 30°C.

Based on these adsorption results, we performed further catalytic tests in sugar dehydration both in aqueous phase as well as in a one-phase system in

2-butanol. Due to low reactivity of glucose in the direct dehydration to HMF, we extended the catalytic tests towards the more reactive initial product fructose. The reason for the tremendous difference in dehydration activity of both sugars is originated from structural properties of the two isomers. The furanose form of fructose directly provides the structural element to follow the cyclic mechanism over the furanosyl cation. In contrast, glucose requires an epimerization over the acyclic conformer which is abundant in only diminutive quantities ($< 0.005\%$).

The comparative dehydration experiments between glucose and fructose were performed at 150°C in a 200 ml Parr® autoclave. A sampling valve allowed sampling during the catalytic reaction. **Figure 8** shows the HMF yield versus reaction time for the BLANK reaction compared to the use of 250 mg BTs catalyst in the dehydration of glucose in 2-butanol, fructose in 2-butanol and fructose in water, respectively. Under these reaction conditions glucose is essentially inactive. For fructose dehydration, the use of 2-butanol instead of water as solvent increases the HMF yield significantly.

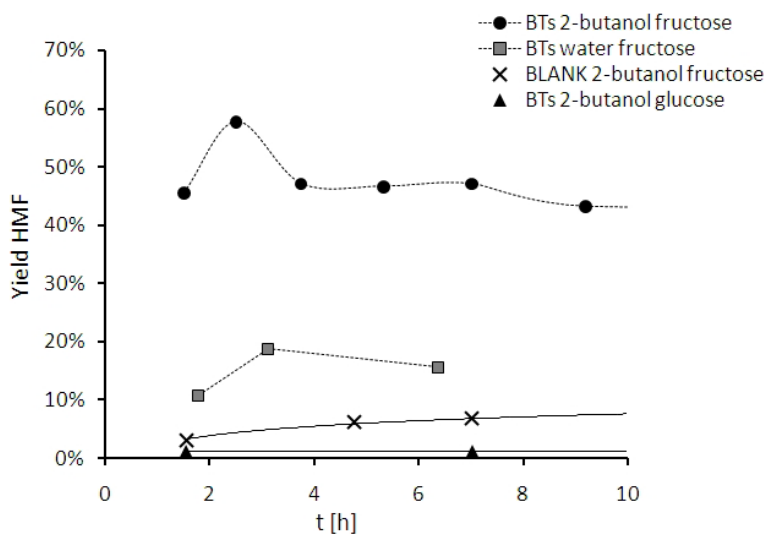


Figure 8: HMF yield over reaction time for the dehydration of glucose and fructose in aqueous phase in comparison to the one-phase system in 2-butanol at 150°C , respectively

Based on these results, we changed our testing conditions into a one-phase system of 2-butanol and focused on the dehydration of fructose to HMF, in order to achieve a better comparison of the catalysts.

IV.3.2 Dehydration of Fructose in 2-butanol

In the following comparison of different acidified carbon catalysts, the 2-butanol one phase system was used. The use of 2-butanol as the only reaction solvent has the disadvantage that the fructose solubility is low in comparison to that in water. For this reason we used 2.5 wt% solutions of fructose. However, the change in reaction conditions has several advantages. First, the product adsorption onto the catalyst surface is lower, as described above. Furthermore, side reactions that require water as reactant are suppressed. Thus the formation of levulinic acid and formic acid can be avoided which themselves lead to a lowering in the pH and continuously increase the amount of catalyst; making the reaction in this state difficult to control. The disadvantages of water as reaction solvent have been widely discussed in the literature [17, 18] and a wide range of different solvents have been tested for the dehydration of monosaccharides^[19]. Most effective apart from ionic liquids were DMSO, DMF or biphasic systems using methyl isobutylketon (MIBK) or 2-butanol as extraction solvents. However, all those solvents have certain disadvantages. Most challenging is the product separation of the reaction mixture due to the high boiling points, e.g. for DMSO of 189°C^[10, 20-23]. Furthermore the processes lead to impurities in the HMF-product that can be problematic in subsequent processing steps, such as S- and N-containing solvent or salt residues from the biphasic process. Since hydrogenolysis as well as oxidation reactions require metal containing catalysts, that are highly sensitive against poisoning by the impurities named, costly purification processes would be required.

In the one-phase system in 2-butanol, 2.5 g fructose were loaded together with 100 ml 2-butanol. If not stated differently 250 mg catalyst were added and the system was heated under stirring (450 rpm) to 130°C. All reactions were performed in a 200 ml Parr® autoclave. During the reaction the solid fructose dissolves in 2-butanol prior to dehydration into HMF. The schematic reaction assembly is depicted in **Figure 9**.

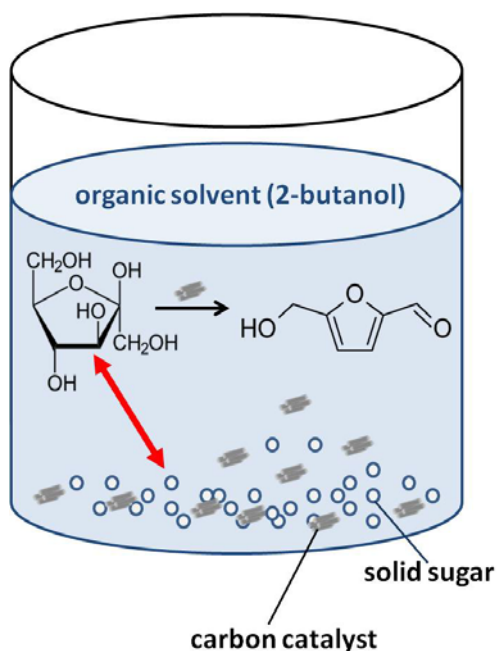


Figure 9: Schematic reaction assembly of one phase system in 2-butanol

In order to test for catalyst stability, four different testing modes were applied (**Figure 10**). First the catalyst was tested in a standard experiment as describes above (RUN1). Following the catalyst was filtered off and reused in a second experiment under identical reaction conditions, which is further referred to as recycling run (RECYCL). The stability of immobilized functional groups was tested in a separate leaching test (LEACH). Here the catalyst was stirred in the reaction solvent 2-butanol at 130°C for 15 h. Subsequently, the catalyst was filtered off and 2.5 g fructose were added to the 2-butanol filtrate. If the catalyst is stable the activity of the leaching test should be equal to the blank

experiment (BLANK), i.e. a blind test under identical reaction conditions as RUN1 but without the addition of any catalyst. The catalyst remained from the first step of the leaching experiment was tested separately as preconditioned material (PC). The pretreatment in 2-butanol at 130°C for 15 h can be repeated several times which will be further assigned to as PC1 to PC4. The letter stands for the test of a catalyst that has been preconditioned in 4 successive preconditioning steps.

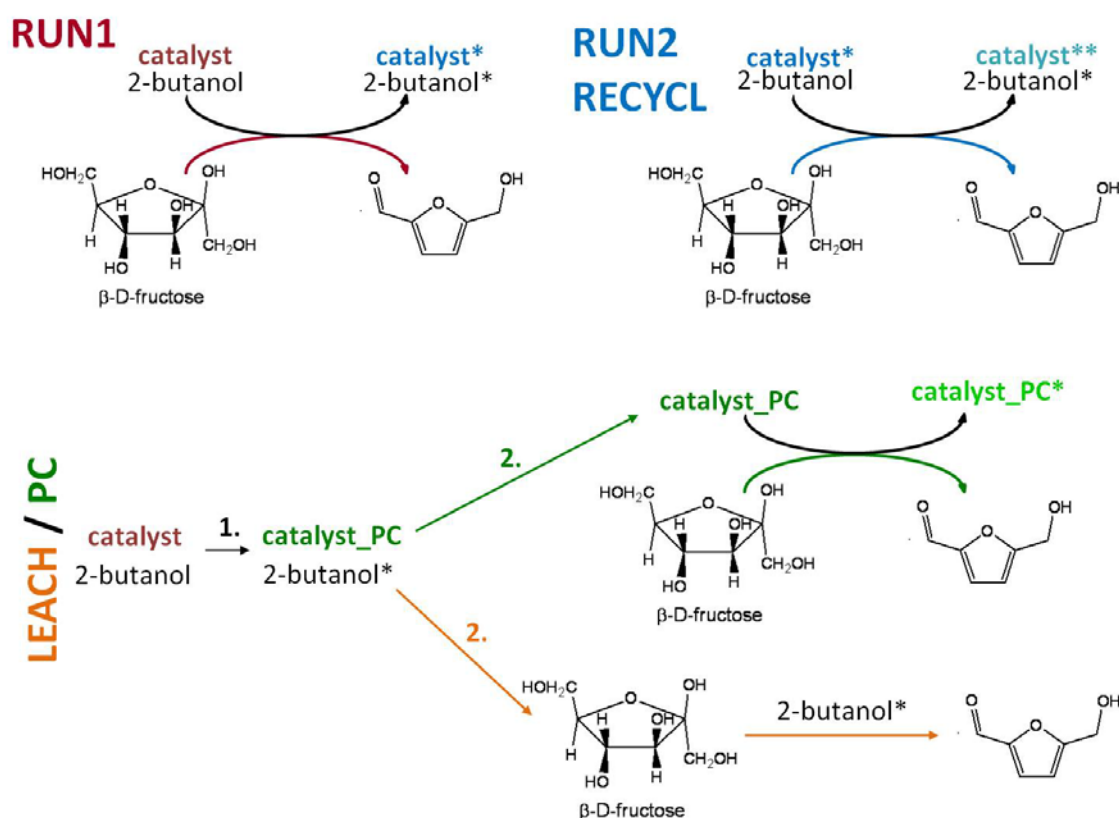


Figure 10: Catalytic testing modes

As described before the major side reaction in sugar dehydration is the formation of humins. In order to discriminate between side blocking by humin formation and other catalyst deactivation modes, the catalyst was studied in a probe reaction. The esterification of acetic acid in ethanol is performed at

milder reaction conditions (80°C) and in the absence of humin-forming side streams. For this reason it was considered as suitable reference reaction.

The catalytic performance of the acidified carbon nanotube catalyst BTs is summarized in **Figure 11**. Here the contribution of leaching experiment is significant. A major part of the activity found in RUN1 can be assigned to unstable acid functional groups that come off the catalyst surface during the reaction. After one preconditioning step in 2-butanol, the BTs catalyst loses the most of its activity. Similar behavior was found in the esterification reaction (**Figure 12**). Although the esterification is performed under milder conditions of only 80°C and the formation of humins can be excluded, the catalyst loses almost all activity after only one reaction run. Comparing the results of the esterification and the dehydration reactions, it can be concluded that in the case of BTs the deactivation mainly occurs due to loss of acid functional groups or leaching of the catalyst.

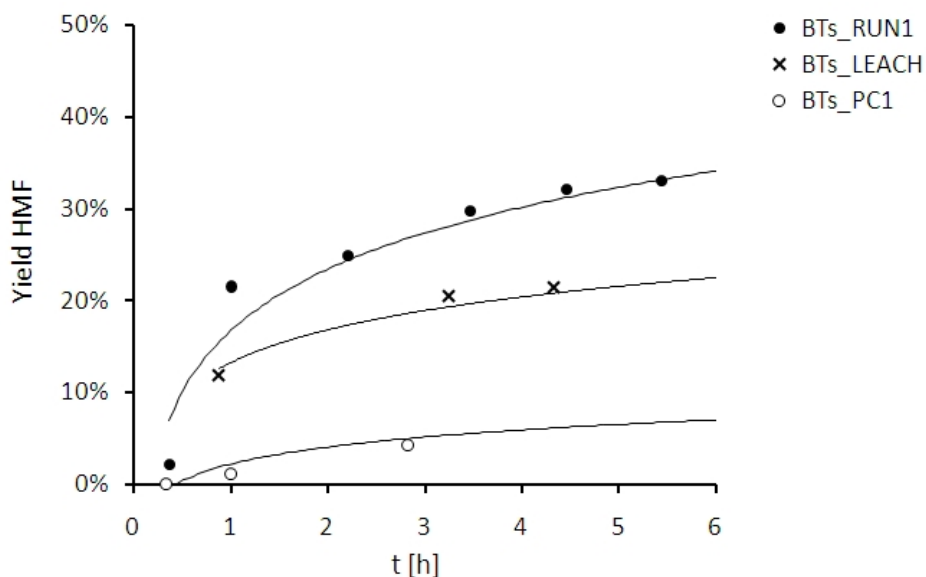


Figure 11: BTs catalyst in the dehydration of fructose in 2-butanol. Reaction performance in first reaction run (RUN1) vs. leaching test (LEACH) and test of preconditioned catalyst (PC1) at 130°C, 7 bar N₂ using 2.5 g fructose in 100 ml 2-butanol and 250 mg BTs-catalyst. After $t = 0.33$ h the system reached 130°C reaction temperature.

Since the functionalization by sulfuric acid is a defect functionalization, it is possible that strongly functionalized amorphous carbon fractions can be dissolved from the CNT surface during the reaction. For this reason, further attempts have been made to improve the stability of the functional groups in using a highly graphitized carbon support, i. e. after temperature treatment at 3000°C, which shows a minimum content in amorphous carbon. Under this aspect, a commercial carbon nanofiber (CNF) named PR24XT-HHT from Applied Sciences® was chosen^[24]. The benzene sulfonic acid was grafted by diazotization onto the CNF surface, resulting into covalently bond acid functional groups. The functionalized CNF catalyst, further named as BS-CNF, was tested in the dehydration of fructose in 2-butanol (**Figure 13**). Similar to BTs, the BS-CNF catalyst shows significant activities in the leaching experiment. In that respect, the grafting of benzene sulfonic acid onto highly graphitized CNFs did not result in more stable functional groups.

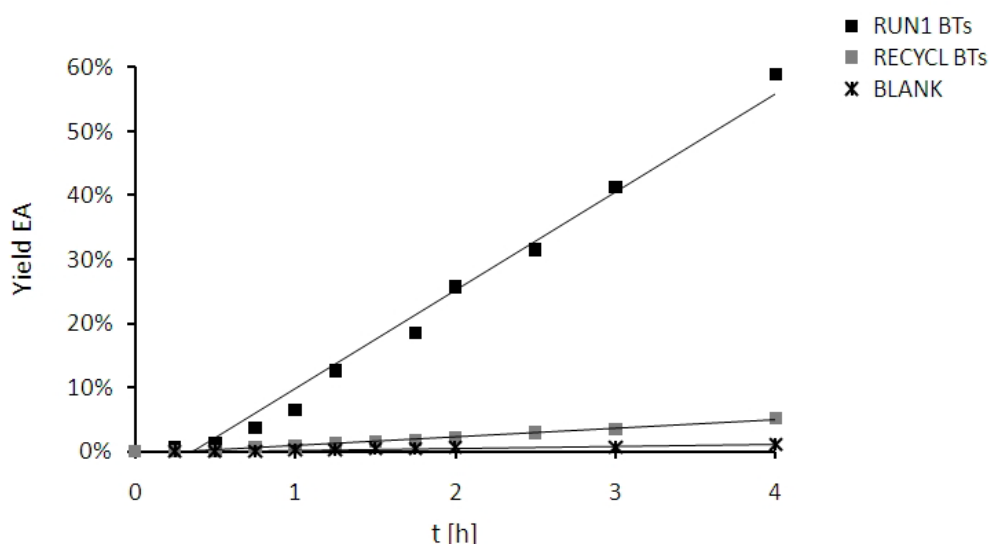


Figure 12: BTs catalyst in the esterification of acetic acid. Comparison of catalytic performance in the first reaction run (RUN1) vs. catalyst recycling (RECYL) at 80°C, 20 bar N₂ using 25 mmol acetic acid in 2.5 mol ethanol and 250 mg BTs-catalyst. At t = 0.33 h the reaction temperature of 80°C is reached

As reference the ion exchange resins Amberlyst® 15 and Nafion® were also tested in the fructose dehydration (**Figure 14**). Both materials showed leaching activities, although they carry only covalently bond sulfonic acid functional groups. In the case of Nafion the activity difference between the first run, the leaching experiment and the recycling run is very similar. The simple recycling of Nafion consequently would not point to deactivation of the material due to unstable functional groups. Since both materials carry a high number of acid functional groups, they can be “recycled” although they continuously lose active sites. However, for longterm application these materials are not suitable.

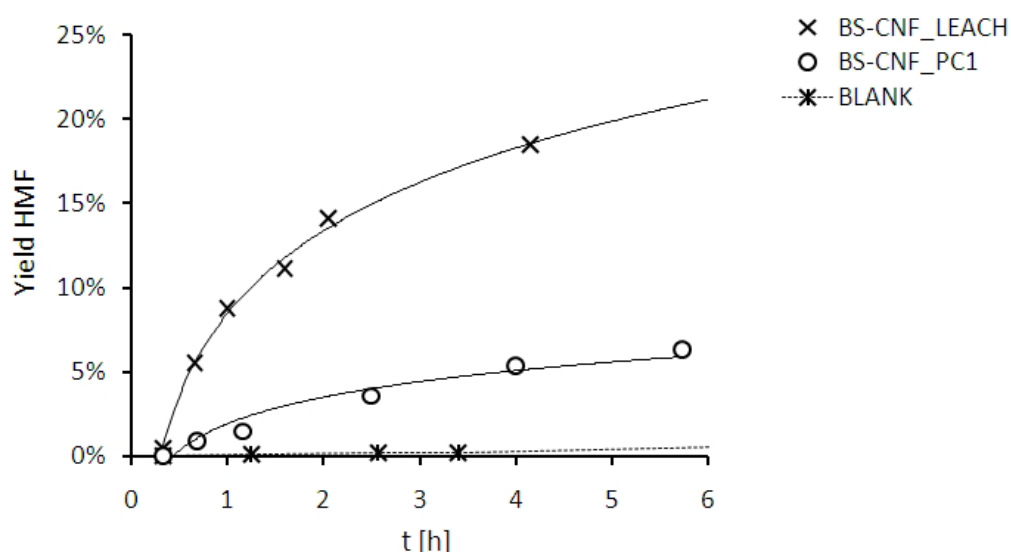


Figure 13: Catalytic performance of BS-CNF in the dehydration of fructose in 2-butanol. Comparison of leaching test (LEACH) with BS-CNF after preconditioning (PC1). At $t = 0.33$ h the reaction temperature of 130°C is reached

Since it was not possible to stabilize a high number of acid functional groups onto the tubular structured, highly graphitic BTs or BS-CNF catalysts, an acidified amorphous carbon (AGP) was tested as alternative. The carbon support was synthesized by pyrolysis of glucose in argon atmosphere at 400°C . After the treatment in sulfuric acid the amorphous carbon support was

functionalized by 1.7 mmol/g acid functional group, as determined by titration, which is in agreement with the literature^[3].

The stability of the functional groups was tested over four successive preconditioning steps at 130°C in 2-butanol for 15 h each. The remaining acid functional groups have been determined by titration (**Figure 15**). The main loss of acidity was detected after the first preconditioning. After two pretreatment runs the amount of acid functional groups decreased to 0.4 mmol/g and this value was retained over another two preconditioning steps. The catalyst preconditioned in this way (AGPs_PC4) was tested in the dehydration of fructose (**Figure 16**). The HMF productivity decreased from 55 % HMF yield ($t = 3$ h) in the first run of AGPs to 39 % HMF yield for the preconditioned catalyst. However, the material did not show activity due to leaching. Here leaching was tested by filtering off the catalyst after 2 h reaction time and continuing the reaction under the same conditions. No further HMF production could be determined.

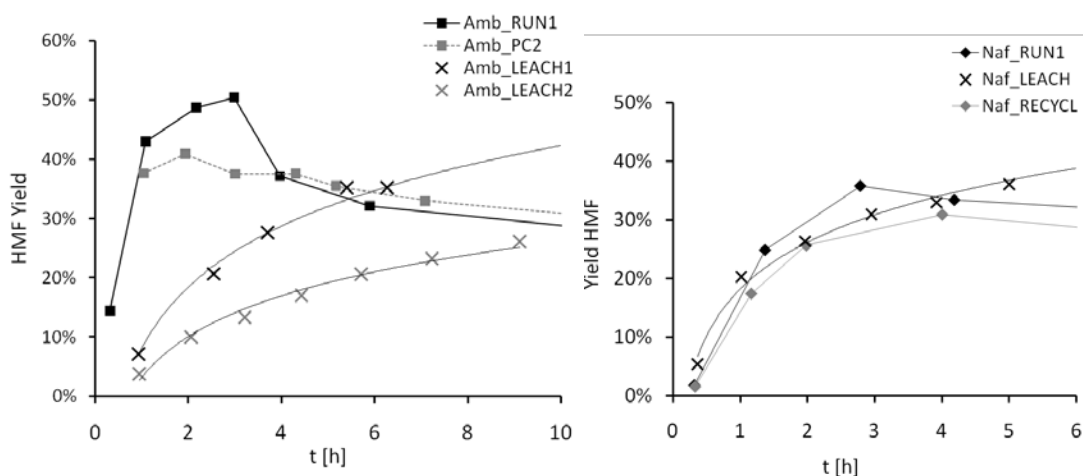


Figure 14: Left: Amberlyst® 15 (Amb) in the fructose dehydration. Comparison of first run (RUN1), catalyst testing after two successive preconditioning steps (PC2), leaching test of 2-butanol after the first pretreatment (LEACH1) and 2-butanol of the second, subsequent pretreatment (LEACH2). Right: Nafion® (Naf) in the fructose dehydration. Comparison of first run (RUN1), leaching test (LEACH) and reuse of the catalyst after RUN1 in a recycling run (RECYCL)

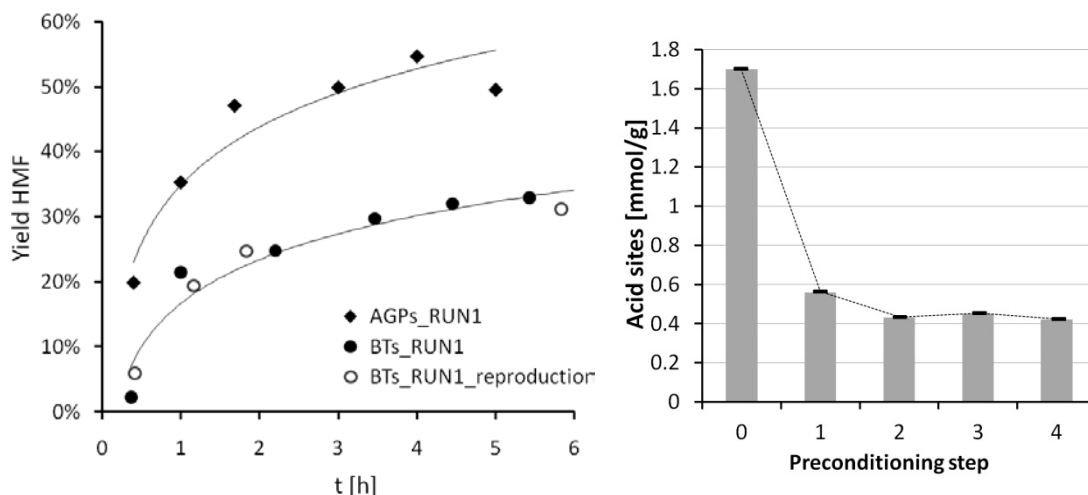


Figure 15: Left: Comparison of first run activities of AGPs and BTs. At $t = 0.33$ h the reaction temperature of 130°C is reached. Right: Number of acid functional groups determined by titration as a function of preconditioning steps

Although the AGP material was tested to be stable against leaching after suitable preconditioning steps, the catalyst could not be recycled. The deactivation of the material during the fructose dehydration must have a different origin. The reference experiment showed that AGPs_PC4 can be recycled in the esterification of acetic acid in ethanol at 80°C . The recyclability in the esterification (**Figure 15**) can be seen as further proof that the material is stable against leaching after sufficient preconditioning. According to this evidence, the reason for the deactivation in the fructose dehydration is most likely humin formation and site blocking by solid byproducts.

Another carbon material tested was ordered mesoporous carbon (OMC). OMC was chosen, since it combines an amorphous structure, predestinated for a high degree of functionalization by sulfuric acid, with high surface area and a mesoporous structure suitable for bulky solvated fructose molecules. After the functionalization in sulfuric acid the OMCs catalyst carried 0.45 mmol/g acid functional groups. However, catalytic tests of preconditioned OMCs showed deactivation of the material in the dehydration of fructose, since the material

cannot be recycled for this reaction (**Figure 17**). Furthermore, OMCs showed leaching activity already under the milder conditions of the esterification reaction.

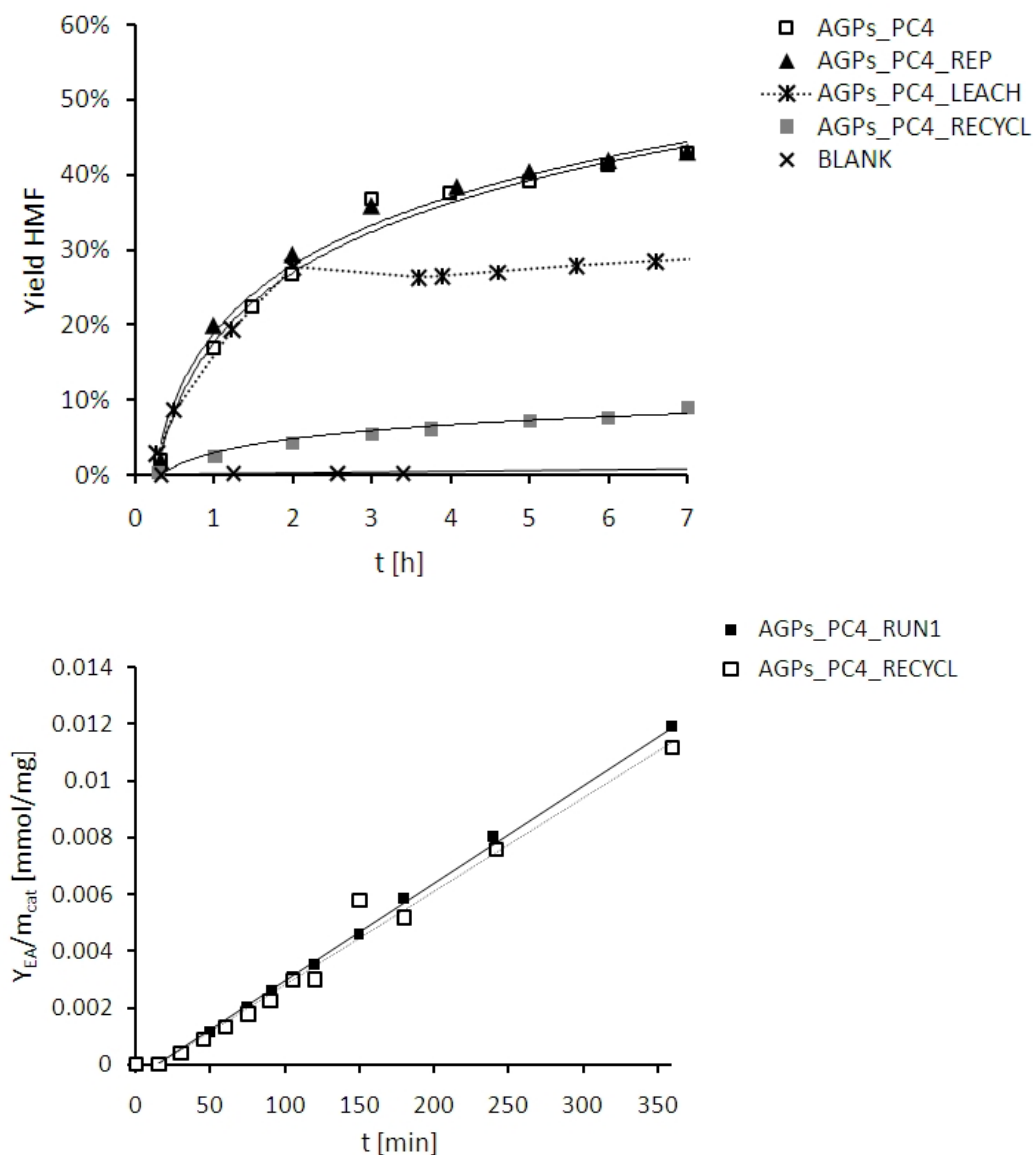


Figure 16: Upper: Catalytic performance of AGPs after four preconditioning step (AGPs_PC4) in dehydration of fructose in 2-butanol. Lower: Recyclability of AGPs_PC4 in the esterification reaction

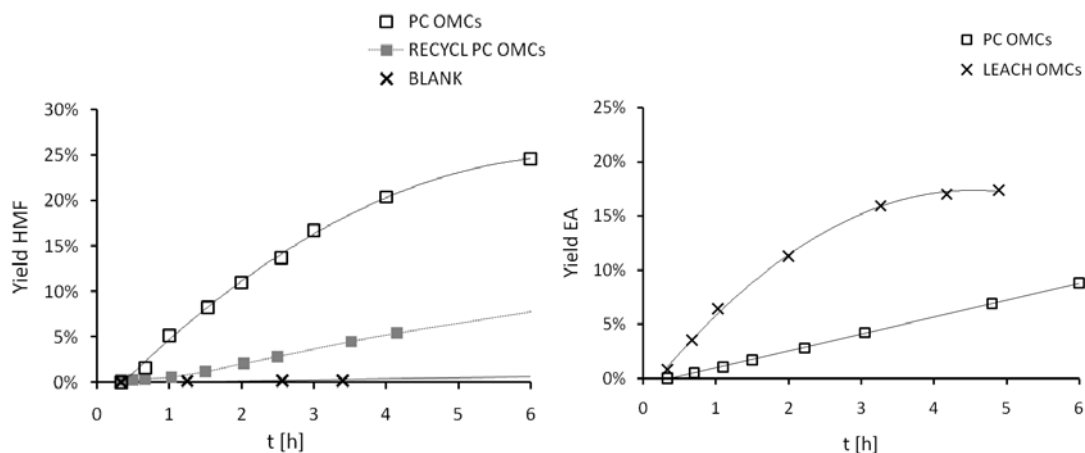


Figure 17: Left: OMCs in the dehydration of fructose in 2-butanol after preconditioning (PC), and recycling of the preconditioned OMCs (RECYCL). Right: Leaching activity of OMCs in the esterification of acetic acid (LEACH)

In the synthesis of OMC functional groups can be incorporated by the choice of suitable monomers for the polymerization process. For the incorporation of sulfur functional groups, 4,4'-thiodiphenol (TDP) was used to replace 20% of the resorcinol in the polymer. After carbonization at 600°C, sulfonic acid functional groups were formed by oxidation in H₂O₂. The obtained mesoporous catalyst, further referred to as TDP0.2, carried 0.25 mmol/g acid functional groups and showed high activities in the first run of fructose dehydration (**Figure 18**). Already after 1 h reaction time, HMF yields of 60% were achieved, whereas the leaching activity of TDP0.2 is comparably low. However, the material strongly deactivated after preconditioning in 2-butanol at 130°C. The activity of the preconditioned material is close to the one of the recycling run. Hence the major deactivation of TDP0.2 seems to happen by the contact with the solvent.

The catalytic performance of TDP0.2 in the esterification of acetic acid in ethanol is depicted in **Figure 19**. Similar behavior as in the fructose dehydration reaction could be detected. The leaching activity is comparably low. However,

the pretreatment in the reaction solvent ethanol leads to significant deactivation. Deeper investigations of surface changes after exposure to alcoholic solvents have been done using insitu-XPS and will be intensively discussed in the following chapter.

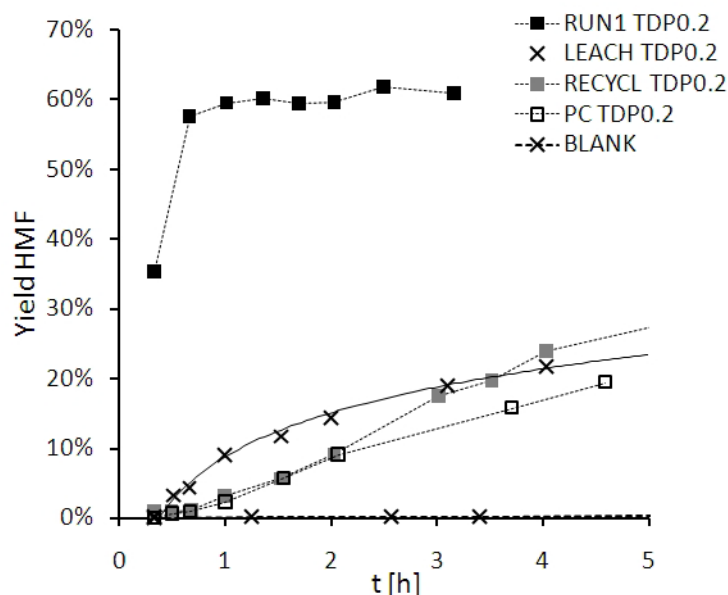


Figure 18: Mesoporous carbon catalyst TDP0.2 in the dehydration of fructose in 2-butanol

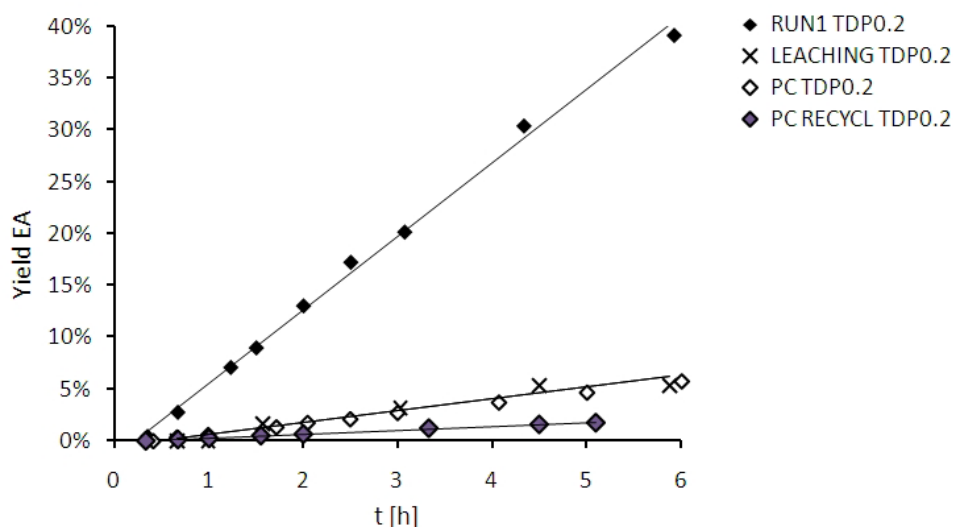


Figure 19: Mesoporous TDP0.2-catalyst in the esterification of acetic acid.

IV.4 Summary and Conclusion

As the catalytic tests of acidified carbon materials have shown, several deactivation procedures can be distinguished during the dehydration of fructose. A first idea of the stability of the catalyst can be extracted from the RUN1-activity plots. In the case of homogeneous acids (LEACHing solutions) or the extensively pretreated catalyst AGPs_PC4, the HMF yield development over reaction time corresponds to a logarithmic curve shape. Any deviation from the typical curve shape points to the superposition of several processes and thus can be seen as first hint for catalyst deactivation.

Table 3: Overview of results on catalyst deactivation tests

Catalyst	Yield HMF [%]	BET [m ² /g]	r_0^* $\left[\frac{\mu\text{mol HMF}}{2\text{h}\cdot\text{m}^2} \right]$	Leach	Active after PC	Stable in esterification	Recyclable in dehydration
BTs	28	245	56.1	yes	no	no	no
BS-CNF	4.1 ^a	36.1	48.5	yes	no	n.d.	no
AGPs	50; 37 ^b	-	-	no ^b	yes ^b	yes ^b	no
OMCs	17	683	7.8	yes	no	no	no
MC_TDP	61	654	51.5	little	no	no	no
Naf	36	flexible structure, swellable in liquid phase	-	yes	yes	n.d.	no
Amb	50		-	yes	yes	n.d.	no

All catalytic tests were performed in a one-phase system of 2-butanol at 130°C. The yields (calculated per mol initial fructose) refer to the amount of HMF formed after t = 3 h.

r_0^* specific apparent initial rate

^a HMF yield for the preconditioned catalyst (catalyst was pretreated one time in 2-butanol at 130°C for 15 h each)

^b HMF yield for the preconditioned catalyst (catalyst was pretreated 4 times in 2-butanol at 130°C for 15 h each)

Furthermore, the stability of acid functional groups was found to be critical for all materials and determined as the major deactivation process for the BTs catalyst (compare **Table 3**). Hence appropriate pretreatments are required, and leaching tests are essential for thorough proof of catalyst stability.

Even if the deactivation by leaching can be diminished by suitable pretreatments of the catalyst, and the stability of the groups is proven by leaching tests and recyclability in the reference reaction esterification, as in the case of AGPs, the catalyst deactivates in the fructose dehydration. Humin formation and accumulation of the active surface of the catalyst by those byproducts, is most likely the reason for the catalyst deactivation. The third aspect comprises catalyst deactivation by exposure to alcoholic solvents, as found for the mesoporous carbon material TDP0.2.

Finally, it can be concluded that independent from the choice of the carbon backbone, the covalently bond acid functional groups are not stable in water and alcohol under the described reaction conditions. This result contradicts the general hypothesis of considering carbon as hydrolytically stable support material. The correlation of the amount of functional groups with the number of defects in the carbon structure leads to a decrease in stability of the carbon support upon functionalization. Further investigation and better understanding of carbon degradation processes, i. e. carbon hydrolysis, could lead to knowledge-based optimization of carbon functional materials in catalysis, as well as in electrocatalytic applications.

V References

- [1] Y. Roman-Leshkov, J. N. Chheda, J. A. Dumesic *Science*. **2006**, 312, 1933-1937.
- [2] J. N. Chheda, Y. Roman-Leshkov, J. A. Dumesic *Green Chemistry*. **2007**, 9, 342-350.
- [3] A. Takagaki, M. Toda, M. Okamura, J. N. Kondo, S. Hayashi, K. Domen, M. Hara *Catalysis Today*. **2006**, 116, 157-161.
- [4] B. Hu, K. Wang, L. H. Wu, S. H. Yu, M. Antonietti, M. M. Titirici *Advanced Materials*. **2010**, 22, 813-828.
- [5] R. Rinaldi, F. Schuth *Energy & Environmental Science*. **2009**, 2, 610-626.
- [6] J. K. Chinthaginjala, K. Seshan, L. Lefferts *Industrial & Engineering Chemistry Research*. **2007**, 46, 3968-3978.
- [7] P. Wenmakers, J. van der Schaaf, B. F. M. Kuster, J. C. Schouten *Journal of Materials Chemistry*. **2008**, 18, 2426-2436.
- [8] A. Hirsch *Angewandte Chemie-International Edition*. **2002**, 41, 1853-1859.
- [9] D. Tasis, N. Tagmatarchis, A. Bianco, M. Prato *Chemical Reviews*. **2006**, 106, 1105-1136.
- [10] B. F. M. Kuster *Starch-Starke*. **1990**, 42, 314-321.
- [11] A. I. Torres, P. Daoutidis, M. Tsapatsis *Energy & Environmental Science*. **2010**, 3, 1560-1572.
- [12] C. A. Dyke, J. M. Tour *Journal of the American Chemical Society*. **2003**, 125, 1156-1157.
- [13] X. C. Zhao, A. Q. Wang, J. W. Yan, G. Q. Sun, L. X. Sun, T. Zhang *Chemistry of Materials*. **2010**, 22, 5463-5473.
- [14] J. P. Yuan, F. Chen *Food Chemistry*. **1999**, 64, 423-427.
- [15] R. Weingarten, G. A. Tompsett, W. C. Conner, Jr., G. W. Huber *Journal of Catalysis*. **2011**, 279, 174-182.
- [16] Y. Roman-Leshkov, C. J. Barrett, Z. Y. Liu, J. A. Dumesic *Nature*. **2007**, 447, 982-985.
- [17] H. E. Van Dam, A. P. G. Kieboom, H. Van Bekkum *Starch*. **1986**, 38, 95-101.
- [18] X. L. Tong, Y. Ma, Y. D. Li *Applied Catalysis a-General*. **2010**, 385, 1-13.

- [19] A. A. Rosatella, S. P. Simeonov, R. F. M. Frade, C. A. M. Afonso *Green Chemistry*. **2011**, 13, 754-793.
- [20] P. Vinke, H. van Bekkum *Starch-Starke*. **1992**, 44, 90-96.
- [21] D. W. Brown, A. J. Floyd, R. G. Kinsman, Y. Roshanali *Journal of Chemical Technology and Biotechnology*. **1982**, 32, 920-924.
- [22] G. A. Halliday, R. J. Young, V. V. Grushin *Organic Letters*. **2003**, 5, 2003-2005.
- [23] X. H. Qi, M. Watanabe, T. M. Aida, R. L. Smith *Industrial & Engineering Chemistry Research*. **2008**, 47, 9234-9239.
- [24] J. P. Tessonnier, D. Rosenthal, T. W. Hansen, C. Hess, M. E. Schuster, R. Blume, F. Girgsdies, N. Pfander, O. Timpe, D. S. Su, R. Schlögl *Carbon*. **2009**, 47, 1779-1798.

V REACTIVITY OF MESOPOROUS CARBON AGAINST WATER – AN IN-SITU XPS STUDY

Authors: Sylvia Reiche, Raoul Blume, Xiao Chen Zhao, Dangsheng Su,
Edward Kunkes, Malte Behrens, Robert Schlögl*

Abstract

Thiodiphenol (TDP) modified mesoporous carbon catalysts can be used in the acid catalyzed dehydration of fructose to 5-hydroxymethyl furfural (HMF). However, strong deactivation can be observed after preconditioning of the material in the solvent 2-butanol. Surface changes caused by the pretreatment have been studied by a XPS. The comparison of the pristine sample and the pretreated carbon sample showed similar distribution of oxygen functional groups by ex-situ XPS, as well as similar behavior during heating in vacuum. However, the addition of 0.1 mbar vapor pressure and subsequent heating to 130°C exhibited prominent differences in the evolution of the O1s, as well as for the C1s spectra of the two samples. Changes in the surface termination and hydrophobicity of the materials are discussed under the aspect of possible reactions of surface functional groups with the alcoholic solvent and water.

V.1 Introduction

Mesoporous carbon materials from resorcinol-formaldehyde aerogels have attracted enormous attention due to their advantageous properties and multiple potential applications, ranging from electrode materials in supercapacitors and fuel cells, over filters, down to catalytic supports or catalysts^[1, 2]. Several studies on material texture and pore structure are reported^[3]. However, the detailed chemical surface structure is still under investigation. Surface analytical methods, such as X-ray photoelectron spectroscopy (XPS), have been used to quantify the total surface oxygen content of the mesoporous carbon^[4]. However, the identification of the nature and the abundance of specific oxygen functional groups are still not understood. Based on the structural elements of the monomers and the polymerization mechanism suggested by Pekala^[5] (**Figure 1**), there is a general agreement on the functional groups of the aerogel. Isotope exchange experiments combined with ¹³C-NMR confirmed the abundance of methylene bridges and ether bridges in the polymer^[6]. The elucidation of the surface functional groups of the carbonized material was the intention of the present study. The focus was on an improved understanding of observations from prior catalysis tests of acidified mesoporous carbon materials^[7].

Acidified carbon catalysts can be applied in the acid catalyzed dehydration of fructose to 5-hydroxymethyl furfural (HMF, **Figure 2**). The general finding of the catalytic tests, as reported elsewhere^[7, 8], we observed a significant deactivation of the carbon based materials already in the first recycling run. The deactivation was found to have two causes; the loss of acid functional groups, which was determined by leaching tests, and surface poisoning by insoluble humins, as concluded from comparison to a reference esterification reaction.

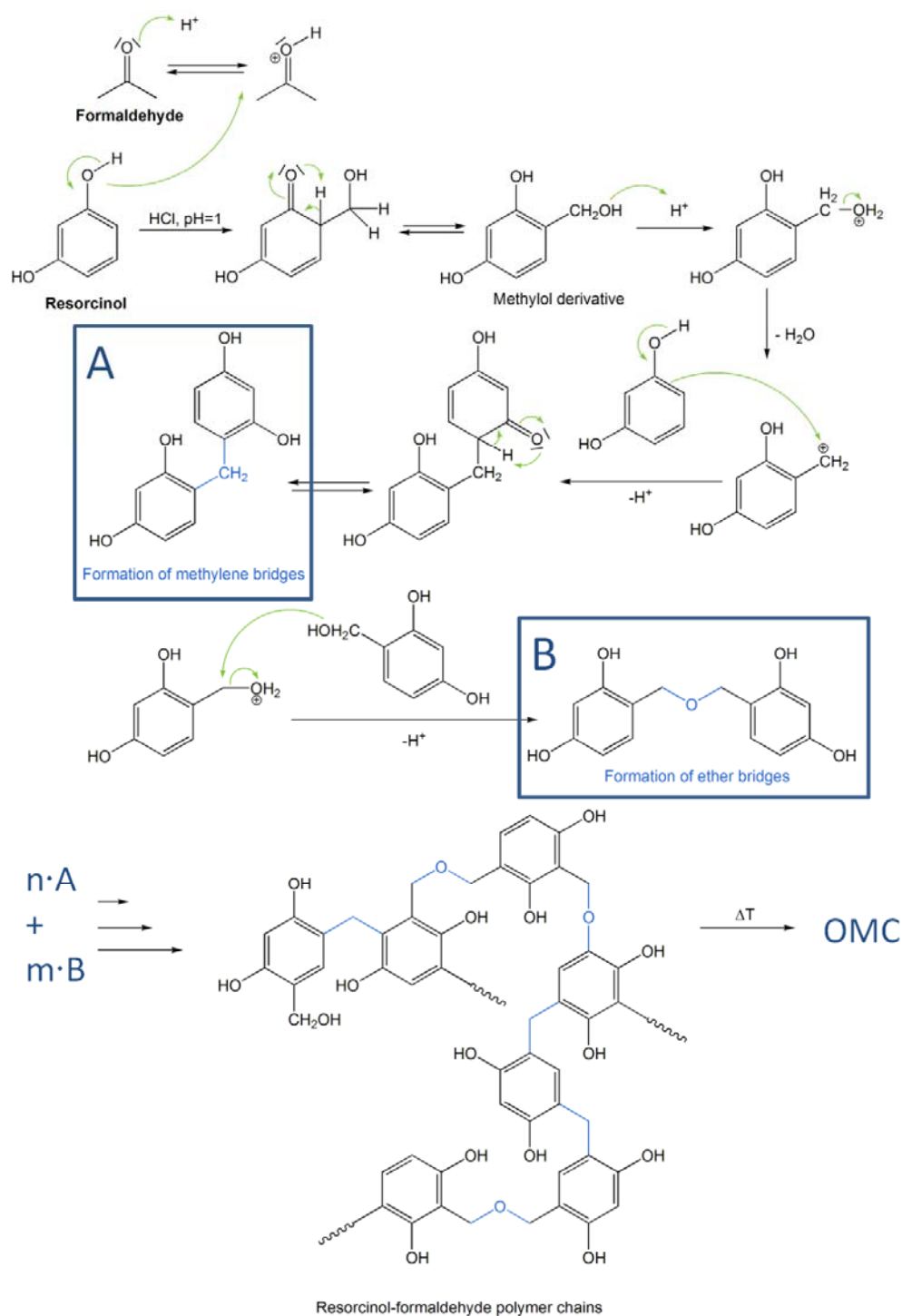


Figure 1: Possible reaction mechanism for the formation of the resorcinol-formaldehyde polymer as the precursor for OMC synthesis^[5, 9]

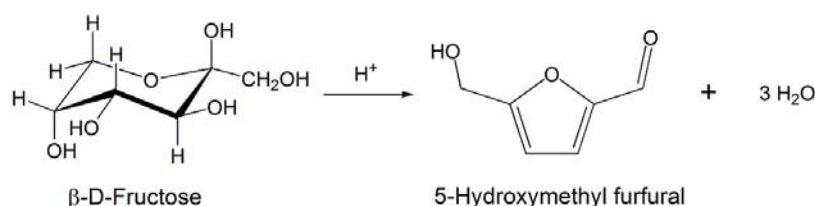


Figure 2: Fructose dehydration into 5-hydroxymethyl furfural under liberation of 3 molecules of water

For one group of materials, the thiodiphenol (TDP) modified mesoporous carbon, we could observe very promising HMF yields of 60% after 1 h reaction time (**Figure 3**, left). The leaching activity was comparably low. However, the catalyst deactivated after the preconditioning in 2-butanol. In a subsequent catalytic test of the preconditioned material we observed a delayed initialization of HMF formation, as well as a lower total activity. The behavior of the preconditioned material is very similar to the catalyst in the recycling run. Hence, major contribution to the deactivation of the catalyst occurred from exposure to the solvent. The better understanding of this deactivation procedure is necessary for the development of stable heterogeneous catalysts.

We further found that the initial activity of TDP0.2 is not, as originally expected, a function of the thiodiphenyl content (**Figure 3**, right). The TDP-free catalyst MC_1 shows identical activity as TDP0.2 and TDP0.6. The oxidation treatment in hydrogen peroxide most likely introduces surface species that are responsible for the dehydration activity of the materials. Hence all further considerations are based on TDP-free samples of mesoporous carbon.

In order to investigate changes in surface structure and oxygen functional groups during the pretreatment in 2-butanol, we have chosen two representative samples for insitu XPS experiments. The first mesoporous carbon sample was functionalized in hydrogen peroxide at pH 1 and corresponds to an active catalyst in the dehydration of fructose into HMF (MC_1), as shown in **Figure 3**. Secondly, a sample MC_2 was obtained by a

pretreatment of MC_1 in reaction solvent at reaction temperature, i. e. in 2-butanol at 130°C. In addition, a reference sample MC_0 was examined ex-situ by XPS. MC_0 is an ordered mesoporous carbon sample which has not been oxidized by H₂O₂.

We investigated dynamic changes in surface structures and in the distribution of oxygen functional groups under vapor exposure and heat treatments to the reaction temperature of 130°C by in-situ XPS. The vapor pressure of 0.1 mbar was applied in order to study the reactivity of the functionalized carbon surface towards water. Furthermore, the addition of vapor simulates the water evolution of 3 H₂O molecules per synthesized HMF molecule during the dehydration reaction of fructose.

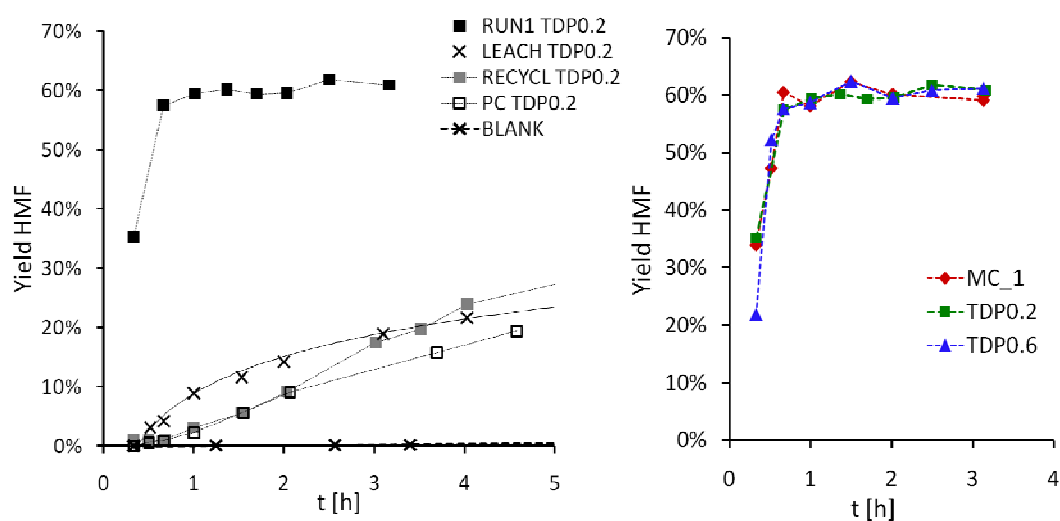


Figure 3: Catalytic performance of mesoporous carbon materials in the dehydration of fructose to HMF. Left: Deactivation of the material after the pretreatment in 2-butanol (PC TDP0.2). Right: Comparison of samples of different TDP content.

V.2 Experimental

V.2.1 Material synthesis and preliminary characterization

For the synthesis of MC_0, 5.5 g of resorcinol and 5.0 g of formaldehyde solution (37 wt%) undergo an acid catalyzed polymerization in 50 ml of a water-ethanol-mixture (1:1 by weight). The obtained polymer is carbonized in N₂ atmosphere at 350°C and 600°C for 2h, respectively. The detailed procedure of OMC synthesis is described elsewhere^[2].

After the carbonization, the mesoporous carbon is oxidized by H₂O₂ in a mixture of methanol and 2 M HCl (1:1, V:V) to obtain MC_1^[2].

The preconditioned material MC_2 was synthesized of MC_1 by stirring in 2-butanol at 130°C for 15h.

All materials are mesoporous carbons. The BET surface areas were determined by measuring the adsorption-desorption-isotherms with a Quantachrome Autosorb automatic BET-sorptometer at -196°C with nitrogen as analysis gas. For data evaluation the Quantachrome software Autosorb1 (version 1.54) was used. A full list of BET isotherms and plots for the BJH pore size distribution can be found in the supplementary information.

The number of acid functional groups was determined by titration using an automatic titrator (Mettler Toledo). For each measurement, 100 mg catalyst were dispersed in 10⁻³ mol KCl-solution and stirred over night. Following the dispersion was titrated under Ar atmosphere, using a 0.1 M NaOH solution.

Table 1: Summary of material basis including BET areas and titration results

Sample	Material description	BET [m ² /g]	Acid sites [mmol/g]
MC_0	ordered mesoporous carbon	789	-
MC_1	mesoporous carbon, functionalized by H ₂ O ₂ at pH = 1	596	0.24 ^a
TDP0.2	mesoporous carbon, 20mol% of building block recorcinol replaced by thiodiphenyl	654	0.25 ^a
MC_2	mesoporous carbon, MC_1 after preconditioning in 2-butanol at 130°C for 15 h	604	-

^a density of acid sites determined by titration of the material (100 mg in 50 ml KCl 0.001 M) with 0.01 M NaOH

V.2.2 Instrumental

In-Situ XPS experiments were performed at the synchrotron radiation source BESSY II of the Helmholtz Zentrum Berlin (HZB). The in-situ chamber was designed by FHI^[10, 11]. A schematic sketch of the set up is depicted in **Figure 4**. The high-pressure reaction cell is separated from the X-ray source by an X-ray transparent window. The emitted electrons attain the hemispherical electron analyzer through a differentially pumped aperture.

During in-situ XPS analysis of MC_1 and MC_2, the samples were heated stepwise to 130°C in vacuum and subsequently exposed to water at 0.1 mbar. In a second experiment, the samples were heated from RT to 130°C in water atmosphere (0.1 mbar). Spectra of the C1s, O1s and Cl2p regions as well as their respective Fermi edges were recorded with an electron kinetic energy of ~150eV.

All spectra are normalized to the background on the high binding energy side for better comparison of the peak shape of the main component. The spectra were fitted with a set of peaks derived from a differential spectra survey of a large number of functionalized and unfunctionalized carbon samples^[12].

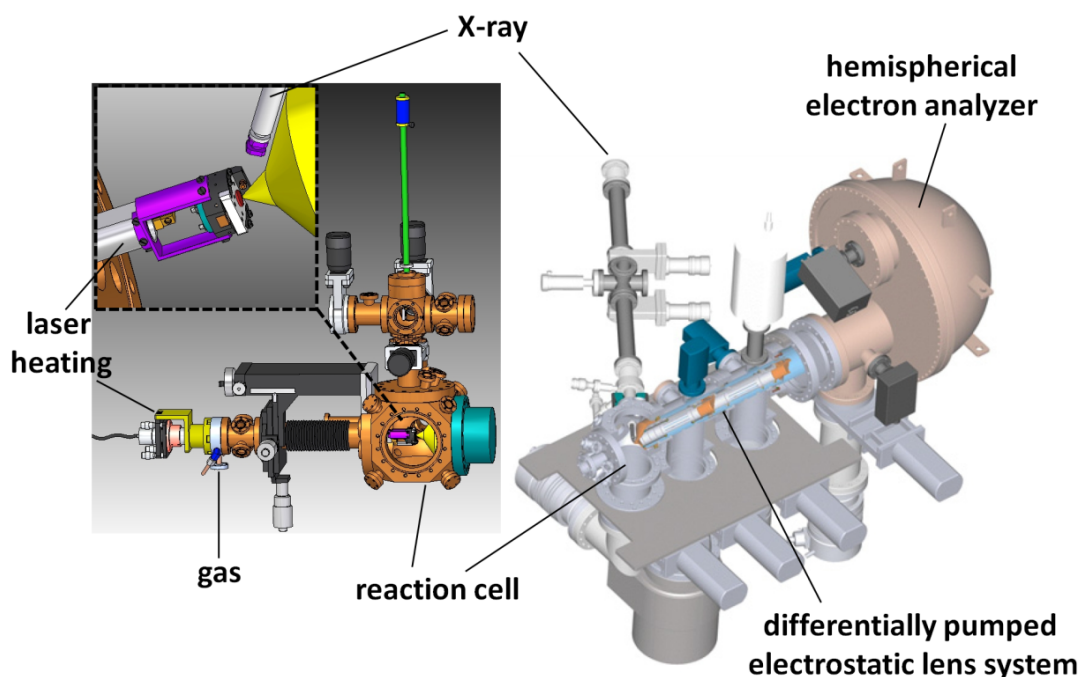


Figure 4: Schematic drawing of the high pressure XPS system at BESSY II^[11].

V.3 Results and Discussion

V.3.1 Differences in original carbon samples

In a first step the samples MC_1 and MC_2 were investigated ex-situ and compared to the reference sample MC_0 that represents the mesoporous carbon before any oxidation treatment. According to Blume et al.^[12], the O1s spectra were fitted by 6 different components of the peak positions 530.5 eV, 531.2 eV, 531.9 eV, 532.7 eV, 533.5 eV and 534.2 eV (**Table 2**). An additional feature for the measurements under water vapor was detected at 535 eV and corresponds to the water gas phase peak^[13].

Table 2: O1s peak assignment according to the literature

No.	Peak position [eV]	Oxygen functional group	Supporting References	
I	530.5	C=O in quinones	[13-16]	[17, 18]
II	531.2	C=O in ketones, aldehydes		[17, 18]
III	531.9	C-O-C in aromates (furan), or keto-enol tautomers	[13-15, 18]	
IV	532.7	OH in phenol or aliphatic alcohols		[16]
		chemisorbed H ₂ O		
V	533.5	C-O-C in ethers, esters, anhydride		[16, 19]
VI	534.2	C-OH in carboxylic acid	[16, 18]	
		chemisorbed H ₂ O	[13-15]	[19]
VII	535	gas phase H ₂ O		[13]

The assignments of specific features in the O1s peak are intensively and partially controversially debated in the literature. It is generally agreed to the discrimination of minimum two different oxygen species, the double bonded oxygen at lower binding energies (~531 eV) and the single bonded oxygen at higher binding energies (~533 eV)^[20]. Additionally, a third species at higher binding energies is commonly considered in the fit, assigned to adsorbed water or oxygen^[13-15]. Clark et al. performed more detailed studies in the systematic comparison of well defined polymers and suggested the discrimination of four different oxygen species: double-bonded oxygen in esters, carbonates and acids (~532.8–532.9 eV), oxygen in ketons, ethers and alcohols (~533.6–533.7 eV), single-bonded oxygen in acids and esters (~534.3 eV) and single-bonded oxygen in carbonates (~535.0–535.2 eV)^[21]. The high resolution of modern XPS instruments, the use of synchrotron radiation sources, and the consideration of the thermostability of different oxygen functional groups lead to verification of the Clark model^[18, 22] and further differentiation of the O1s peak^[16, 17, 19, 23].

For the present work we also tried to involve considerations on structural elements that are predetermined by the synthesis procedure. Based on the polymeric precursor of the mesoporous carbon (compare **Figure 1**) a broad variety of oxygen functional groups is possible for the carbon samples. Most likely the material still contains phenolic and aliphatic OH-groups, as well as ether groups after the carbonization procedure. Due to possible condensation reactions at the applied temperatures (600°C for 2 h during carbonization), lactones, furans or quinones are further possible structural elements. During the oxidation in hydrogen peroxide an increase in carbonyl and carboxyl groups is expected, as well as further hydroxyl functional groups through the oxidation of double bonds.

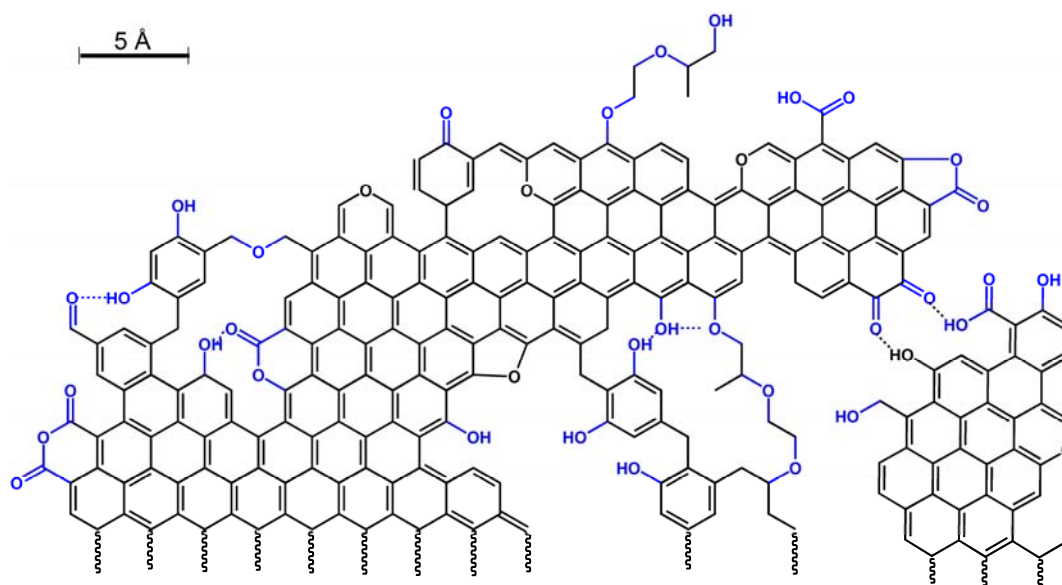


Figure 5: Scheme of possible carbon structure for the samples investigated in consideration of the structural elements of the polymeric precursor and ideas reported in the literature^[23, 24]. In blue: functional groups that can interact with water molecules under the formation of hydrogen bonds or in hydrolysis reactions

Comprising the knowledge of the building blocks, the synthesis procedure and experiences reported in the literature^[23, 24], a schematic carbon structure can be proposed for the materials (**Figure 5**). In the following, this structural idea will be compared to the result of the XPS experiments.

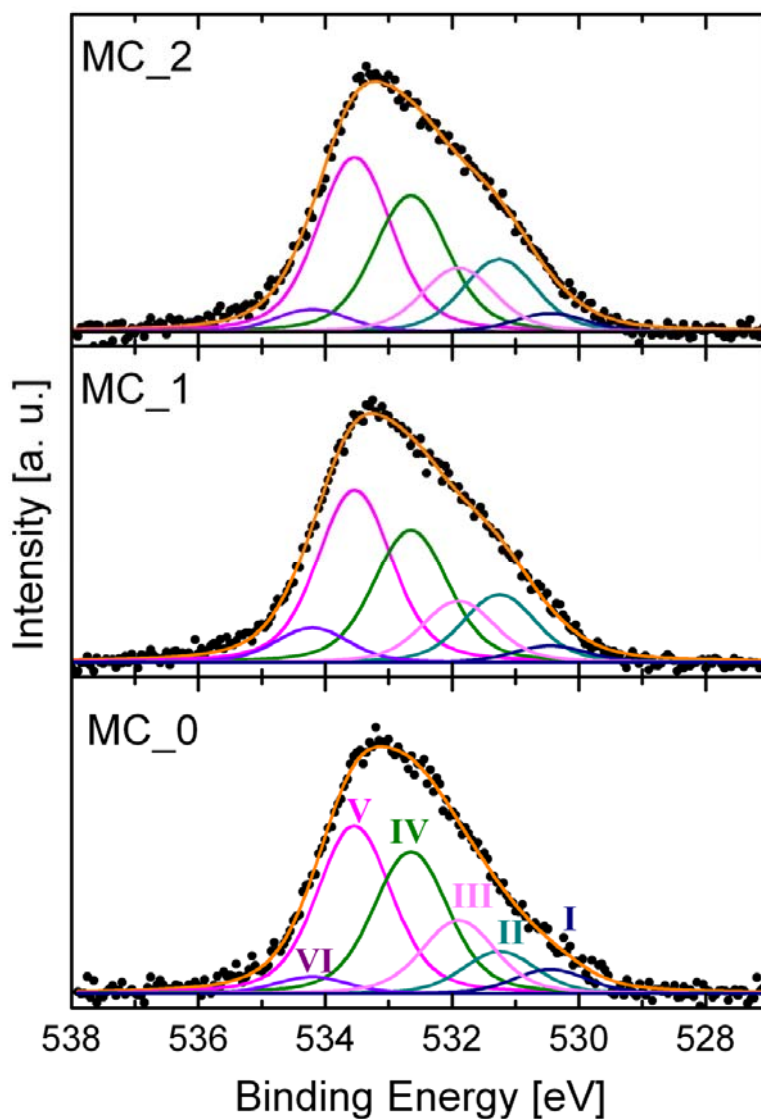


Figure 6: O1s fits of MC_0, MC_1 and MC_2 of ex-situ XPS measurements

Ex-situ measurements of MC1 and MC_2 show O1s spectra of similar line shape for both samples (**Figure 6**). There is only a small difference in the total oxygen content of about 1% (**Table 3**). The small intensity difference is equally distributed between the species II-V. However, the component VI at 534.2 eV, which can be assigned to carboxylic acid functional groups^[16, 18] or chemisorbed water^[13-15] according to the literature, is abundant in slightly higher proportion in sample MC_1 in comparison to the sample MC_2 after the butanol treatment. Either assignment could support the idea of possible surface changes of MC_1 during the treatment in alcoholic solvents. In the case of the assignment to carboxylic acid functional groups, the lower content for MC_2 could be explained by possible esterification reactions in the alcoholic solvent. If assigned to adsorbed water, the higher content of the species at 534.2 eV points to a higher hydrophilicity for MC_1 which can be seen as indirect evidence for surface modifications by 2-butanol in the case of MC_2.

Table 3: Quantification of oxygen species of MC_0, MC_1 and MC_2 by ex-situ XPS [%]

Sample	530.5 eV	531.2 eV	531.9 eV	532.7 eV	533.5 eV	534.2 eV	Total oxygen content
MC_0	0.3	0.5	0.8	1.6	1.9	0.2	5.3
MC_1	0.4	1.5	1.4	3.0	4.0	0.8	11.1
MC_2	0.4	1.8	1.6	3.4	4.4	0.5	12.1

In contrast to the oxidized samples, the O1s spectrum of the reference sample MC_0 differs in line shape due to the lower influence of features at lower binding energies. After the oxidation, the carbonyl species at 531.2 eV contributed stronger to the overall line shape for the samples MC_1 and MC_2.

Table 4: C1s peak assignment according to literature

No.	Peak position [eV]	Carbon functional group	Supporting References	
I	284.4	C=C, sp ² carbon	[15-17, 25]	
II	284.7	C-C, sp ³ carbon	[15-17, 25]	
III	285.2	aliphatische C-H, C-O in alcohols, phenols, ethers	[15-17, 25]	
IV	285.9	C=C-O in keto-enolic equilibria or furans	[15, 17]	[16, 25]
V	286.6	C=O		[16, 25]
VI	287.9	COOH, COOR in carboxylic acids or esters	[15-17, 25]	
VII	288.5	carbonate	[15, 16]	[26]
VIII	289.1			[26]

Similar to the O1s spectra, the C1s peaks (**Figure 7**) were fitted by a set of fitting parameters derived from a differential spectra survey of a large number of functionalized and unfunctionalized carbon samples^[12]. Within the C1s peak, eight features at the positions 284.4 eV, 284.7 eV, 285.2 eV, 285.9 eV, 286.6 eV, 287.9 eV, 288.5 eV and 289.1 eV were discriminated (**Table 4**). However, due to the dominant influence of the asymmetry of the sp² carbon peak ($I_{\max} = 284.4$ eV) up to high binding energies, the quantification of the oxygen species in the C1s is rather difficult. Small errors in the subtraction of the graphitic peak can lead to large errors in the evaluation of the functional groups, in particular due to their minor contribution^[27].

Comparing the fits of the C1s spectra for the three samples, a clear difference in the proportion of graphitic carbon to amorphous carbon and/or unsaturated bonds can be found. The higher percentage of graphitic surface carbon for MC_2 could be explained by partial removal of amorphous carbon species during the pretreatment in 2-butanol. Another explanation could be partial structural reorientation of the surface as a consequence of pretreatment. The esterification

of carboxylic acid functional groups, for instance, could lead to a decrease of structure determining hydrogen bonds (compare Fig.). As a consequence, the influence of π - π -stacking interactions increases which could result in more densely packed regimes of graphitic carbon. The peaks III-VIII correspond to the oxygen functional groups. Based on the quantification of the same, lower oxygen content could be determined for the reference sample MC_0 (Table 5) which is in agreement to the findings of the O1s spectra evaluation.

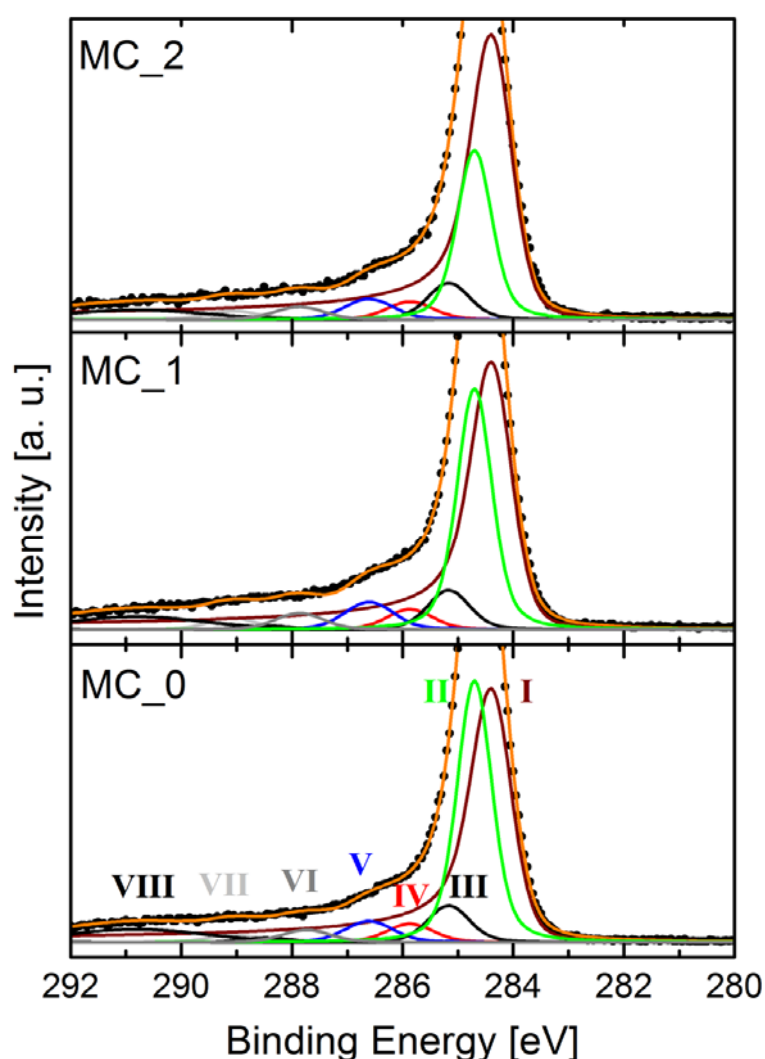


Figure 7: C1s fits of MC_0, MC_1 and MC_2 of ex-situ XPS measurements

Table 5: Quantification of carbon species in the C1s pectra of MC_0, MC_1 and MC_2 obtained by ex-situ XPS [%]

Sample	284.4 eV	284.7 eV	285.2 eV	285.9 eV	286.6 eV	287.9 eV	288.5 eV	289.1 eV	Total carbon content
MC_0	40.0	27.7	4.7	2.4	2.9	1.8	5.9	1.2	94.8
MC_1	37.0	26.7	4.9	3.0	4.0	2.4	0.6	1.8	88.6
MC_2	43.0	15.7	5.1	2.9	3.4	2.3	0.5	1.1	87.7

V.3.2 Differences during heating in vacuum

The O1s spectra show similar behavior for MC_1 and MC_2 while heating the materials in vacuum. For both samples, a decrease in the total oxygen content of about one quarter for MC_1 and about one third for MC_2 can be determined (**Table 3**). Even the water exposure at 130°C does not change the trend of the gradual decrease of most oxygen components. The major change in the oxygen species distribution is observed for the feature at 532.7 eV which can be assigned to temperature sensitive OH-groups, according to the literature. Due to the mild temperatures applied, the loss of adsorbed water species from the highly porous materials (compare BET surface areas in **Table 1**) seems to be another plausible conclusion. TG-MS experiments were performed in order to check for carbon decomposition reactions under CO₂ evolution at the temperatures applied in the in-situ experiments. It could be confirmed that water is the only released species within the investigated temperature range (**Figure 8**). The most pronounced intensity after the heating experiments corresponds to an oxygen species at 533.5 eV. As described before this feature can be assigned to ether-like oxygen functional groups which were expected to be stable in the applied temperature treatment. Due to the pronounced intensity

loss in this regime and water being the only species evolved below 130°C, the 533.5 eV peak has to be associated with water.

Table 6: Quantification of oxygen species of MC_1 and MC_2 during heating in vacuum and subsequent addition of water (0.1 mbar) at 130°C

	Process step	Total oxygen content [%]
MC_1	RT	11.1
	80°C	9.8
	130°C	9.5
	130°C _{vapor}	8.6

	Process step	Total oxygen content [%]
MC_2	RT	12.1
	80°C	10.9
	130°C	9.8
	130°C _{vapor}	8.3

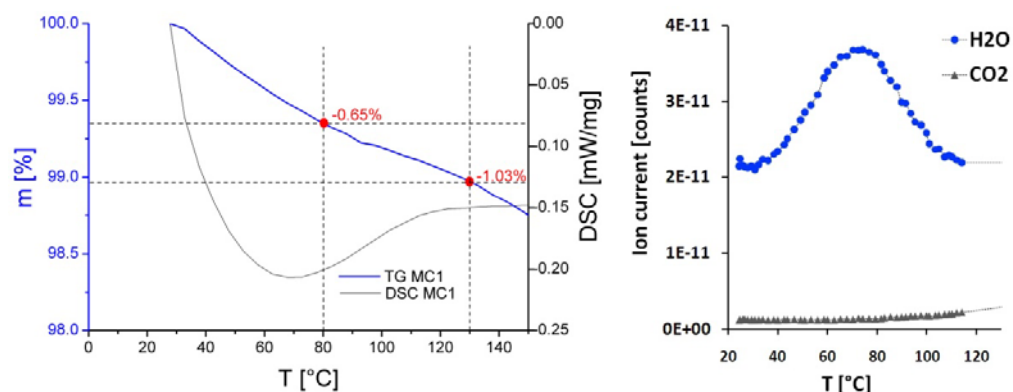
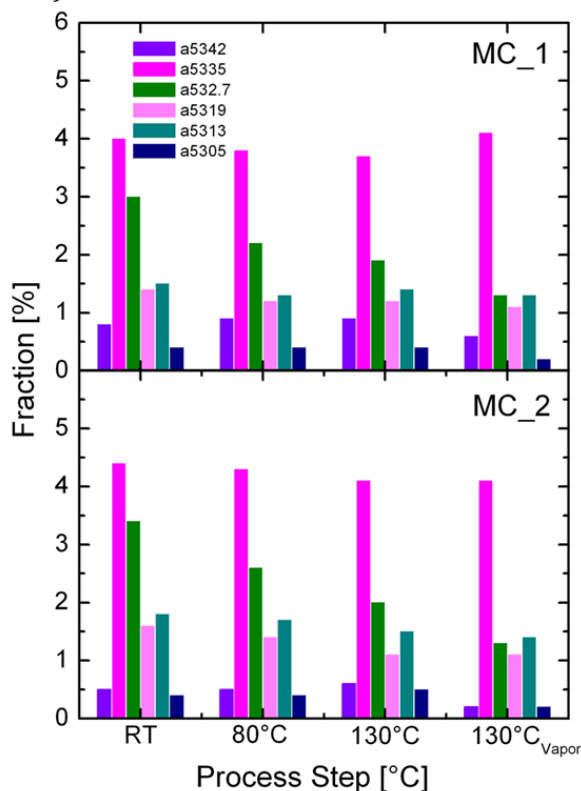


Figure 8: TG-MS experiment of MC_1. Left: mass loss over temperature treatment, Right: MS-signal for CO, CO₂, OH and H₂O

Despite the similarity in the evolution of the O1s spectra, differences can be observed comparing the C1s spectra of the two samples (**Figure 9**). In case of MC_1 the carbon structure of the material remains almost unchanged during heating in vacuum. In contrary, an increase in amorphous surface carbon can be determined for MC_2. Generally the formation of amorphous surface carbon can be explained by the removal of oxygen functional groups while less ordered amorphous structures are retained. However, since the O1s spectra of both samples show similar losses in oxygen functional groups, this idea does not provide a satisfying explanation of the observations in the C1s spectra. For this reason, we would like to refer to the initial differences of the C1s spectra as discussed for the ex-situ XPS measurements. The effect of possible esterification reactions during the pretreatment in 2-butanol could be partially reversed by the water evolved during heating. Thus, hydrolysis and re-formation of hydrogen bonds can lead to structural changes. The increase in wettability and intercalation of water can result in the exfoliation of the structure. It is possible that less stable amorphous components can be partially transported towards the surface by the water evolved, resulting in the detection of higher amounts of amorphous surface carbon.

Since for none of the oxygen related features at higher binding energies of the C1s spectra a pronounced loss was observed, the strong changes in O1s spectra for both samples are unlikely to be related to the cleavage of C-O-bonds. More plausible for the explanation of the changes in the feature at 532.7 eV is the removal of structural water, e. g. from water incorporation of the pores or the solvation of oxygen functional groups.

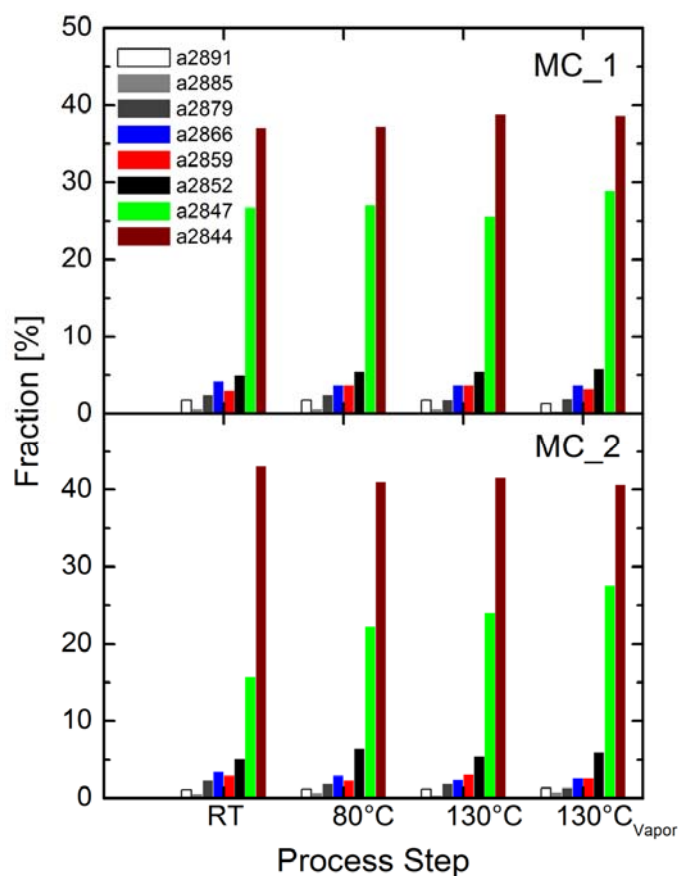


Figure 9: Evolution of C1s components during heating in vacuum and subsequent addition of water (0.1 mbar) at 130°C

V.3.3 Behavior during heating in water atmosphere

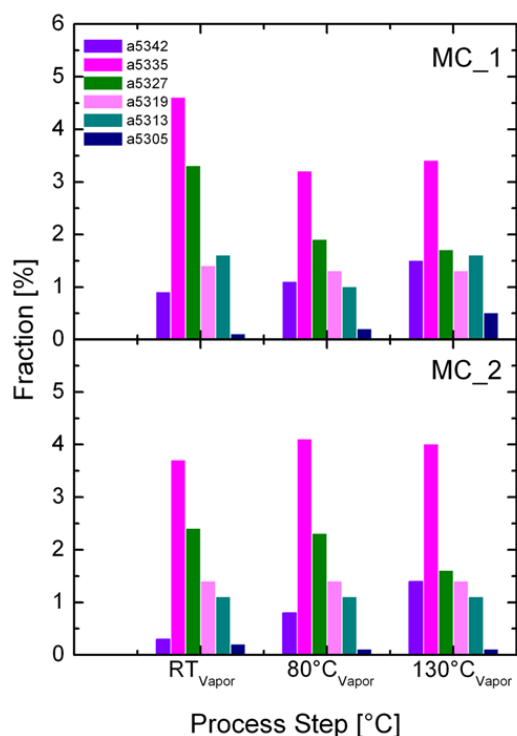
Compared to the experiments in vacuum, there are significant differences in the behavior of the two samples MC_1 and MC_2 while heating under water vapor of 0.1 mbar. The presence of water induces the additional reactivity of hydrolysis to the sequence of chemical events upon thermal treatment. The latter commonly leads to condensation reactions. Whereas the overall oxygen content for MC_2 does not change significantly under the heat treatment in

vapor (even shows a tendency to rise up to 80°C), the total O-content for MC_1 decreases from 11.1% to 9.5% (**Table 7**).

Table 7: Quantification of oxygen species for MC_1 and MC_2 during heating in 0.1 mbar vapor

	Process step	Total oxygen content [%]
MC_1	RT _{aq}	11.1
	80°C _{aq}	9.8
	130°C _{aq}	9.5

	Process step	Total oxygen content [%]
MC_2	RT _{aq}	9.1
	80°C _{aq}	9.8
	130°C _{aq}	9.6



The signal at 533.5 eV, which was stable for both samples during the heat treatment in vacuum, decreases for MC_1 while heating in water atmosphere. This indicates that parts of the ether or ester groups of MC_1 are sensitive against hydrolysis. In case of MC_2, the structural changes of the samples during the pretreatment in 2-butanol, i. e. the reordering towards a more graphitic surface termination (compare result of ex-situ XPS, **Figure 7**), seems to stabilize the material against the intrusion of water and hydrolytic effects of the heat treatments in vapor.

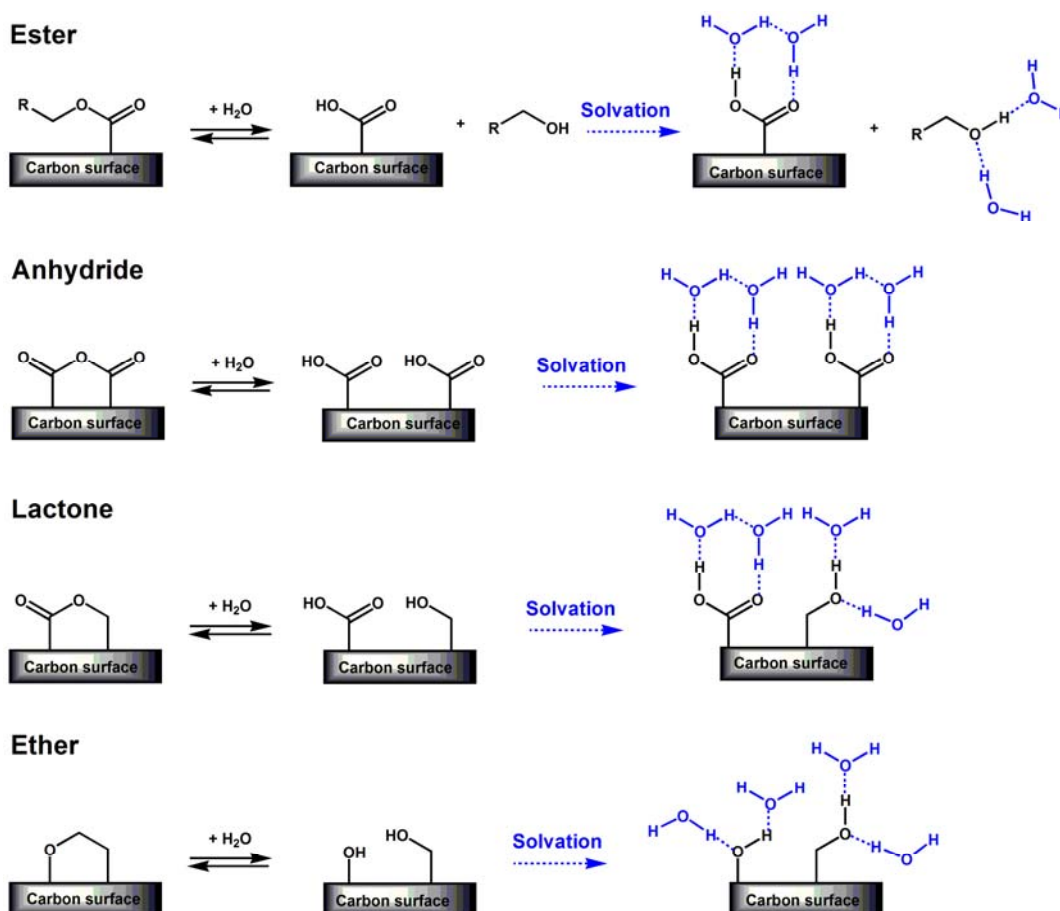


Figure 10: Reactivity of different oxygen functional groups towards water^[28] and consequential changes in the solvation chemistry.

Hydrolysis reactions have an oxygen introducing effect. Thus the small changes in the overall oxygen content for MC_2 could be the result of two simultaneous processes: Firstly, the loss of oxygen species (water removal) due to the increasing temperature and secondly the partial introduction of oxygen functional groups by possible hydrolysis reactions. **Figure 10** summarizes potential hydrolysis reactions for the prior suggested surface functional groups of the materials. As a result of the hydrolysis, the surface solvation is enhanced, due to the increase in functional groups that are capable of hydrogen bond

formation. Solvation or the incorporation of water molecules could be one explanation of restructuring forces as discussed before.

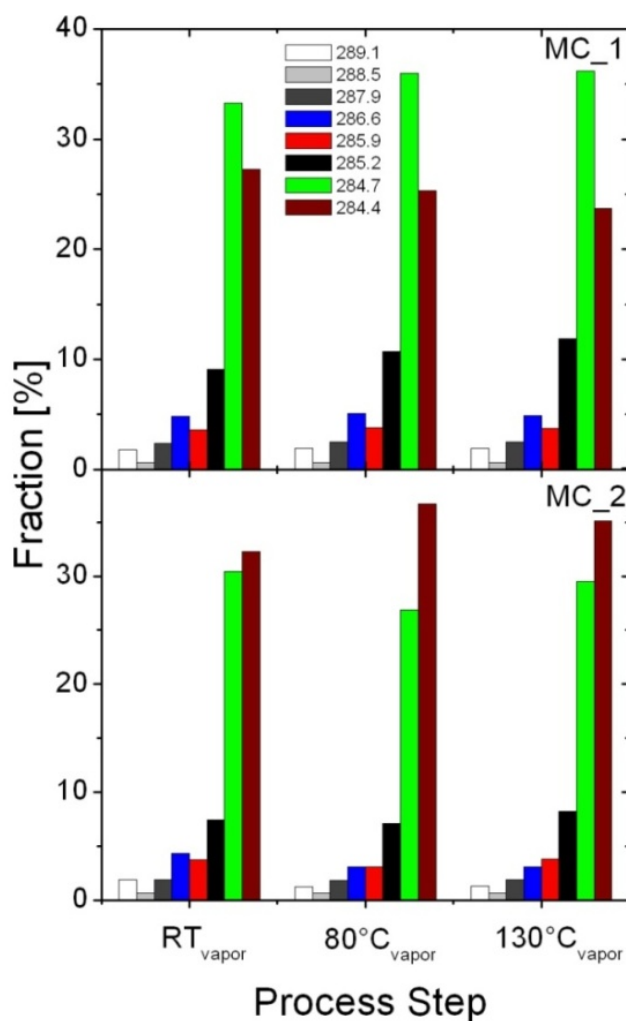


Figure 11: Evolution of C1s components during heating in vacuum and subsequent addition of water (0.1 mbar) at 130°C

As a common trend of the O1s spectra, both samples, MC_1 and MC_2, exhibit a decrease of the peak located at 532.7 eV, also observed under vacuum. At the same time, the feature at the binding energy of 534.2 eV increases in intensity. The opposite trend of development of both peaks supports the idea of two

simultaneous processes. The correlation of the peak at 534.2 eV to OH-species in carboxyl functional groups corresponds to an often reported assignment in the literature^[15-17, 25]. In addition, carboxyl groups are preferentially formed in most hydrolysis reactions (**Figure 10**). Based on the reaction conditions applied, i. e. mild temperatures and vapor atmosphere, the decrease in the peak at 532.7 eV is most likely related to adsorbed water from pore incorporation or material solvation.

The C1s spectra for the experiments in water atmosphere reveal a stronger contribution of amorphous carbon for both samples (**Figure 11**), in comparison to the water-free experiments. In case of MC_1 a dramatic increase of the amorphous carbon can be followed during heating in vapor. Similar to the observations from the O1s spectra, MC_1 seems to be less stable against water.

V.3.4 Cl impurities and their evolution during heat and vapor treatment

The acidic pH during the oxidation treatment in hydrogen peroxide is achieved by the addition of hydrochloric acid to the reaction mixture. As observed in the survey spectra, part of the hydrochloric acid reacted with the carbon material and formed chloro-functionalized surface species on the material. In order to give a complete comparison of the two samples MC_1 and MC_2 in terms of catalytic activity, it is important to also consider differences in the amount of the Cl-species and their changes under reaction conditions. Therefore the Cl2p peaks have been examined in detail.

The main feature of the Cl2p is located at ~200.4 eV. This can be related to chlorinated polymers like polyethylene or chlorinated benzene-like molecules^[29]. Sample MC_2 exhibits a smaller amount of Cl than sample MC_1 at room temperature (**Table 8**) and only MC_1 shows a decrease of the Cl signal with increasing T under vacuum conditions. This effect proceeds also under

water exposure at 130°C, where the intensity of MC_1 reaches values comparable to the average Cl signal of MC_2.

Table 8: Quantification of Cl species of MC_1 and MC_2 during in-situ XPS

Experiment: Heating in vacuum and subsequent addition of 0.1 mbar vapor			Experiment: Heating in 0.1 mbar vapor pressure		
	Process step	Total Cl content [%]		Process step	Total Cl content [%]
MC_1	RT	0.4	MC_1	RT _{vapor}	0.3
	80°C	0.2		80°C _{vapor}	0.3
	130°C	0.2		130°C _{vapor}	0.2
	130°C _{vapor}	0.1	MC_2	RT _{vapor}	0.2
MC_2	RT	0.2		80°C _{vapor}	0.2
	80°C	0.1		130°C _{vapor}	0.3
	130°C	0.1			
	130°C _{vapor}	0.1			

The heating of the carbon material under water atmosphere in seems to stabilize the Cl-functional groups in both samples. Minor differences could be detected both for the different samples MC_1 and MC_2, as well as for the different temperature steps.

Although the total amount of chlorine functional groups is with < 0.5% small in comparison to 12% oxygen content, it cannot be excluded that the differences in the Cl-content between MC_1 and MC_2 influenced the catalytic performance of the two materials. The nucleophilic attack of the alcoholic solvent on the chlorinated carbon could lead to the release of HCl under the formation of butylether groups at the carbon surface. The amount of 0.4% Cl for MC_1 corresponds to an acidity of approximately 0.3 mmol/g, in case of a thorough substitution of the Cl-functional groups by etherification. This value is in close

agreement with the results of the titration experiments. However, since the leaching activity, as shown for TDP0.2 (**Figure 3**), was low in comparison to the activity of the oxidized carbon material, the question of the function of the heterogeneous catalyst remains. It is possible that the in-situ formation of HCl is more effective, since side reaction, e. g. with the solvent, can be avoided. Another possible explanation is given by the oxygen functional groups. Brønsted acidic carboxylic acid functional groups could also be the active species in the dehydration reaction. However, their esterification with the alcoholic solvent could lead to fast deactivation of the acidified carbon. Experiments under the addition of homogeneous organic acids, such as acetic acid and oxalic acid, at the same reaction conditions lead to diminutive HMF yields in comparison to the use of homogeneous mineral acids. The reason also here is the competitive reaction of solvent esterification.

V.4 Conclusions

The results of the presented in-situ XPS experiment can be evaluated under various aspects. First we wanted to gain further insight into the deactivation mechanism of acidified mesoporous catalyst in the dehydration of fructose. Here we found evidence for two different deactivation procedures, whereas the weighting of the final influence of the same would need further investigations by complementary methods.

On the one hand the difference in Cl-content could be an explanation for the unequal catalytic performance of MC_1 and MC_2. However, the low activity in the leaching tests points to other influencing factors. On the other hand the catalytically more active sample MC_1 exhibits a higher content of the oxygen

species at 534.2 eV which can be assigned to carboxylic acid according to the literature^[15-17, 25]. The deactivation of the catalyst during the pretreatment in alcoholic solvents can be due to possible esterification reactions. As indirect evidence of surface changes by esterification, the structural differences obtained from the ex-situ XPS and the different behavior of the two samples under heating in water atmosphere were discussed.

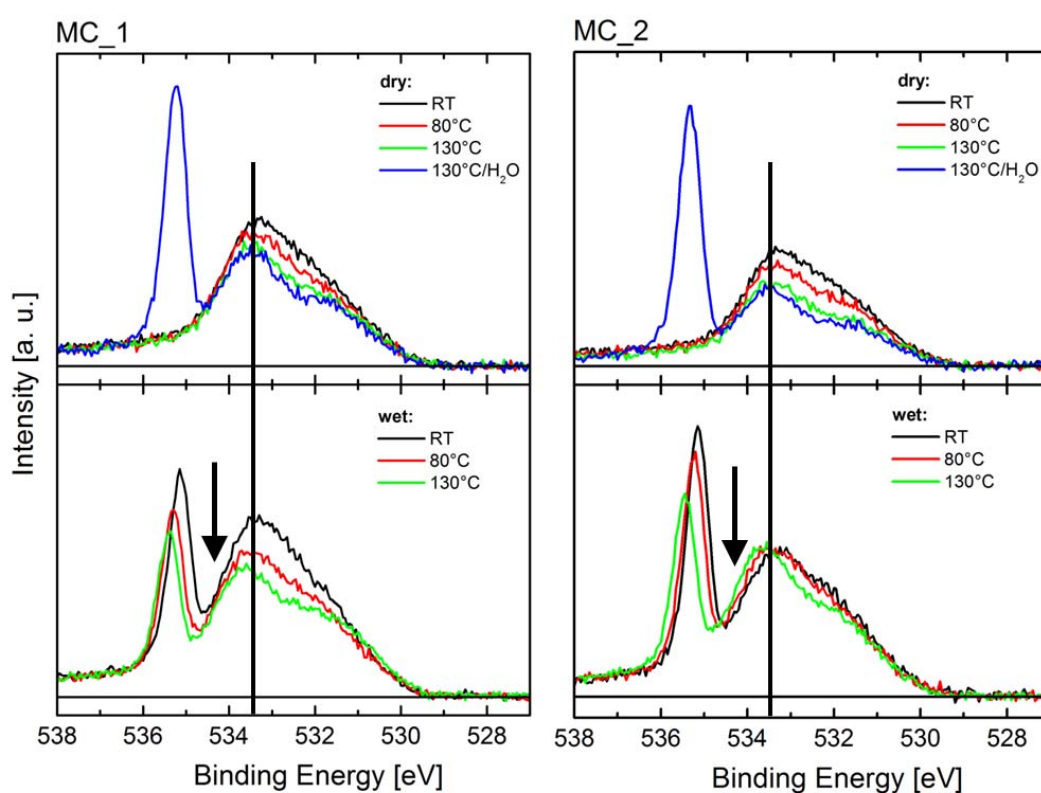


Figure 12: In-situ XPS spectra of sample MC1 (left) and MC2 (right). The line in the figure corresponds to the main intense 533.4 eV peak. The arrow points to a new feature developing while water exposure.

Apart from the results relevant for the catalytic application of the materials in biomass conversion reactions, the experiments provided crucial information on general properties of oxygen functionalized carbon in contact of water. **Figure 12** reveals the different behavior of the two carbon materials MC₁ and

MC_2 by direct comparison of the O1s spectra. Despite the similarities in the oxygen content and the evolution of the O1s peak during heating in vacuum, the addition of water and adjacent heat treatments revealed significant differences in the behavior of the two samples.

Following it can be concluded that carbon materials are not necessarily inert towards water if they carry oxygen functional groups. Carbon, if not graphitic, exhibits a dynamic behavior under the influence of water. Since the in-situ XPS experiment have been performed in only 0.1 mbar vapor pressure and mild temperatures of maximal 130°C, more drastic changes in the structure of carbon materials can be expected under “real” hydrothermal or electrochemical conditions. Several conclusions of the behavior of carbon materials under the influence of aqueous media, e. g. for electrode materials, can be reconsidered based on the finding of the presented XPS experiments.

V.5 References

- [1] H. Probstle, C. Schmitt, J. Fricke, *Journal of Power Sources* **2002**, *105*, 189-194; L. Wencui, G. Reichenauer, J. Fricke, *Carbon* **2002**, *40*, 2955-2959; C. Moreno-Castilla, F. J. Maldonado-Hodar, J. Rivera-Utrilla, E. Rodriguez-Castellon, *Applied Catalysis a-General* **1999**, *183*, 345-356.
- [2] X. C. Zhao, A. Q. Wang, J. W. Yan, G. Q. Sun, L. X. Sun, T. Zhang, *Chemistry of Materials* **2010**, *22*, 5463-5473.
- [3] Y. Hanzawa, H. Hatori, N. Yoshizawa, Y. Yamada, *Carbon* **2002**, *40*, 575-581; W. C. Li, A. H. Lu, S. C. Guo, *Carbon* **2001**, *39*, 1989-1994.
- [4] P. V. Samant, F. Goncalves, M. M. A. Freitas, M. F. R. Pereira, J. L. Figueiredo, *Carbon* **2004**, *42*, 1321-1325.
- [5] R. W. Pekala, *Journal of Materials Science* **1989**, *24*, 3221-3227.
- [6] A. W. Christiansen, *Journal of Applied Polymer Science* **2000**, *75*, 1760-1768.

- [7] S. Reiche, X. C. Zhao, M. Aronson, K. Friedel, E. Kunkes, J.-P. Tessonnier, M. Behrens, D. S. Su, R. Davis, S. B. Abdul Hamid, R. Schlögl, **2012**.
- [8] S. Reiche, E. Kunkes, N. B. Asari Mansor, X. C. Zhao, K. R. Yuyyuru, A. Villa, D. S. Su, M. Behrens, P. Strasser, R. Schlögl, **2012**.
- [9] G. C. Ruben, R. W. Pekala, T. M. Tillotson, L. W. Hrubesh, *Journal of Materials Science* **1992**, 27, 4341-4349.
- [10] H. Bluhm, M. Haevecker, A. Knop-Gericke, M. Kiskinova, R. Schloegl, M. Salmeron, *Mrs Bulletin* **2007**, 32, 1022-1030; A. Knop-Gericke, E. Kleimenov, M. Haevecker, R. Blume, D. Teschner, S. Zafeiratos, R. Schloegl, V. I. Bukhtiyarov, V. V. Kaichev, I. P. Prosvirin, A. I. Nizovskii, H. Bluhm, A. Barinov, P. Dudin, M. Kiskinova, *Advances in Catalysis, Vol 52* **2009**, 52, 213-272; M. Salmeron, R. Schlogl, *Surface Science Reports* **2008**, 63, 169-199.
- [11] E. M. Vass, M. Haevecker, S. Zafeiratos, D. Teschner, A. Knop-Gericke, R. Schloegl, *Journal of Physics-Condensed Matter* **2008**, 20.
- [12] R. Blume, in *unpublished work*, **2011**.
- [13] G. Ketteler, P. Ashby, B. S. Mun, I. Ratera, H. Bluhm, B. Kasemo, M. Salmeron, *Journal of Physics-Condensed Matter* **2008**, 20.
- [14] R. Schlogl, G. Loose, M. Wesemann, *Solid State Ionics* **1990**, 43, 183-192; M. T. Martinez, M. A. Callejas, A. M. Benito, M. Cochet, T. Seeger, A. Anson, J. Schreiber, C. Gordon, C. Marhic, O. Chauvet, J. L. G. Fierro, W. K. Maser, *Carbon* **2003**, 41, 2247-2256; E. Desimoni, G. I. Casella, A. Morone, A. M. Salvi, *Surface and Interface Analysis* **1990**, 15, 627-634.
- [15] S. Biniak, G. Szymanski, J. Siedlewski, A. Swiatkowski, *Carbon* **1997**, 35, 1799-1810; H. Darmstadt, C. Roy, S. Kaliaguine, *Carbon* **1994**, 32, 1399-1406.
- [16] J. L. Figueiredo, M. F. R. Pereira, *Catalysis Today* **2010**, 150, 2-7.
- [17] M. E. Schuster, M. Havecker, R. Arrigo, R. Blume, M. Knauer, N. P. Ivleva, D. S. Su, R. Niessner, R. Schlogl, *Journal of Physical Chemistry A* **2011**, 115, 2568-2580.
- [18] J. L. Figueiredo, M. F. R. Pereira, M. M. A. Freitas, J. J. M. Orfao, *Carbon* **1999**, 37, 1379-1389.
- [19] B. Frank, A. Rinaldi, R. Blume, R. Schlogl, D. S. Su, *Chemistry of Materials* **2010**, 22, 4462-4470.
- [20] S. Kundu, Y. M. Wang, W. Xia, M. Muhler, *Journal of Physical Chemistry C* **2008**, 112, 16869-16878.

- [21] D. T. Clark, B. J. Cromarty, A. Dilks, *Journal of Polymer Science Part a-Polymer Chemistry* **1978**, *16*, 3173-3184; D. T. Clark, A. Dilks, *Journal of Polymer Science Part a-Polymer Chemistry* **1979**, *17*, 957-976.
- [22] D. Rosenthal, M. Ruta, R. Schloegl, L. Kiwi-Minsker, *Carbon* **2010**, *48*, 1835-1843; G. P. Lopez, D. G. Castner, B. D. Ratner, *Surface and Interface Analysis* **1991**, *17*, 267-272.
- [23] A. Stein, Z. Wang, M. A. Fierke, *Advanced Materials* **2009**, *21*, 265-293.
- [24] M. S. Akhter, A. R. Chughtai, D. M. Smith, *Applied Spectroscopy* **1985**, *39*, 143-153; D. M. Smith, A. R. Chughtai, *Colloids and Surfaces a-Physicochemical and Engineering Aspects* **1995**, *105*, 47-77; P. E. Fanning, M. A. Vannice, *Carbon* **1993**, *31*, 721-730.
- [25] U. Zielke, K. J. Huttinger, W. P. Hoffman, *Carbon* **1996**, *34*, 983-998.
- [26] M. E. Schuster, Technische Universität Berlin (Berlin), **2011**.
- [27] E. Desimoni, G. I. Casella, T. R. I. Cataldi, A. M. Salvi, T. Rotunno, E. Dicroce, *Surface and Interface Analysis* **1992**, *18*, 623-630.
- [28] E. Breitmaier, G. Jung, *Organische Chemie - Grundlagen, Stoffklassen, Reaktionen, Konzepte, Molekülstruktur*, 5 ed., Georg Thieme Verlag, Stuttgart, New York, **2005**.
- [29] J. Moulder, W. Stickle, P. Sobol, *Handbook of X Ray Photoelectron Spectroscopy*, **1992**.

VI FINAL DISCUSSION AND OUTLOOK

Several heterogeneous catalysts have been tested in the acid catalyzed dehydration of fructose to 5-hydroxymethyl furfural (HMF) with the result of a severe deactivation of the materials already after the first reaction run. The critical comparison of measured catalytic activities to literature data has shown a lack of stability studies on heterogeneous catalyst applied in this reaction. Furthermore, the variety of catalytic test conditions hampers the direct comparison of data. Often applied multi-component systems lead to additional complexity hindering the basic understanding of the influence of single reaction parameters. We developed a one-phase solution for the dehydration of fructose. The use of 2-butanol as the only reaction solvent inhibits the product accumulation on hydrophobic catalysts (e.g. functionalized carbon nanotubes), as confirmed by adsorption studies. In addition, the rehydration to the side products levulinic acid and formic acid are suppressed. The process avoids impurities in the HMF-product that can be problematic in subsequent processing steps, such as S- and N-containing solvents or salt residues applied in the biphasic process^[1]. Hence the one-phase system in 2-butanol would require lower purification costs than other established processes.

Comparative studies on carbon based heterogeneous catalysts revealed three different deactivating processes: (1) the leaching of instable acid functional groups, (2) the surface coverage or side blocking by insoluble polymeric byproducts (humins)

and (3) the surface passivation by the solvent. The stability of acid functional groups was investigated by activity tests of the solvent after preconditioning of the catalyst (leaching tests). It was found that leaching is a common problem for all post-functionalized, e. g. sulfonated, catalysts and appropriate pretreatments are required, in order to start with a stable fraction of acid functional groups. Leaching tests are essential for thorough proof of catalyst stability and hence are suggested to be adapted as common test for heterogeneous catalysts in fructose dehydration.

Furthermore we established the comparison to the reference reaction, the esterification of acetic acid in ethanol, as successful tool for the estimation of catalyst stability. The deactivation by leaching or solvent reactions can be traced by the reference reaction. However, the successful recycling in the esterification reaction does not guarantee a stable catalyst in the fructose dehydration. It could be shown that the preconditioned catalyst AGPs (sulfonated amorphous carbon from glucose pyrolysis) can be recycled successfully in catalyzing the conversion of the monofunctionalized reactant in the reference reaction. However, the cascade reaction fructose dehydration (**Figure 1**) cannot be catalyzed in a controlled way, avoiding the formation of surface covering humins.

Under the focus of gaining further inside into the solvent deactivating process (3), in-situ XPS studies have been performed. It was shown that the catalyst pretreated in the solvent 2-butanol exhibits less structural changes in the O1s as well as the C1s spectra while heating in vapor atmosphere. Consequently, we concluded a higher hydrophobicity for the pretreated sample. As possible passivating reaction the esterification of surface carboxylic acid groups by the alcoholic solvent was discussed. The formed ester groups lead to a more hydrophobic surface termination which could prevent the intrusion of water. As consequence for the dehydration reaction, the lower abundance of acid functional groups can explain the decrease in catalytic activity.

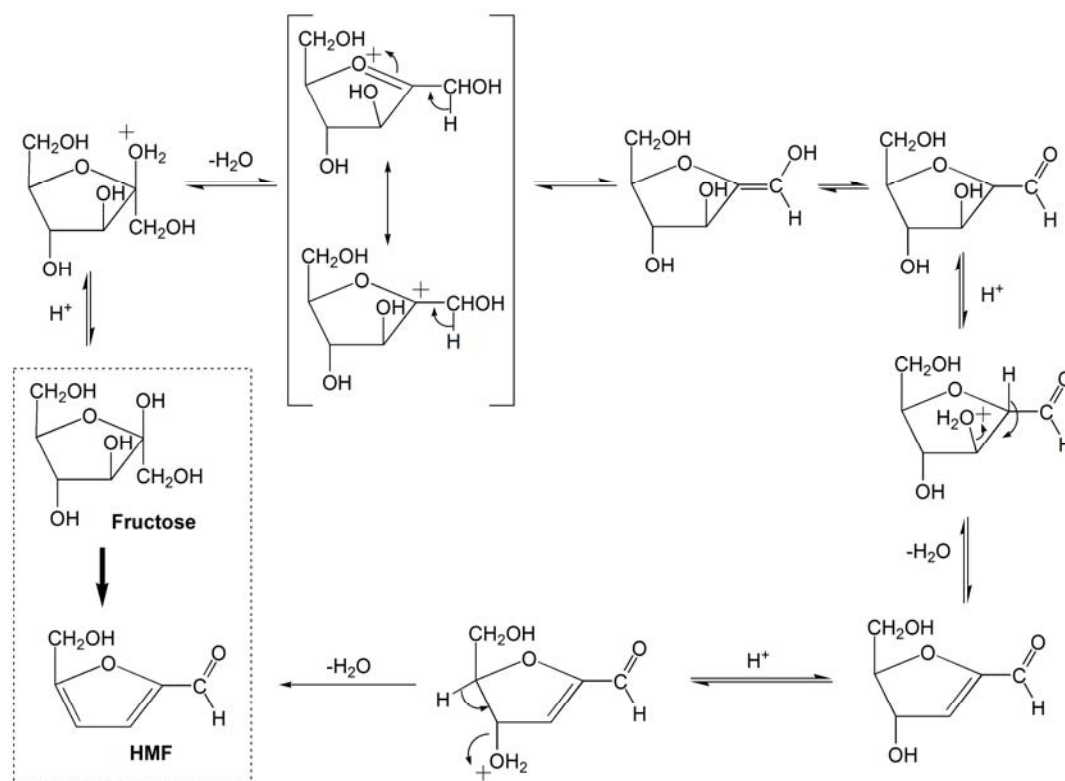


Figure 1: Mechanism of fructose dehydration catalyzed by homogeneous acids

Future studies could be directed into more mechanistic understanding of the fructose dehydration on heterogeneous catalysts. **Figure 1** shows the mechanism of the dehydration reaction of fructose (possible side reactions neglected) for the homogeneously catalyzed case. In comparison to the homogeneous case, where the proton concentration is constant over the total reaction medium, the protons at the surface of the heterogeneous catalyst are localized at the “active site”. The constrained local environment of the active proton plays a major role in the reactivity of the catalyst and the selectivity of the total reaction. The reactant can be stabilized in certain conformations by complexation by surface functional groups. Additionally, side reactions can be provoked if further reactive groups are situated in close proximity to the active site. So far, neither the actual nor the ideal local environment of an active site is known for fructose dehydration. Some groups discussed the general positive or

negative effect of additional Lewis acid sites on the reaction with controversial conclusions^[2].

Due to the incomplete knowledge on the requirements of the heterogeneous catalyst, model systems carrying only one type of acid functional groups would be needed. Preferentially, the support should be variable in pore size and inert to the reaction conditions, as well as to the reactant fructose. In the case of oxides, the stability against hydrolysis is limited and the influence of Lewis acid and basic sites add complexity. Furthermore, the redox activity cannot be excluded for some systems, such as the promising niobium-based catalysts. For this reason we have chosen carbon catalysts, although the recovery of by calcination is not possible. Under the aim of further mechanistic understanding of the heterogeneously catalyzed fructose dehydration, carbon stays an interesting support material. However, higher precision in the functionalization process is required which includes the thorough purification of an – at best – graphitic carbon support and the selective introduction on only one type of functional group. There are ongoing research efforts towards this direction in our department.

Based on a controlled functionalization process, the optimal density of acid sites could be determined. According to the present state of the literature, it is not known how many acid sites participate in the formation of one HMF molecule. It is possible that more than one acid site can be involved in the course of the reaction. Hence, the local proton density would affect the devolution of the cascade reaction of three subsequent dehydration steps (**Figure 1**) and consequently can be seen as an important selectivity criterion.

Under the focus of the short term development of an economic process for fructose dehydration the use of calcinable, oxidic catalysts provide a possible starting point. The use of two parallel reactors would provide the possibility of alternating processing and reactivation / calcinations steps under constant HMF production. Also here, the basis of successful process development is the careful investigation of the deactivation behavior of the catalyst. Typical deactivation procedures and essential stability tests have been described in this thesis.

- [1] Y. Roman-Leshkov, C. J. Barrett, Z. Y. Liu, J. A. Dumesic *Nature*. **2007**, 447, 982-U985.
- [2] R. Weingarten, G. A. Tompsett, W. C. Conner, Jr., G. W. Huber *Journal of Catalysis*. **2011**, 279, 174-182.

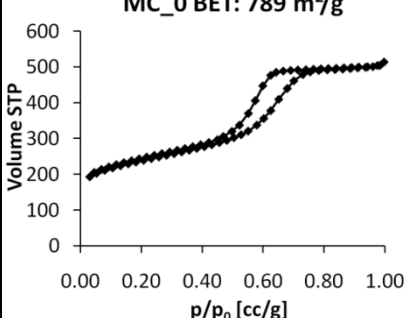
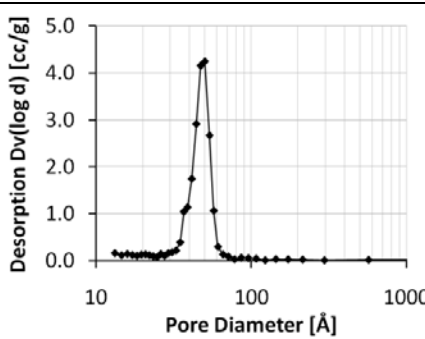
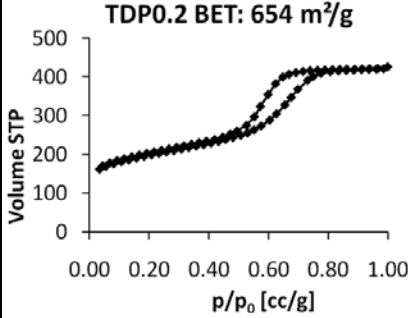
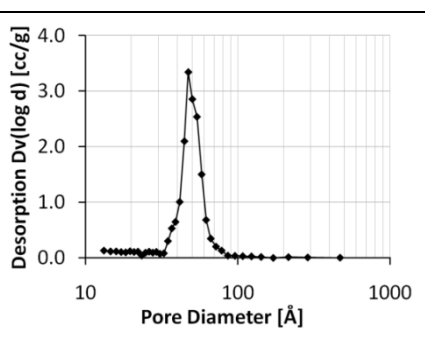
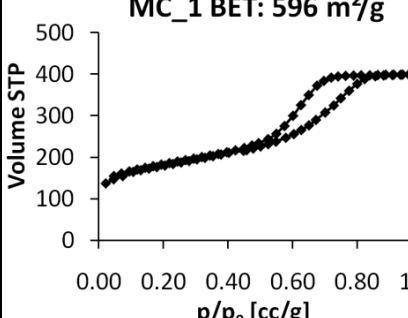
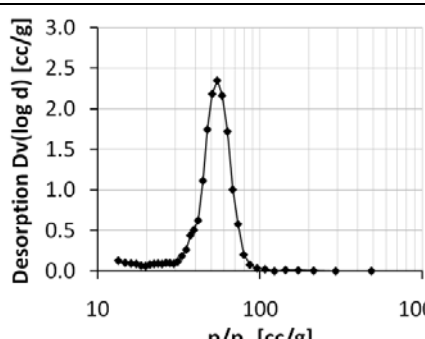
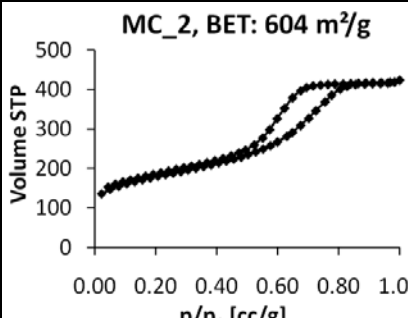
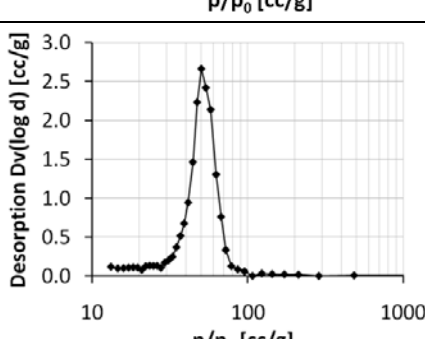
VII SUPPLEMENTARY INFORMATION

VII.1 Database Sample Numbers

Abbreviation	Material description	Sample Number
BT ₀	pristine Baytubes® from Bayer	3832, 8819
BTs	Baytubes® functionalized by H ₂ SO ₄	8234, 8032, 8879
BTsG200	Baytubes® gas phase functionalized in oleum at 200°C	9121
BTsG600	Baytubes® gas phase functionalized in oleum at 600°C	9187
BTn	Baytubes® functionalized by HNO ₃	8240
BTb	Baytubes® functionalized by B(OH) ₃	8241
BS-CNF	PR24XT-HHT from Applied Sciences, grafted by benzene sulfonic acid	12001
AGP	amorphous carbon from glucose pyrolysis	9922, 10121, 10122
AGPs	amorphous carbon from glucose pyrolysis functionalized by H ₂ SO ₄	9933, 10279
OMC (MC_0)	ordered mesoporous carbon	10921
OMCs	ordered mesoporous carbon functionalized by H ₂ SO ₄	10956
MC_TDP (TDP0.2)	mesoporous carbon, 20mol% of building block recorcinol replaced by thiodiphenyl	11108, 11454
MC_H ₂ O ₂ (MC_1)	mesoporous carbon, functionalized by H ₂ O ₂ at pH = 1	11466
MC_H ₂ O ₂ _2B (MC_2)	mesoporous carbon, after functionalization by H ₂ O ₂ at pH = 1 and subsequent treatment in 2-butanol (130°C, 15 h)	11690
Nafion®	Nafion® NR50 from Aldrich	10281
Amberlyst®	Amberlyst® 15 from Aldrich	12375
Sulfated zirconia	Sulfated zirconia from MEL Chemicals	3006
H-mordenite	H-mordenite (H-MOR 14) from Südchemie	6188
H-ZSM5	H-ZSM5, Degussa, Si/Al=19, #KM-426	9378
NbPO ₄	niobium phosphate from CBMM	12318
(VO) ₂ P ₂ O ₇	vanadyl pyrophosphate from Ecole Polytechnique Montréal	12351

VII.2 BET Isotherms

Table 1: BET isotherms of mesoporous carbon samples investigated by XPS

Sample	SN	BET isotherm	BJH poresize distribution
MC_0	10921	<p>MC_0 BET: 789 m²/g</p> 	
TDP0.2	11108	<p>TDP0.2 BET: 654 m²/g</p> 	
MC_1	11466	<p>MC_1 BET: 596 m²/g</p> 	
MC_2	11690	<p>MC_2, BET: 604 m²/g</p> 	

VII.3 XPS

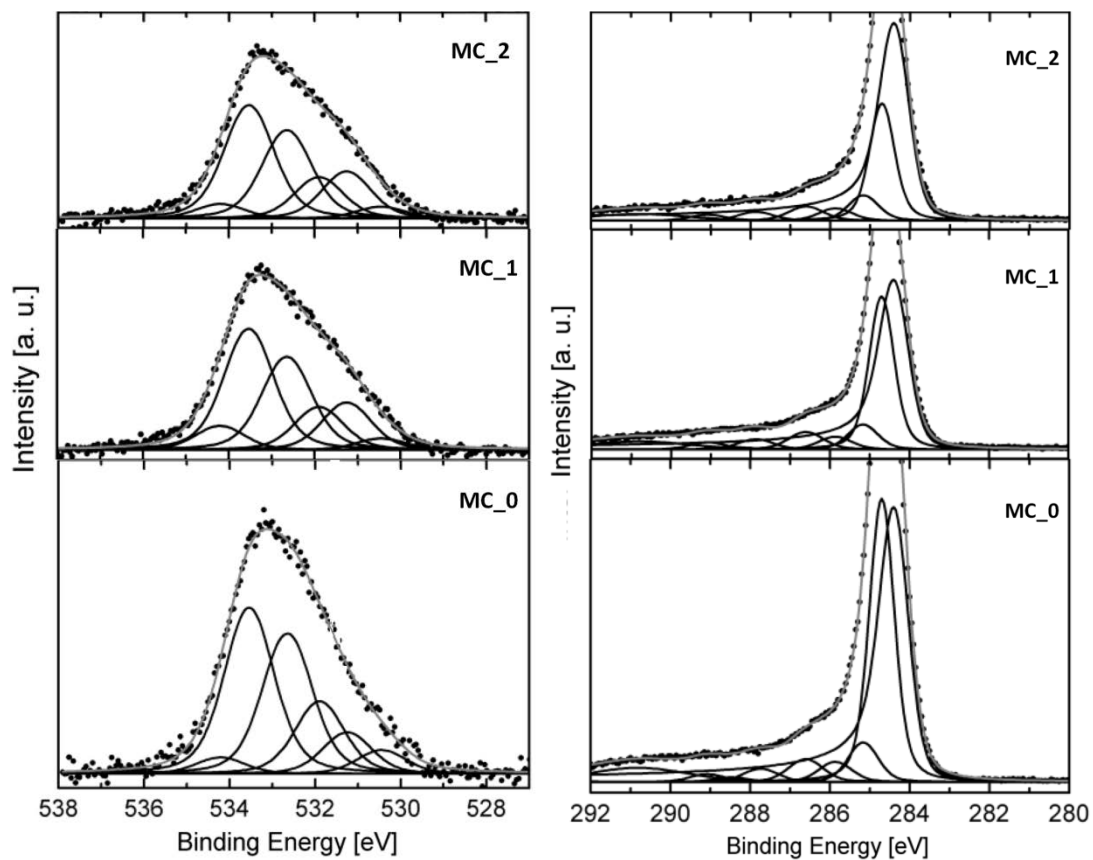


Figure 1: O1s fits (left panel) and C1s fits (right panel) of MC_0, MC_1 and MC_2 obtained by ex-situ XPS

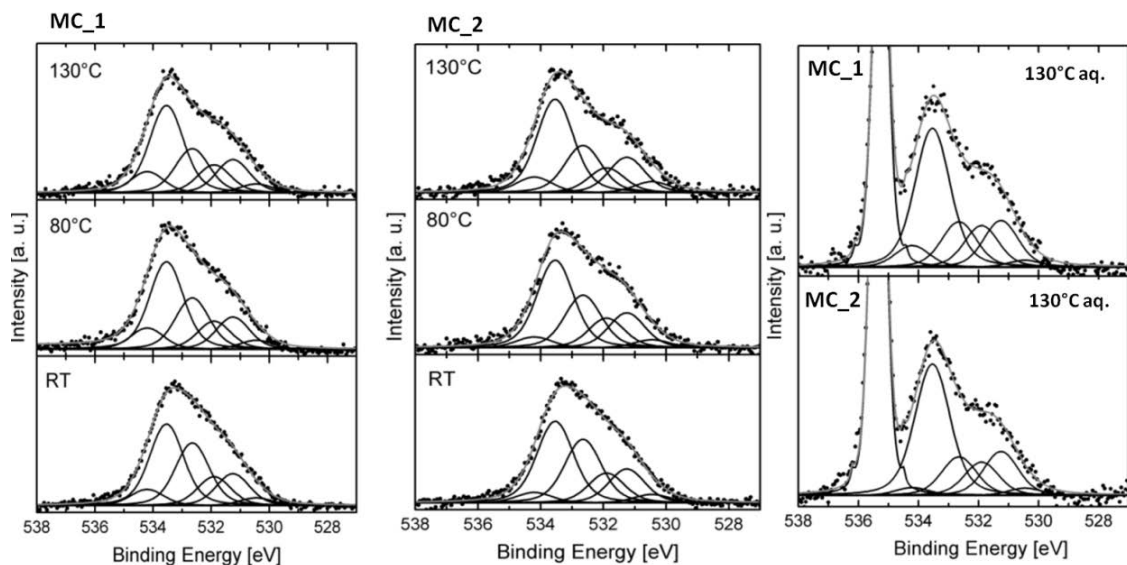


Figure 2: Fits for O1s spectra of MC_1 and MC_2 during heating in vacuum

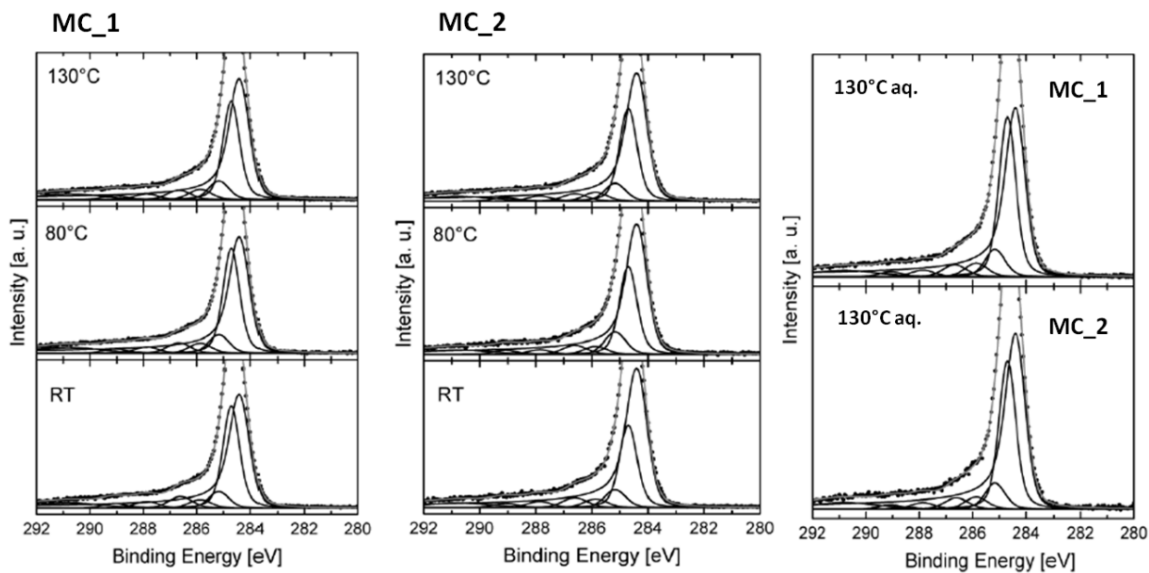


Figure 3: Fits for C1s spectra of MC_1 and MC_2 during heating in vacuum

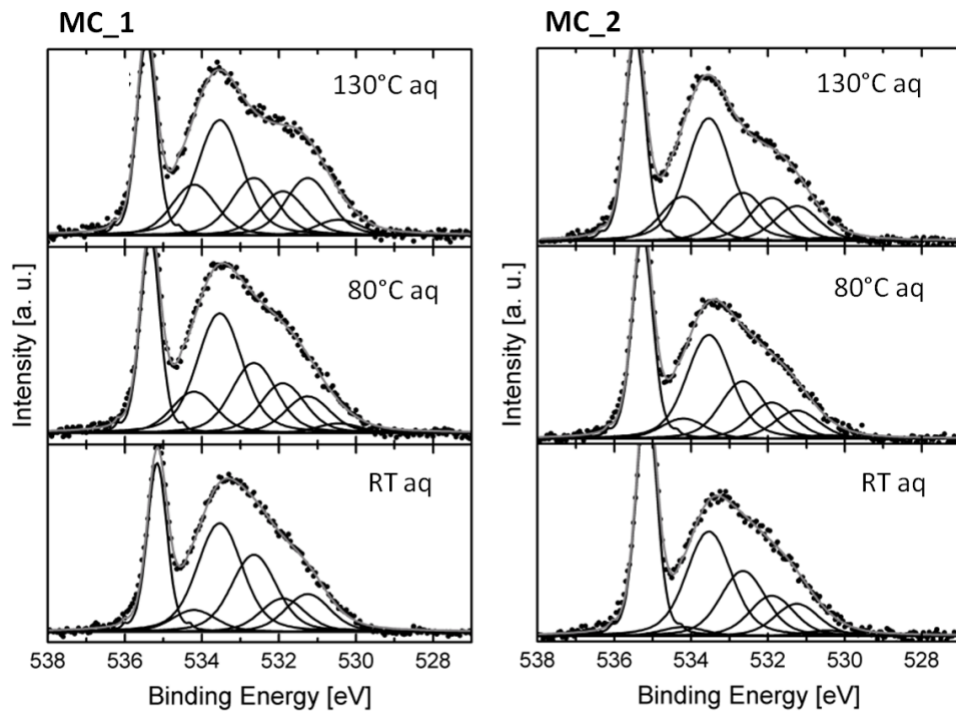


Figure 4: Fits for O1s spectra of MC_1 and MC_2 during heating in 0.1 mbar vapor

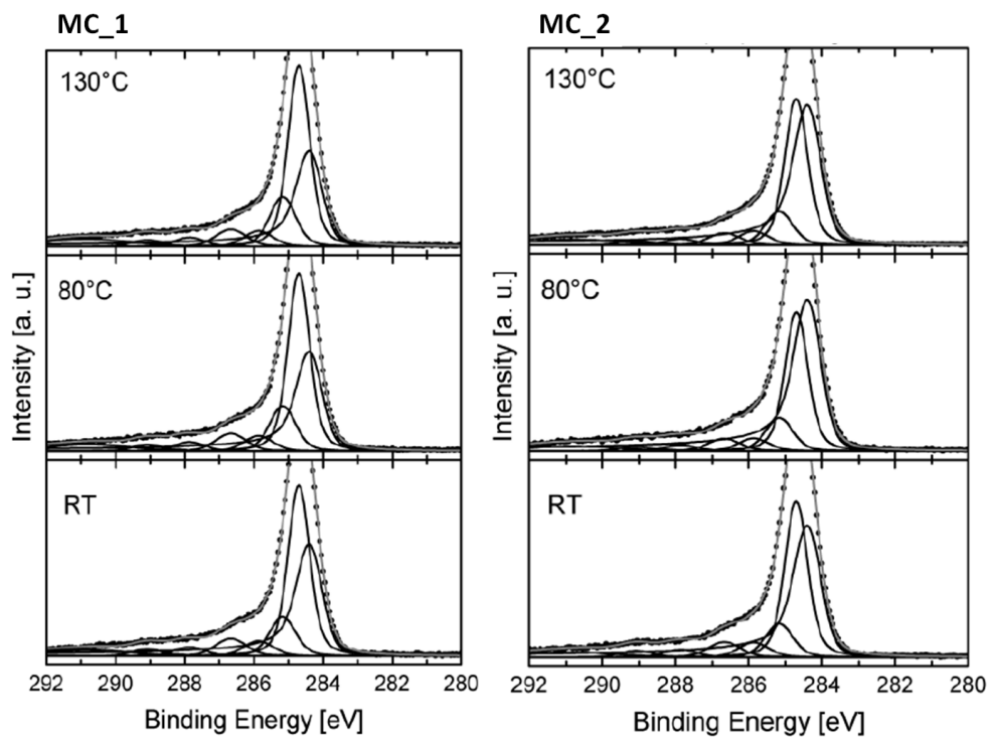


Figure 5: Fits for C1s spectra of MC_1 and MC_2 during heating in 0.1 mbar vapor

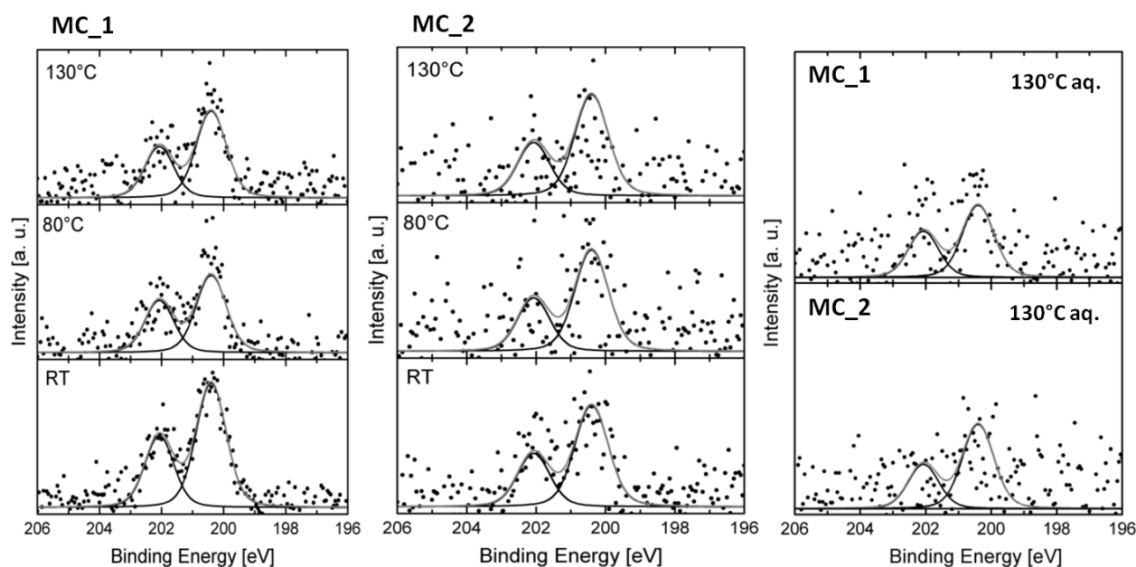


Figure 6: Cl 2p spectra for MC_1 and MC_2 during heating in vacuum

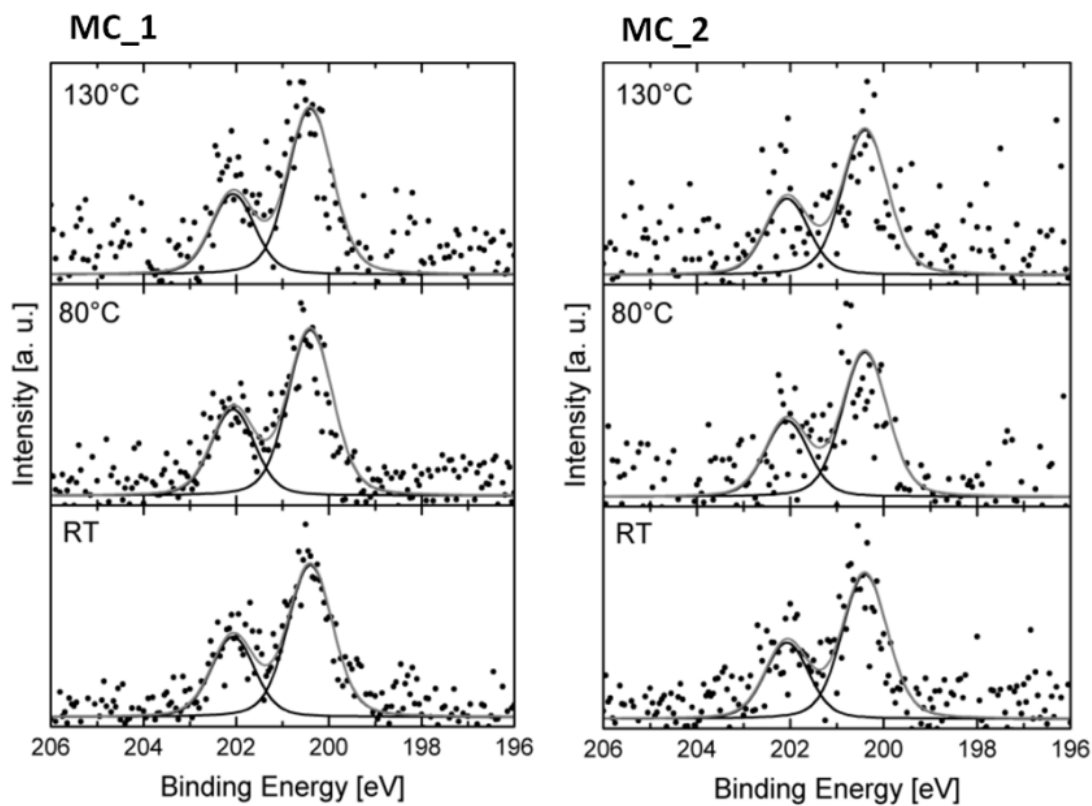


Figure 7: Cl 2p spectra for MC_1 and MC_2 during heating in vapor

Supplementary Information

Table 2: Quantification of carbon species in the O1s peak during heating in vacuum and subsequent addition of water at 130°C (carbon fraction in %)

Sample	Process step	530.5 eV	531.2 eV	531.9 eV	532.7 eV	533.5 eV	534.2 eV	Total oxygen content
MC_1	RT	0.4 (4)	1.5 (14)	1.4 (13)	3.0 (27)	4.0 (36)	0.8 (7)	11.1
	80°C	0.4 (4)	1.3 (13)	1.2 (12)	2.2 (22)	3.8 (39)	0.9 (9)	10.3
	130°C	0.4 (4)	1.4 (15)	1.2 (13)	1.9 (20)	3.7 (39)	0.9 (10)	9.4
	130°C aq	0.2 (2)	1.3 (15)	1.1 (13)	1.3 (15)	4.1 (48)	0.6 (7)	8.5
MC_2	RT	0.4 (3)	1.8 (15)	1.6 (13)	3.4 (28)	4.4 (36)	0.5 (4)	12.1
	80°C	0.4 (4)	1.7 (16)	1.4 (13)	2.6 (24)	4.3 (40)	0.5 (5)	10.9
	130°C	0.5 (5)	1.5 (15)	1.1 (11)	2.0 (20)	4.1 (42)	0.6 (6)	9.8
	130°C aq	0.2 (2)	1.4 (17)	1.1 (13)	1.3 (16)	4.1 (49)	0.2 (2)	8.3

Table 3: Quantification of carbon species in the C1s peak during heating in vacuum and subsequent addition of water at 130°C (carbon fraction in %)

Sample	Process step	284.4 eV	284.7 eV	285.2 eV	285.9 eV	286.6 eV	287.9 eV	Total carbon content
MC_1	RT	37.0 (42)	26.7 (30)	4.9 (6)	3.0 (3)	4.0 (5)	2.4 (3)	88.6
	80°C	37.2 (42)	27.0 (30)	5.4 (6)	3.6 (4)	3.6 (4)	2.4 (3)	89.4
	130°C	38.8 (43)	25.5 (28)	5.4 (6)	3.6 (4)	3.6 (4)	1.8 (2)	90.4
	130°C aq	38.6 (43)	28.9 (32)	5.8 (6)	3.2 (4)	3.6 (4)	1.9 (2)	91.3
MC_2	RT	43.0 (49)	15.7 (18)	5.1 (6)	2.9 (3)	3.4 (4)	2.3 (3)	87.7
	80°C	41.0 (46)	22.2 (25)	6.4 (7)	2.3 (3)	2.9 (3)	1.8 (2)	88.9
	130°C	41.5 (46)	24.0 (27)	5.4 (6)	3.0 (3)	2.4 (3)	1.8 (2)	90.1
	130°C aq	40.6 (44)	27.5 (30)	5.9 (6)	2.6 (3)	2.6 (3)	1.3 (2)	91.6

Supplementary Information

Table 4: Quantification of carbon species in the O1s peak during heating in 0.1 mbar vapor pressure (carbon fraction in %)

Sample	Process step	530.5 eV	531.2 eV	531.9 eV	532.7 eV	533.5 eV	534.2 eV	Total oxygen content
MC_1	RTaq	0.1 (1)	1.6 (13)	1.4 (12)	3.3 (28)	4.6 (39)	0.9 (8)	11.8
	80°Caq	0.2 (2)	1.0 (12)	1.3 (15)	1.9 (22)	3.2 (37)	1.1 (13)	8.7
	130°Caq	0.5 (5)	1.6 (16)	1.3 (13)	1.7 (17)	3.4 (34)	1.5 (15)	9.9
MC_2	RTaq	0.2 (2)	1.1 (12)	1.4 (15)	2.4 (26)	3.7 (26)	0.3 (3)	9.2
	80°Caq	0.1 (1)	1.1 (11)	1.4 (14)	2.3 (24)	4.1 (42)	0.8 (8)	9.8
	130°Caq	0.1 (1)	1.1 (12)	1.4 (1.6)	1.6 (17)	4.0 (42)	1.4 (15)	9.5

Table 5: Quantification of carbon species in the C1s peak during heating in 0.1 mbar vapor pressure (carbon fraction in %)

Sample	Process step	284.4 eV	284.7 eV	285.2 eV	285.9 eV	286.6 eV	287.9 eV	Total carbon content
MC_1	RTaq	27.3 (31)	33.3 (38)	9.1 (10)	3.6 (4)	4.8 (6)	2.4 (3)	87.9
	80°Caq	25.3 (28)	36.0 (40)	10.7 (12)	3.8 (4)	5.1 (6)	2.5 (3)	91
	130°Caq	23.7 (26)	36.2 (40)	11.9 (13)	3.7 (4)	4.9 (6)	2.5 (3)	89.9
MC_2	RTaq	32.3 (36)	30.4 (34)	7.4 (8)	3.7 (4)	4.3 (5)	1.9 (2)	90.6
	80°Caq	36.7 (41)	26.9 (30)	7.1 (8)	3.1 (3)	3.1 (3)	1.9 (2)	90
	130°Caq	35.1 (39)	29.5 (33)	8.2 (9.1)	3.8 (4)	3.1 (3)	1.9 (2)	90.2

Acknowledgment

A good friend kept telling me: "If you really want something the whole universe will come together and help you to make it happen." This phrase gives a very suitable expression for the dimensions of help and support during my PhD, I would like to gratefully acknowledge for in fewer words than probably adequate.

First I would like to thank Prof. Robert Schlögl for the opportunity to work on this challenging and multi-disciplinary project in such a great environment. The scientific input as well as continuous encouragement and motivation helped me to keep track and to overcome the one or other hurdle. Furthermore, I thank my two group leaders during my time at FHI, Dr. Dangsheng Su and Dr. Malte Behrens for scientific as well as moral support. I would like to thank my first supervisor Dr. Jean-Philippe Tessonier for sharing his broad knowledge in carbon research and catalysis. The open office discussions facilitated my start at FHI and generated a fruitful spirit of interactive exchange. In this regards, I am also grateful for my permanent office mate Weiqing Zheng who patiently handled my curiosity and openly answered all kind of questions on Chinese culture, which widened my view towards other perspectives. Special thank goes to Dr. Alberto Villa for his supervision and his experience in the preparation of metal colloids and liquid phase catalysis.

I would like to thank Nuruzatulifah Bt. Asari Mansor, Xiao Chen Zhao, Klaus Friedel and Matthew Aronson for their collaboration in the material synthesis and the PIRE program, in particular Keenan Deutsch, Prof. Brent Shanks and Prof. Robert Davis for fruitful exchange of experience in biomass conversion chemistry. Furthermore, I highly appreciate the collaboration with Prof. Sharifah Bee Abdul Hamid who gave me the opportunity to use the high-throughput facilities at Universiti Malaya in Kuala Lumpur for my experiments.

I am particularly grateful for the support by Dr. Edward Kunkes. His long-ranging experience in the catalytic conversion of biomass, as well as the talent to oversee complex problems with an immediate focus on critical points, gave me a big push forward. I highly appreciate the scientific input and all the efforts in teaching me the engineer's point of view, as well as the time taken for the correction of my English writing.

For their help in the analysis of the materials I would like to thank Gisela Lorenz for the BET measurements, as well as Edith Kitzelmann and Dr. Andrey Tarasov for TG-MS. The microscopy group, in particular Achim Klein-Hoffman, Gisela Weinberg, Norbert Pfänder and Dr. Marc Willinger I would like to thank for their support and the introduction into the microscopes. My special thank goes to Dr. Raoul Blume for technical support at BESSY, the fits of the XPS spectra and intensive scientific discussions.

I thank all members of the AC department of FHI for creating this characteristic scientific spirit that I enjoyed very much. Countless discussions set new impulses in the project and led to a continuous learning process. For my “daily lecture” during coffee break or lunch I thank Christian Heine, Andreas Östereich, Klaus Friedel, Pierre Kube, Stefan Zander, Gregor Wowsnick, Julia Neuendorf, Antje Ota und Steffi Kühl. In particular in the last months some daily routine gave me stability and mental strength in stressful times.

At the Technische Universität Berlin I thank Prof. Peter Strasser and Koteswara Rao Vuyyuru for the collaboration and fruitful input. I am grateful that I could be a part of UniCat and the BIG-NSE, and want to thank for the financial support, as well as the scientific interactions. I send my special thanks to my BIG-NSE-batch, including Kirstin Hobiger, Sara Bruun, Subhamoy Bhattacharya, Sardor Mavlyankariyev, Stanislav Jaso, Changzhu Wu, Manuel Harth and Carlos Carrero, as well as to Dr. Jean-Philippe Lonjaret who spared no efforts to make this BIG-NSE time enjoyable and memorable.

From the beginning till the end, I could always rely on Steffi Kühl and Antje Ota who offered help intuitively even before I could ask for. I wanna thank for all efforts and support, and for the little reminders that prevented me from trouble multiple times.

I thank my family – my island of continuity, stability and love that I can always land on. I wanna thank my parents and my brother Martin because they always stand beside me, no matter what. And I thank my fiancé Christoph for his love and all the weight he carried on his broad shoulders, in particular during the last months.

Danke

CURRICULUM VITAE

- Sylvia Reiche -

- born on November 24th 1983 in Oschatz (Germany) -

EDUCATION

From 7/2008	PhD thesis <i>Insights into Heterogeneous Catalysts for HMF synthesis from Biomass</i> Prof. Dr. Robert Schlögl (co-advisor, Fritz Haber Institute), Prof. Dr. Peter Strasser (co-advisor, Technische Universität Berlin)	Fritz Haber Institute Berlin, Germany Technische Universität Berlin, Germany
From 10/2008	Berlin International Graduate School of Natural Sciences and Engineering (BIG-NSE)	Technische Universität Berlin, Germany
04/2008	M. Sc. <i>Preparation and Characterization of Silver Nanoparticles for Printable Electronics</i> Prof. Dr. Dan Goia (co-advisor, Clarkson University), Prof. Dr. Berthold Kersting (co-advisor, Universität Leipzig)	Universität Leipzig Leipzig, Germany Clarkson University Postdam, NY, United States
10/2005	B. Sc. <i>Determination of the Degree of Phosphorylation of the TAU-Protein by Antibodies</i> Prof. Dr. Ralf Hoffmann	Universität Leipzig Leipzig, Germany

PROFESSIONAL EXPERIENCE

10/2009	Research visit Combinatorial Technologies and Catalysis Research Centre (COMBICAT), Universiti Malaya Prof. Dr. Sharifah Bee Abd. Hamid	Universiti Malaya Kuala Lumpur, Malaysia
06/2006– 03/2007	Employee R&D of Contact Materials (Dept: TM-ETM-FE), preparation of silver dispersions, scale up Dr. Bernd Kempf, Dr. Sebastian Fritzsche	Umicore AG & Co. KG Hanau, Germany
02/2007 and 10/2007– 03/2008	Research visit Center for Advanced Material Processing (CAMP), cooperated partner of Umicore AG & Co. KG Prof. Dr. Dan Goia	Clarkson University Postdam, NY, United States

HONORS AND AWARDS

10/2008 – 10/2011	Scholarship from Berlin International Graduate School of Natural Sciences and Engineering (BIG-NSE), graduate school of the Cluster of Excellence "Unifying Concepts in Catalysis" (UniCat)
08/2010	Invitation to BASF International Summer Courses 2010

REFERENCES

Oral presentations:

S. Reiche, M. Aronson, X. C. Zhao, K. Friedel, R. Blume, E. Kunkes, J.-P. Tessonnier, M. Behrens, D. S. Su, R. Davis, R. Schlögl, *Acidified Carbon Catalysts for Liquid Phase Reactions in Biomass Conversion Chemistry*, EuropaCat X, August 2011, Glasgow, Scotland

S. Reiche, M. Aronson, X. C. Zhao, K. Friedel, R. Blume, E. Kunkes, J.-P. Tessonnier, M. Behrens, D. S. Su, R. Davis, R. Schlögl, *Heterogeneous Catalysts in the Dehydration of Fructose to HMF*, AIChE Annual Meeting, October 2011, Minneapolis (MN), United States

Poster presentations:

A. Demund, D. Wett, S. Reiche, R. Szargan, R. Denecke, *Study of formation and thermal stability of Fe layers on ZnO surfaces* (Poster), DPG Annual Meeting, February 2008, Berlin, Germany

S. Reiche, M. Aronson, X. Ch. Zhao, E. Kunkes, J.-P. Tessonnier, M. Behrens, D. S. Su, R. Davis, R. Schlögl, *Acidified Carbon Catalysts for Liquid Phase Reactions in Biomass Conversion Chemistry*, 44. Jahrestreffen Deutscher Katalytiker, March 2011, Weimar, Germany

Publications:

S. Sahin, P. Maki-Arvela, J.-P. Tessonnier, A. Villa, S. Reiche, S. Wrabetz, D. S. Su, R. Schlögl, T. Salmi, D. Y. Murzin, *Palladium catalysts supported on N-functionalized hollow vapor-grown carbon nanofibers: The effect of the basic support and catalyst reduction temperature*, Applied Catalysis A – General **2011**, 408, 1-2, 137-147

S. Reiche, E. Kunkes, N. B. Asari Mansor, X. C. Zhao, K. R. Vuyyuru, A. Villa, J.-P. Tessonnier, D. S. Su, M. Behrens, P. Strasser, R. Schlögl, *Heterogeneous Catalysts in the Dehydration of Fructose to HMF (to be submitted)*

S. Reiche, X. C. Zhao, M. Aronson, K. Friedel, E. Kunkes, J.-P. Tessonnier, M. Behrens, D. S. Su, R. Davis, S. B. Abdul Hamid, R. Schlögl, *Deactivation Pathways of Carbon Catalysts in the Dehydration of Fructose (to be submitted)*

S. Reiche, R. Blume, X. C. Zhao, E. Kunkes, D. S. Su, M. Behrens, R. Schlögl, *Reactivity of Mesoporous Carbon Against Water: An In-Situ XPS Study (to be submitted)*

„Groß ist die Aufgabe, die vor mir steht und bescheiden sind die Kenntnisse und Kräfte, die für ihre Bewältigung ausreichen sollen. Aber Aufgaben sind da, um gelöst zu werden, und welcher Schlachtruf wäre wohl besser geeignet, den Ermatteten mit neuem Mut zu erfüllen, als das Wort: Energie?“

Wilhelm Ostwald